Friction factors and Nusselt numbers for laminar flow in ducts

Daniel Petrus Rocco Venter

B.Sc. (Hons), B.Eng. (Mechanical)

Dissertation submitted for the degree

Master of Engineering

in the

School of Mechanical Engineering,

Faculty of Engineering

at the

North-West University.

Supervisor: Prof. C.G. du Toit

Potchefstroom

South Africa

2009

ABSTRACT

By using the finite element method to solve the appropriate momentum and energy equations the friction factors and Nusselt numbers for fully developed laminar flow were determined for one- and two-dimensional flow systems. The Nusselt numbers were determined for domain boundaries subjected to a constant heat flux (H1) or a constant surface temperature (T) around the computational boundaries and in the axial directions. C++ programs, that were rewritten and extended from previous programs, were used to solve the laminar flow and to determine the values. The required wall shear stresses and heat fluxes were directly obtained for a duct as part of the primary finite-element solution; these values were then used to determine the Nusselt number and friction factor for the specific duct. The computations were performed for circular-, annular-, trapezoidal-, rectangular- and triangular ducts. Special emphasis was placed on trapezoidal ducts since only a limited number of studies have been performed on trapezoidal duct shapes and none of these studies employed the finite element method.

Excellent agreement was found when the determined values were compared with the values reported in the literature. In general, the agreement of the values improved as the number of elements was increased. It was, therefore, concluded that the methods used in this study yielded friction factors and Nusselt numbers that are very accurate and usable.

Keywoords

Friction factors

Nusselt numbers

Laminar flow

Finite elements

Constant heat flux

Constant surface temperature

OPSOMMING

Deur die gepaste momentum en energie vergelykings met die eindige element metode op te los, was die wrywingsfaktore en Nusseltgetalle vir ten volle ontwikkelde laminêre vloei vir een- en twee-dimensionele vloei bepaal. Nusseltgetalle was bepaal vir domeinrande onderhewig aan konstante hitte-oordrag (H1) of vir konstante oppervlaktemperature (T) reg rondom die berekende grense en ook in die aksiale rigtings. C++ programme wat herskryf en uitgebrei is van vorige programme, was gebruik om die laminêre vloei op te los en die verlangde waardes te bereken. Die nodige skuifspanning en hitteoordrag vir ’n wand was direk verkry as deel van die primêre eindige element oplossing vir die kanaal. Hierdie waardes was dan gebruik om die Nusseltgetal en wrywingsfaktor vir die spesifieke kanaal te bepaal. Die bepalings was gedoen vir ’n annulus, asook sirkelvormige-, trapesiumvormige-, reghoekige- en driehoekige kanale. Spesiale klem was geplaas op trapesiumvormige kanale aangesien daar tot op datum slegs ’n beperkte aantal studies op hierdie tipe kanale gedoen is. Geen studies is in die literatuur gevind waar die waardes vir ’n trapesium met behulp van die eindige element metode bepaal is nie.

’n Uitstekende ooreenkoms was gevind toe die bepaalde waardes met dié in die literatuur vergelyk was. Oor die algemeen het die ooreenstemming van die waardes, wat met behulp van twee-dimensionele C++ programme bepaal is, verbeter namate die aantal elemente vermeerder is. Die gevolgtrekking was dus gemaak dat die metodes wat gebruik was om wrywings faktore en Nusseltgetalle in hierdie studie te bepaal, baie akkuraat en bruikbaar is.

Sleutelwoorde

Wrywingsfaktore

Nusseltgetalle

Laminêre vloei

Eindige elemente

Konstante hitte-oordrag

Konstante oppervlaktemperatuur

ACKNOWLEDGEMENTS

The author of this thesis would like to thank:

- Prof. Jat du Toit, for his insight, enthusiasm and support which inspired me to finish this study;
- my father, Daan Venter for his enthusiasm, support and technical assistance which was of great help;
- my wife, Jeanne-Marie for her love and support;
- the rest of my family (mother Sylvia, and my siblings Nadia, Philip and Brianda), for their love and support; and
- my sponsors, Sasol and Thrip, who made it possible for me to study fulltime.

To God, our loving Father and Saviour, all the honour. He gave me the strength and determination to complete this dissertation successfully.

TABLE OF CONTENTS

ABSTRACT i

OPSOMMING ii

ACKNOWLEDGEMENTS iii

TABLE OF CONTENTS iv

NOMENCLATURE vii

LIST OF FIGURES xiii

LIST OF TABLES xiv

1. Introduction 1

1.1. Background 1
1.2. Duct shapes to be investigated in this study 2
1.3. Scope of this study 4
1.4. C++ programs 4
1.5. Document overview 5
1.6. Summary 7

2. Literature study 8

2.1. Research overview 8
2.2. Fully developed laminar flow 15
2.3. The Galerkin weighted – residual method 16
2.4. Stokes' viscosity law 17
2.5. Conservation laws 18
2.5.1. Conservation of mass 18
2.5.2. Conservation of momentum 19
2.5.3. Conservation of energy 21
2.6. Computational fluid dynamics (CFD) 22
2.6.1. Finite difference method 23
2.6.2. Finite element method 26
2.6.3. The finite volume method 31
2.6.4. Properties of numerical solution methods 33
2.7. C++ programming language 35
2.8. Summary 35

3. The governing equations 37

3.1. One-dimensional governing equations 37
3.2. Two-dimensional governing equations 38
3.3. Constant wall heat flux versus constant wall temperature 39
3.4. Summary 39

4. Analytical equations for calculating Nusselt numbers and friction factors 40

4.1. Nusselt number for a circular duct (H1) 40
4.2. Nusselt number for a circular duct (T) 42
4.3. Friction factor for a circular duct (H1 or T) 43

4.4. Nusselt number for an annular duct with constant heat transfer at the one wall whilst the other wall has no heat transfer 44
4.5. Nusselt number for an annular duct (H1) 48
4.6. Nusselt number for an annular duct (T) 49
4.7. Friction factor for an annular duct (H1 or T) 50
4.8. Summary 50
5. One-dimensional numerical solution: finite element formulation 52
5.1. Finite element formulation 52
5.2. Nusselt number for a circular duct (H1) 55
5.2.1. Wall temperature (T_o) and the temperature gradient $\left(\frac{\partial T}{\partial z}\right)$ are known 56
5.2.2. The uniform heat flux $\left(\overline{q}_o^{"}\right)$ and reference temperature (T_o) at the wall are known 57
5.3. Nusselt number for a circular duct (T) 58
5.4. Friction factor for a circular duct (H1 or T) 58
5.5. Nusselt numbers for an annular duct (H1) 59
5.5.1. Inner (T_i) wall temperatures, outer (T_o) wall temperatures and the temperature gradient $\left(\frac{\partial T}{\partial z}\right)$ known 59
5.5.2. Inner $\left(\overline{q}_i^{"}\right)$ wall heat flux, outer wall heat flux $\left(\overline{q}_o^{"}\right)$ and the outer wall temperature (T_o) known 61
5.5.3. Inner $\left(\overline{q}_i^{"}\right)$ wall heat flux, outer wall temperature (T_o) and the temperature gradient $\left(\frac{\partial T}{\partial z}\right)$ known 61
5.5.4. Outer $\left(\overline{q}_o^{"}\right)$ wall heat flux, inner wall temperature (T_i) and the temperature gradient $\left(\frac{\partial T}{\partial z}\right)$ are known 62
5.6. Friction factor for an annular duct (H1 or T) 63
5.7. Influence coefficients (Nu_{ii}, Nu_{oo}, θ_i^* and $\theta_o^{"}$) for an annulus with constant heat flux at both walls (with $\overline{q}_i^{"}$, $\overline{q}_o^{"}$ and T_o known) 63
5.8. A list of Nu_i and Nu_o at different radius ratios, with constant surface temperature at one wall whilst the other wall has no heat transfer (with T_i, T_o and $\left(\frac{\partial T_m}{\partial z}\right)$ known) 65
5.9. Explicit and implicit computations for a T boundary condition 66
5.10. Summary 67
6. Two-dimensional numerical solution: finite element formulation 68
6.1. Finite element formulation 68
6.2. Create the mesh of the domain 72
6.3. Two-dimensional finite element program 77
6.4. Friction factor and Nusselt numbers for a duct that has an inner and outer boundary (H1) 85
6.5. Friction factor and Nusselt number for a duct that has only an outer boundary (H1) 89
6.6. Friction factor and Nusselt numbers for a duct that has an inner and outer boundary (T) 90
6.7. Friction factor and Nusselt number for a duct that has only an outer boundary (T) 91

6.8. Friction factor and Nusselt numbers for a duct with one boundary at constant surface temperature whilst the other boundary has no heat transfer 92
6.9. Summary 93
7. Comparing the one- and two-dimensional results with known values 94
7.1. Comparisons for a circular duct 94
7.2. Comparisons for annular ducts 96
7.3. Comparisons for trapezoidal ducts 100
7.4. Comparisons for a square duct 102
7.5. Comparisons for a rectangular duct 104
7.6. Comparisons for a triangular duct 106
7.7 Friction factor and Nusselt numbers for annular ducts 108
7.8. Friction factors and Nusselt numbers for trapezoidal ducts 114
7.9. Summary 120
8. Discussion and Conclusions 123
Bibliography 125
Appendix A: Literature study 131

NOMENCLATURE

a_i	Gaussian weighting factor
a	Top side length of trapezium or rectangle
b	Height of trapezium or rectangle
c_p,	Specific heat
c_j	Coefficient for the Galerkin method
$d\vec{A}$	Area vector
ds	Length of a boundary node
e	Energy stored per unit mass
f	Dimensionless Moody friction factor
f	Perimeter average Fanning friction factor
gz	Potential energy
h	Element contribution
h	Heat transfer coefficient
h	Spacing between two consecutive points
$\left[\bar{h}\right]$	Element contribution matrix
k	Thermal conductivity
k	Current iteration value
k_{eff}	Effective thermal conductivity
k_e	Eddy thermal conductivity of liquid metal
m	Number of points in the domain
$\dot{m}$	Mass flow
p	Pressure
q''	Heat-transfer per unit area
$q_i^{''}$	Heat flux on the inner boundary
$\bar{q}_i^{''}$	$-q_i^{''}$
$q_o^{''}$	Heat flux on the outer boundary
$\bar{q}_o^{''}$	$-q_o^{''}$
$q_w^{''}$	Heat flux at wall
$q(x,t)$	Grid point at x at time t

$\{\bar{q}''\}$	Vector that incorporates the unknown heat flux values multiplied by associated lengths (ds) for all the boundary nodal points and multiplied with (-1)
r	Radius
r_i	Inner annulus radius
r_o	Outer annulus radius
s_{BTot_i}	Total inner boundary length
s_{BTot_o}	Total outer boundary length
$s\bar{q}''_{tot_i}$	Total inner boundary heat flux multiplied with associated boundary length
$s\bar{q}''_{tot_o}$	Total outer boundary heat flux multiplied with associated boundary length
sT_{BTot_i}	Sum of all the temperature values multiplied by the associated lengths for the inner boundary nodes
sT_{BTot_o}	Sum of all the temperature values multiplied by the associated lengths for the outer boundary nodes
$s\bar{\tau}_{tot}$	Total boundary shear stress multiplied with associated boundary length
t	Certain period
t_{n+1}	Next time step after time t_n
u	Internal energy
u	Velocity in the x direction
$\bar{u}$	Approximate solution for a differential equation
v	Suitable weighting function
v	Volume
v	Velocity in the y direction
w	Axial velocity
w	Arbitrary weighting function
w_k	Arbitrary weighting function at point k
w_m	Mean velocity
w^N	Finite element approximations for the axial velocity distribution
x_0	Essential boundary condition
$y(x)$	Unknown function

$\vec{B}$	Body force distribution vector
C_i	The ith grid cell
CS	Closed surface
CV	Control volume
D	Diameter
D_h	Hydraulic diameter
E	Energy in the system
E	Number of elements in the mesh
$\{F\}$	Source vector
F_x,	Body force in the x direction
F_y	Body force in the y direction.
$F_{i-0.5}^{n}$	Approximation for the average flux at $x = x_{i-0.5}$
$\overline{G}\left(\overline{Y}\right)$	Vector function
$\overline{H}$	Global coefficient matrix
H1	Constant heat flux at the wall around the computational boundaries and also in the axial direction
J_e	Jacobian
$\overline{J}\left(\overline{Y}_k\right)$	Tridiagonal matrix
K	Value of conductivity
$[K]$	Coefficient matrix
L	Domain length
N	Number of global nodes
N_i	Function of the nodal points
NB	Number of nodal points on the boundary
NBi	Number of nodal points on the inner boundary
NBo	Number of nodal points on the outer boundary
NE	Number of nodal points associated with an element
NG	Number of Gauss/integration points
Nu	Nusselt numbers
Nu_{ii}	Nusselt number at the inner wall with constant heat transfer at the inner wall and no heat transfer at the outer wall

Nu_{oo}	Nusselt number for the outer wall, with constant heat transfer at the outer wall and no heat transfer at the inner wall
P	Perimeter length
Pr	Prandtl number
Q	Heat added to the system
Q_o	Natural boundary condition
Q_i^n	Approximate value for $q(x,t)$
R	Residual due to an approximation
Re_D	Reynolds number for a circular duct
RE	Relevant elements associated with node I
S	Source term
T	Constant surface temperature at the wall around the computational boundaries and also in the axial direction
T	Temperature
T_i	Inner wall surface temperature
T_m	Bulk temperature
T_{m_i}	Mean inner boundary temperature
T_{m_o}	Mean outer boundary temperatures
T_o	Outer wall surface temperature
T_s	Wall temperature
T^N	Finite element approximation for the temperature distribution
$\vec{T}^*$	Surface force distribution vector
$\{U\}$	Solution vector
V	Velocity component
$\vec{V}$	Velocity vector
W	Work done on the system
$\left(\overline{Y}_0\right)$	Starting vector
Z	Numerical flux function
α_1	Triangle's bottom left angle
α_2	Triangle's bottom right angle

δx	width of the elemental area
δy	height of the elemental area
ε_H	Eddy diffusivity of heat
ε_M	Eddy diffusivity of momentum
ϕ_J	Trail or basis function
φ	Velocity potential
γ	Aspect ratio
η	Gaussian integration point or natural coordinate
μ	Dynamic viscosity
θ	Base angle
θ_i^*	Influence coefficient used to adjust Nu_{ii}
θ_o^*	Influence coefficient used to adjust Nu_{oo}.
ρ	density
σ_x	Compressive stress in the x direction
σ_y	Compressive stress in the y direction
$\{\bar{\tau}\}$	Vector that incorporates the values of unknown shear stress values multiplied by the associated lengths for the boundary nodes and multiplied with (-1)
τ_i	Inner wall shear stress
$\vec{\tau}_i$	$-\tau_i$
τ_o	Outer wall shear stress
$\vec{\tau}_o$	$-\tau_o$
τ_w	Wall shear stress
τ_{ij}	Viscous stress component
τ_{xy}	Shear stress in the y direction
τ_{yx}	Shear stress in the x direction
υ	Kinematic viscosity
ξ	Gaussian integration point or natural coordinate
ψ_i	Interpolation (shape) function at the given Gauss point

ψ_j^e	Element interpolation function associated with the element node j
Δx	Cell length
Δt	Step length
Φ_J	Global interpolation function associated with the global node J
Ω	Whole domain
Γ	Boundary of problem domain
$^1/_4 f\mathrm{Re}$	Friction factors
b/a	Aspect ratio
$\frac{r_i}{r_o}$	Radius ratio
$\frac{\partial p}{\partial z}$	Axial pressure gradient
$\frac{\partial T}{\partial z}$	Axial temperature gradient
$\left(\frac{V^2}{2}\right)$	Kinetic energy

LIST OF FIGURES

Figure 2.1. Boundary-layer growth at the entrance of a well-rounded pipe (Shames, 2003:406). 16
Figure 2.2. Elemental area with flow through it. 18
Figure 2.3. Stress notation on a two-dimensional elemental area. 19
Figure 2.4. Basic concepts of the finite element method. 27
Figure 2.5. An element with eight nodal points. 28
Figure 6.1. Triangle divided into three blocks. 73
Figure 6.2. A block divided into four elements by using natural coordinates. 73
Figure 6.3. Boundary line divide into two element lines. 74
Figure 6.4. A block with nodal point numbering for an eight-node quadrilateral finite element. 74
Figure 6.5. A Block with nodal point numbering for a nine-node quadrilateral finite element. 79
Figure 7.1. Circular duct divided into five blocks. 95
Figure 7.2. Circular duct divided into 20 elements. 95
Figure 7.3. An annulus with its inner and outer radius. 97
Figure 7.4. A trapezium. 101
Figure 7.5. A square divided into 16 elements. Note that each element is defined by nine nodal points. 103
Figure 7.6. A rectangular duct with variables *a* and b. 105
Figure 7.7. A triangle with its left (α_1) and right (α_2) base angles. 106
Figure 7.8a. Friction factor and influence coefficients for an annular duct, subjected to constant heat flux, versus radius ratio (from Table 7.12) 111
Figure 7.8b. Influence coefficients for an annular duct, subjected to constant heat flux, versus radius ratio (from Table 7.12). Results shown for $r_i/r_o \geq 0.25$. 111
Figure 7.9a. Nu_{ii} (H1) and Nu_{oo} (H1) versus radius ratio, for an annular duct subjected to equal heat transfer at the inner and outer boundaries (from Table 7.12) 113
Figure 7.9b. Nu_{oo} (H1) versus radius ratio, for an annular duct subjected to equal heat transfer at the inner and outer boundaries (from Table 7.12). Results shown for $r_i/r_o \geq 0.35$. 113
Figure 7.10. Nu_i (H1) versus Base angle, for a trapezoidal duct, subjected to different aspect ratios (from Tables 7.13 – 7.17). 118
Figure 7.11. Nu_i (T) versus Base angle, for a trapezoidal duct, subjected to different aspect ratios (from Tables 7.13 – 7.17). 118
Figure 7.12. ¼ *f*Re versus base angle, for a trapezoidal duct, subjected to different aspect ratios (from Tables 7.13 – 7.17). 119
Figure 7.13. This figure illustrates the hyperbolic relationships between *Nu* (H1), *Nu* (T), ¼ *f*Re and different *b*/*a* ratios (at 20º base angle) of trapezoidal ducts. 119

LIST OF TABLES

Table 1.1 List of Nusselt numbers and friction factors for the duct shapes to be investigated (Shah & London, 1978: 200-394). 3
Table 2.1 Friction factors and Nusselt numbers for a trapezium (H1) (Shah and London, 1978:259). 14
Table 2.2 Friction factors and Nusselt numbers for a trapezium with a 60^o base angle at different grid sizes, and $b/a = 1$ (Yuan *et al*., 2001:4052)..... 15
Table 4.1. Inner and outer Nusselt numbers for annular ducts with constant heat transfer at one wall whilst the other wall has no heat transfer (Dwyer, 1963b:337). 48
Table 7.1. Comparing the computed Nusselt numbers (*Nu* (H1) and *Nu* (T)) and friction factors with published values for circular ducts. 96
Table 7.2. Comparing the computed Nusselt numbers and friction factors to published values. All these values were obtained for annular ducts with one wall at constant surface temperature, whilst the other wall was adiabatic and $r_i/r_o = 0.5$. 98
Table 7.3. Comparing the computed Nusselt numbers (Nui and Nuo) and friction factors with published values. All these values were obtained for annular ducts subjected to a constant heat flux at the walls, and $r_i/r_o = 0.6$. 99
Table 7.4. Comparing the computed Nusselt numbers (Nu_i and Nu_o) and friction factors with published values. All these values were obtained for annular ducts subjected to a constant surface temperature at the walls, and $r_i/r_o = 0.5$. 100
Table 7.5. Comparing the computed Nusselt numbers (*Nu* (H1) and *Nu* (T)) and friction factors with published values for trapezoidal ducts ($b/a = 1$ and $\theta = 45^o$). 101
Table 7.6. Comparing the computed Nusselt numbers (*Nu* (H1) and *Nu* (T)) and friction factors with published values for trapezoidal ducts ($b/a = 1$ and $\theta = 60^o$). 102
Table 7.7. Comparing the computed Nusselt numbers (*Nu* (H1) and *Nu* (T)) and friction factors with published values for square ducts. 104
Table 7.8. Comparing the computed Nusselt numbers (*Nu* (H1) and *Nu* (T)) and friction factors with published values for rectangular ducts ($b/a = 1/4$). 105
Table 7.9. Comparing the computed Nusselt numbers (*Nu* (H1) and *Nu* (T)) and friction factors with published values for triangular ducts ($\alpha_1 = \alpha_2 = 60^o$). 107
Table 7.10. Computed Nusselt numbers (*Nu* (H1) and *Nu* (T)) and friction factors for rectangular- ($b/a = 1/4$), trapezoidal- ($b/a = 1/4$ and $\theta = 60^o$) and triangular ducts ($\alpha_1 = \alpha_2 = 60^o$). 108
Table 7.11. Computed Nusselt numbers and friction factors for annular ducts with various radius ratios. All these values were obtained for annular ducts with one wall at constant surface temperature whilst the other wall was not subjected to heat flux. 109
Table 7.12. Computed influence coefficients, Nusselt numbers and friction factors for annular ducts with various radius ratios, subjected to the H1 boundary condition. 110
Table 7.13. Computed Nusselt numbers and friction factors for trapezoidal ducts with different base angles and $b/a = 1/4$. 114
Table 7.14. Computed Nusselt numbers and friction factors for trapezoidal ducts with different base angles and $b/a = 1/2$. 115
Table 7.15. Computed Nusselt numbers and friction factors for trapezoidal ducts with different base angles and $b/a = 1$. 115
Table 7.16. Computed Nusselt numbers and friction factors for trapezoidal ducts with different base angles and $b/a = 2$. 116
Table 7.17. Computed Nusselt numbers and friction factors for trapezoidal ducts with different base angles and $b/a = 4$. 116

1. Introduction

1.1. Background

Heat exchangers play a crucial role in our modern society. Nuclear and coal power stations would have been very inefficient or impossible to operate if it were not for heat exchangers.

Open cycle power stations employ heat exchangers to increase their efficiency by preheating the incoming fluid/gas with the excess heat in the cycle. On the other hand, closed cycle power stations use heat exchangers to decrease the temperature of the final fluid/gas so that it can be re-used in the cycle.

Heat exchangers are generally classified into three groups (Rousseau, 2007:42-85):

- Compact heat exchangers: they consist of plates with some form of corrugated surface pattern, which form narrow passages for flow.
- Finned-tube heat exchangers: they consist of expanded round tubes in a block of parallel continuous fins, with flow (usually liquid) through the tubes and flow (usually gas) over the tubes.
- Shell-and-tube heat exchangers: they consist of a shell with tubes inside the heat exchanger. In these exchangers a liquid/gas flows through the tubes, whilst another liquid/gas flows over the tubes, located inside the shell.

For a recuperative gas turbine cycle, heat exchangers have the ability to increase the thermal efficiency with up to 40% for an open cycle and as much as 60% for a combined cycle (Aquaro & Pieve, 2007:391).

The determination of the wall shear stress and the heat flux at the wall of a duct is of utmost importance in the analysis and design of applications such as heat exchangers (Du Toit, 2002b:201). The friction factors (¼ fRe[1]) and Nusselt numbers (Nu) are used to calculate the friction coefficients and the heat transfer coefficients, which are then used to calculate the wall shear stresses and the heat fluxes.

[1] In this study ¼ f Re denotes the friction factor, whilst some authors use f Re.

Friction factors and Nusselt numbers depend to a great extent on the particular shape of the duct in question. Annular or circular duct shapes are usually used in heat exchangers, but this does not mean that ducts with other shapes may not be used. For example, hexagonal duct shapes are encountered in lamella type compact heat exchangers, which are used in pulp and paper, alcohol, petrochemical and chemical industries. Trapezoidal duct shapes are used in plate-fin heat exchangers and in micro-channel electronic cooling modules (Sadasivam *et al*., 1999:4321-4322).

The so-called circular tube thermal entrance problem (also known as the Graetz problem), was first investigated by Graetz in 1883, and then later (independently) by Nusselt in 1910. These two heat transfer theory pioneers evaluated the first three terms of an infinite series solution for hydrodynamically developed and thermally fully developed flow for the constant surface temperature boundary condition. Their asymptotic Nusselt number for fully developed flow was calculated as $Nu = 3.66$, which is very close to the more accurate $Nu = 3.6567935$ (for negligible axial heat conduction, viscous dissipation, and thermal energy sources within the fluid) (Shah & London, 1978:79).

In principle, the volume flux, velocity distribution, friction factor and Nusselt number can be solved analytically for laminar flow in the cross section of any duct. But as the duct's cross section becomes more complex, the analytical solution also becomes more complex, or even impossible to solve. For this reason these parameters must be determined numerically (Du Toit, 2002a: 397).

The wall shear stresses and the heat fluxes are often determined by differentiating the numerical solution (for example, the finite element solution) and evaluating the required quantities from the derivatives, which is part of the post processing of the solution. The wall stresses and heat fluxes may also be determined by performing a secondary computation by using the assembled linear finite element equations. The latter procedure has been shown to be very accurate and has high rates of convergence for the fluxes. This procedure requires some extra computation, because the previously computed stiffness and forcing contributions can be preassembled and used directly in the flux projection. This boils down to a partitioning of the original system of assembled finite element equations (Du Toit, 2002a: 398).

1.2. Duct shapes to be investigated in this study

The different duct shapes to be investigated are:

- Circular pipe

- Annulus
- Trapezium
- Square
- Rectangle
- Triangle

Table 1.1 shows a list of friction factors and Nusselt numbers, as reported in the literature, for the above mentioned ducts (Shah & London, 1978: 200-394). The Nusselt numbers are given for boundaries subjected to a constant heat flux (H1) or a constant surface temperature (T) around the computational boundaries and also in the axial directions.

Table 1.1 List of Nusselt numbers and friction factors for the duct shapes to be investigated (Shah & London, 1978: 200-394).

Duct shape	***Nu* (H1)**	***Nu* (T)**	**¼ *f*Re**
Circular pipe	4.364	3.657	16.000
Trapezium ($\frac{b}{a}=1$, and θ = 45°)	3.268		13.827
Trapezium ($\frac{b}{a}=1$, and θ = 60°)	3.495		14.151
Square	3.60795	2.976	14.22708
Rectangle (with $\frac{b}{a}=\frac{1}{4}$)	5.33106	4.439	18.23278
Triangle (with $\alpha_1 = \alpha_2$ = 60°)	3.111	2.47	13.333
	Nu_i	Nu_o	**¼ *f*Re**
Annulus: one wall at constant surface temperature whilst the other wall has no heat transfer, $\left(\frac{r_i}{r_o}=0.5\right)$.	5.7382	4.4293	23.813
Annulus: uniform heat flux at both walls, $\left(\frac{r_i}{r_o}=0.5\right)$.	9.979	7.185	23.813
Annulus: constant surface temperature at both walls, $\left(\frac{r_i}{r_o}=0.5\right)$	9.441	6.401	23.813

The parameters r_i, r_o, b, a, θ, α_1 and α_2 are the inner annulus radius, outer annulus radius, height of trapezium or rectangle, top side length of trapezium or rectangle, trapezium's base angles, triangle's bottom left angle, and triangle's bottom right angle respectively. See Figures 7.2, 7.3, 7.5 and 7.6 in Chapter 7.

The Nusselt numbers and friction factors will be determined for all these duct shapes, mentioned in Table 1.1, by employing a finite element program (written in C++).

1.3. Scope of this study

The aim of this study is to investigate the friction factors and Nusselt numbers for fully developed laminar flow in a variety of duct shapes, by programming a finite element research code in C++. The investigation will be performed on circular, annular, triangular, rectangular and trapezoidal duct shapes. Special emphasis will be placed on trapezoidal duct shapes.

If the friction factors and Nusselt numbers are, however, determined successfully for these duct shapes, then it would also be possible to determine the shear stresses and heat fluxes of these ducts at the wall. The obtained results may then be used in the analysis and design of any application that requires one or more of these duct shapes.

1.4. C++ programs

C++ programs will be employed in this study to solve the one- and two-dimensional fully developed laminar flow in ducts, and to determine the friction factors and Nusselt numbers applicable to these ducts.

An existing C++ program that only solves one-dimensional flow in a circular or an annular duct and computes the friction factor and Nusselt numbers, for walls subjected to a constant heat flux, will be extended and modified in order to also solve and compute the cases listed below.

- Nusselt number and friction factor for a circular duct, subjected to a constant heat flux at the wall, and different sets of input data.
- Nusselt number and friction factor for a circular duct, subjected to a constant surface temperature at the wall.

- Nusselt numbers and friction factor for an annular duct, subjected to a constant heat flux at the walls, and different sets of input data.
- Nusselt numbers and friction factor for an annular duct with one wall subjected to a constant surface temperature whilst the other wall is adiabatic.
- The influence coefficients that may be used to determine the Nusselt numbers for an annular duct subjected to constant heat fluxes at the walls.

An existing Fortran program that only solves two-dimensional flow and computes the friction factor and Nusselt number for a duct that has only an outer wall, which is subjected to a constant heat flux, will be rewritten in C++ after which it will be extended and modified in order to solve and compute the following.

- Nusselt numbers and friction factor for a duct that has an inner and an outer boundary and where each of these boundaries are subjected to a constant heat flux.
- Nusselt number and friction factor for a duct that has only an outer boundary and where this outer boundary is subjected to a constant heat flux.
- Nusselt numbers and friction factor for a duct that has an inner and outer boundary and where each of these boundaries are subjected to a constant surface temperature.
- Nusselt number and friction factor for a duct that has only an outer boundary and where this outer boundary is subjected to a constant surface temperature.

The finite element formulations, as well as the friction factor and Nusselt number equations that were used in the C++ programs are discussed in Chapters 5 and 6.

1.5. Document overview

The following chapters are included in the remainder of the document:

- Chapter 2:

  Literature study.

- Chapter 3:

  The one- and two-dimensional governing equations, which are used in the finite element method to solve for fully developed laminar flow, are discussed in this chapter.

- Chapter 4:

  The analytical solutions for Nusselt numbers and friction factors, which were reported in the literature for annular and circular ducts, are discussed in this chapter.

- Chapter 5:

  This chapter describes the finite element computations which were used, in the one-dimensional C++ programs, to determine the Nusselt numbers and friction factors for one–dimensional fully developed laminar flow in annular and circular ducts. The computations are described for boundaries that are subjected to a constant heat flux or a constant surface temperature.

- Chapter 6:

  In this chapter it is described how two-dimensional domains are meshed with the C++ mesh program. Finite element computations for two-dimensional fully developed laminar flow are also described. The latter are used in the two-dimensional C++ programs to determine the Nusselt numbers and friction factors for two–dimensional domains. The computations are described for boundaries that are subjected to a constant heat flux or a constant surface temperature.

- Chapter 7:

  In this chapter one- and two-dimensional C++ results are compared with the values reported in the literature.

- Chapter 8:

  The final conclusions and recommendations are given in this chapter.

- Appendix A:

  Short descriptions are given of relevant articles that were used or studied during the literature survey.

1.6. Summary

The friction factors and Nusselt numbers are used to compute the friction coefficients and the heat transfer coefficients. These are then used to determine, for example, the wall shear stress and the heat flux in the heat exchanger. Friction factors and Nusselt numbers are very much dependant on the shape of the duct.

The different shapes that will be investigated are: circular-, annular-, trapezoidal-, rectangular-, triangular- and square ducts.

In the next chapter the literature study concerning Nusselt numbers, friction factors and different numerical methods that may be used to solve for flow in ducts will be discussed.

2. Literature study

An introduction was given in the previous chapter, stating the purpose of Nusselt numbers and friction factors. In the current chapter an overview is given of some of the numerous articles, about Nusselt numbers and friction factors, reported in the literature. Fully developed laminar flow, governing equations which are used to describe the flow, numerical methods used to solve the governing equations, the properties of these equations, as well as their advantages and disadvantages are discussed.

2.1. Research overview

This study will concentrate on the computation of the Nusselt numbers and friction factors for one- and two-dimensional fully developed laminar flow in ducts. The computations will be performed for two different boundary conditions: 1) a constant surface temperature or, 2) a constant heat flux around the computational boundary and also in the axial direction of the duct in question. These conditions are, however, not the only boundary conditions that may prevail. The other possible boundary conditions that may be important, are (Shah & London, 1978:20-21):

- constant axial wall temperature subjected to a finite normal wall thermal resistance,
- nonlinear radiant-flux at the boundary,
- constant axial wall heat flux as well as peripheral wall heat flux,
- constant axial wall flux subjected to finite normal wall thermal resistance,
- constant axial wall flux subjected to finite peripheral wall heat conduction,
- exponential axial wall heat flux, and
- constant axial wall to fluid bulk temperature difference.

Circular and annular shaped ducts are the only shapes that can be analysed in one-dimension. It is thus no surprise that these are the only duct shapes for which analytical solutions are given that may be used to calculate Nusselt numbers and friction factors. Analytical solutions for circular (Incropera & De Witt, 2005:507) and annular ducts (Dwyer, 1963b:337) only exist for the H1 boundary condition. The Nusselt numbers can only be solved iteratively (Incropera & De Witt, 2005:507), (Kays,

1966:110), (Shah & London, 1978:286), or with an infinite series (Kays & Crawford, 1993:117) when circular ducts are subjected to the T boundary condition. The Nusselt numbers can not be obtained analytically for annular ducts, subjected to constant but unequal heat fluxes at the walls, without a trial and error approach (Dwyer, 1963a:55). Irregular duct shapes can only be solved by means of numerical methods.

A considerable amount of work has been done on laminar forced-convective heat transfer for different duct shapes. Numerous studies for calculating Nusselt numbers and friction factors have been reported for the H1 and/or T boundary conditions for circular-, annular-, triangular-, square- and rectangular duct shapes (Incropera & De Witt, 2005), (Kakac *et al*., 1983), (Kays, 1966), (Kays & Crawford, 1993), (Kays & London, 1984), (Shah & London, 1978). It should be noted that Nusselt numbers and friction factors depend on the particular duct shape (Erdogan & Imrak, 2005:87) and the boundary conditions which they are subjected to.

The cases listed below are som e examples of the numerous studies that mainly focussed on more specific matters.

- The effect of eccentricity and thermal boundary conditions on fully developed laminar flow in annular ducts were investigated numerically (Manglik & Fang, 1995:298-306). Large non-uniformities in the axial velocity and temperature fields were found when the eccentricities increased and the radius ratios decreased. The flow was found to stagnate in the narrow sections of the annulus while higher flow velocities were reached in the wider sections. Except for very high eccentricity values it was also found that higher heat transfer coefficients are sustained by the H1 condition relative to the T condition.
- The effect of fully developed laminar flow was described in annuli with very viscous Newtonian fluids (Coelho & Pinho, 2006:3349-3359) and non-Newtonian fluids (Escudier *et al*., 2002:52-73). Coelho and Pinho (2006:3349-3359) presented analytical solutions for Newtonian concentric annular flow that were obtained under imposed asymmetric constant wall heat fluxes as well as under imposed asymmetric constant wall temperatures, taking into account viscous dissipation and for fluid dynamic and thermally fully-developed conditions. Explicit equations for the inner and outer wall temperatures, the temperature profile, the mixing temperature and the inner and outer Nusselt numbers as functions of the radius ratio and the Brinkman number were given. Escudier *et al*. (2002:52-73) presented graphical results

(that were determined with a finite volume method) of the friction factors and other kinematic characteristics, which were obtained for the fully developed laminar flow of inelastic shear-thinning power-law fluids through eccentric annular ducts with inner-cylinder rotation. It was also pointed out by the authors that results found in the literature for this type of flow are incorrect. Some of the conclusions of Meuric *et al*. (1997:363-373) are misleading and some of the results of Beverly and Tanner (1992:85-115) are in error.

- Studies were conducted for circular and rectangular micro channels and micro tubes (Gamrat *et al*., 2005:2943-2954), (Koo & Kleinstreuer, 2004:3159-3169), (Lee *et al*., 2005:1688-1704), (Morini, 2005:3637-3647), (Tiselj *et al*., 2004:2551-2565). Gamrat *et al*. (2005:2943-2954) presented two- and three-dimensional numerical analyses of convective heat transfer in micro channels. It was found that the thermal entrance effects depend on the Reynolds number. It was further also shown that the experimental and numerical heat flux and temperature values correlated poorly for very small (0.1 mm spacing) rectangular micro channels. Koo and Kleinstreuer (2004:3159-3169) have investigated the effects of viscous dissipation on the temperature field and the friction factor using dimensional analysis and experimentally validated computer simulations. They found that the viscous dissipation in micro tubes and micro channels depends mainly on the Reynolds number, aspect ratio, Prandtl number, conduit hydraulic diameter and the Eckart number. Therefore, it is important to note that the accuracy of the simulation may be adversely affected if viscous dissipation is ignored. Lee *et al*. (2005:1688-1704) numerically investigated the laminar natural convection heat and mass transfer in open vertical rectangular ducts subjected to constant surface temperature or constant heat flux at the walls. They established that the simplified thin wall analysis can be used as a computationally economical alternative to a full three-dimensional conjugate analysis. Morini (2005:3637-3647) calculated the temperature distribution in the cross-section of a rectangular duct, under the conditions of Newtonian and incompressible fluid, fully developed laminar flow and steady state regime. They also reported that if the viscous heating and the consequent decrease of fluid viscosity is taken into account, then it is possible to explain the decrease of the friction factor when the Reynolds number increases. Tiselj *et al*. (2004:2551-2565) performed experimental and numerical analysis to evaluate the heat transfer characteristics of water flowing through triangular silicon micro channels. It was found that the bulk water temperature as well as the temperature of the heated wall do not change linearly along the

channel, and that the Nusselt number has a singular point where the difference between the temperatures on the wall and the bulk temperature becomes negative, whilst the flux changes sign.

- Studies conducted for rectangular ducts in the presence of magnetic fields (Teamah, 2008:237-248). Teamah (2008:237-248) studied the convective flow in a rectangular enclosure numerically with the upper and lower surfaces being insulated and impermeable. The left and right walls of the enclosure were subjected to a constant surface temperature. It was found that the strength of the magnetic field and the generation or absorption effect greatly influence the heat and mass transfer mechanism and flow characteristics inside the duct enclosure. It was also reported that the presence of a heat sink increases the Nusselt number whilst a heat source decreases the Nusselt number.

- Studies conducted on the flow through a square duct with a twisted tape insert (Ray & Date, 2003:889-902). Ray and Date (2003:889-902) presented the numerical prediction of the characteristics of laminar, as well as, turbulent flow and heat transfer in a square duct with a twisted tape insert, whose width equals the length of the duct size. They reported that the local laminar Nusselt number varied axially over the pitch for a 180^{o} rotation in a repetitive manner, and that the maximum local Nusselt number is to be found at the cross-section where the tape is aligned with the diagonal of the duct. The axial variation in the Nusselt number, for turbulent flow, was found to be insignificant.

Although many studies (for the circular-, annular, triangular-, square- and rectangular duct shapes) concentrated on laminar flow (Chen *et al*., 2000:209-224), (Du Toit *et al.,* 2000:154-159), (Lee, 1999:4523-4534), (Manglik & Fang, 1995:298-306), (Piva, 1995:815-824) (Syrjala, 2002:89-100), (Uzun & Unsal, 1997:835-848), (Yuan *et al*., 2001:4047-4058) the more complex turbulent flow also received attention (Promvonge & Eiamsaard, 2007:72-82), (Saini & Saini, 1997:973-986), (Wei *et al*., 2005:5284-5296), (Yu *et al*., 2005a:621-634), (Yucel & Dinler, 2006:195-214).

On the subject of flow, a large number of studies have been conducted (for the circular, annular-, triangular-, square- and rectangular duct shapes) on the less complex H1 boundary condition (Barletta, 2002:641-654), (Busedra & Soliman, 1999:527-544), (Du Toit *et al.,* 2000:154-159), (Manglik & Fang, 1995:298-306), (Ray & Date, 2003:889-902), (Syrjala, 1998:191-204), and probably just as much work was done on the more complex T boundary condition (Chen *et al*., 2000:209-224), (Lee *et*

al., 2005:1688-1704), (Sadasivam *et al*., 1999:4321-4331), (Sakalis *et al*., 2002:25-35), (Yuan *et al*., 2001:4047-4058).

Although some of the studies mentioned in the literature employed experimental methods (Lee *et al*., 2005:1688-1704), (Luo *et al*., 2004:5439-5450), (Promvonge & Eiamsaard, 2007:72-82), (Saini & Saini, 1997:973-986), (Tiselj *et al*., 2004:2551-2565), (Wu & Cheng, 2003:2519-2525), numerical methods were mostly employed, since it is much faster and produces results that correspond well with known values published in the literature.

The numerical methods used in the previous studies are:

- finite difference method (Busedra & Soliman, 1999:527-544), (Manglik & Fang, 1995:298-306), (Sadasivam *et al*., 1999:4321-4331), (Sakalis *et al*., 2002:25-35), (Teamah, 2008:237-248), (Uzun & Unsal, 1997:835-848),
- finite element method (Du Toit, 2002a:397-407), (Du Toit, 2002b:201-206), (Du Toit, 2003:50-55), (Du Toit, 2004b:1-16), (Syrjala, 2002:89-100), and
- finite volume method (Chen *et al*., 2000:209-224), (Du Toit *et al.,* 2000:154-159), (Escudier *et al*., 2002:52-73), (Ray & Date, 2003:889-902), (Rosaguti *et al*., 2006:2912-2923), (Valencia, 1995:47-58), (Yeh, 2002:775-784), (Yuan *et al*., 2001:4047-4058), (Yucel & Dinler, 2006:195-214).

In a large percentage of all the studies that used numerical methods specifically reference was made regarding the elegance and accuracy of these methods (Busedra & Soliman, 1999:527-544), (Chen *et al*., 2000:209-224), (Du Toit *et al.,* 2000:154-159), (Gamrat *et al*., 2005:2943-2954), (Lee *et al*., 2005:1688-1704), (Manglik & Fang, 1995:298-306), (Sadasivam *et al*., 1999:4321-4331), (Yu *et al*., 2005a:621-634), (Yu *et al*., 2005b:621-634),

Du Toit (2002a: 404-406) has shown that although the various published values for friction factors and Nusselt numbers are generally in good agreement with each other, there are also discrepancies between some of these published values. For example, in one case the friction factor and Nusselt number for a rectangular duct with a height-to-width ratio of 1:4 differs with 2.56% and 4.35% respectively from the exact values. This is acceptable from an engineering point of view, but from a scientific point of view these small discrepancies may be significant and even unacceptable. It has also been shown that these inaccurate values have been cited by more than one consecutive author.

It is clear from the literature that a large number of studies have been conducted on circular-, annular-, triangular-, square- and rectangular duct shapes, whilst relative few studies had been conducted on trapezoidal duct shapes. This study concentrates mainly on trapezoidal duct shapes and a thorough study regarding trapezoidal duct shapes was conducted.

A survey of the literature concerning trapezoidal duct shapes revealed among others the facts listed below.

- A study conducted by Sadasivam *et al*. (1999:4321-4331) on fully developed laminar flow in trapezoidal ducts subjected to the H1 or T boundary condition was done by using a finite difference method. In this study the following polynomial equation was employed to calculate the Nusselt number and the friction factor:

$$\frac{1}{4} f \,\mathrm{Re} \quad or \quad Nu = b_0\gamma^0 + b_2\gamma^2 + b_3\gamma^3 + b_4\gamma^4 + b_5\gamma^5 + b_6\gamma^6 + b_7\gamma^7$$

  where γ is the aspect ratio ($\gamma = b/a$, see Figure 7.4 in Section 7.3). The results obtained by means of this equation differs with less than 2.5% from results obtained with numerical methods. Every chosen base angle requires its own specific set of coefficients ($b_0 - b_7$) when calculating Nusselt numbers (one set for every boundary condition) and friction factors. Sadasivam *et al*. (1999:4321-4331) published the coefficients at base angles of 30^o, 45^o, 60^o and 75^o.

- An experimental study has been conducted by Wu and Cheng (2003:2519-2525) on the friction factors of laminar flow of deionised water in smooth trapezoidal silicon micro channels with different aspect ratios. The experimental data was found to be in good agreement with existing analytical solutions for incompressible fully developed laminar flow under no-slip boundary conditions for water in micro channels. It was also confirmed that the Navier-Stokes equations (see Section 2.5) are valid for the laminar flow of deionised water in smooth silicon micro channels having hydraulic diameters as small as 25.9 μm.

- Nusselt numbers and friction factors have been published by Shah and London (1978:256-260) for fully developed laminar flow in trapezoidal ducts for the H1 boundary condition. The values obtained for 30^o, 45^o, 60^o, 75^o and 85^o base angles and are given in Table 2.1 and will be compared in Section 7.8 with the values obtained in the current study .

Table 2.1 Friction factors and Nusselt numbers for a trapezium (H1) (Shah and London, 1978:259).

b/a	¼ fRe	Nu (H1)
$\theta = 85^o$		
∞	12.474	2.446
8	17.474	4.366
4	16.740	4.483
2	15.015	3.896
4/3	14.312	3.636
1	14.235	3.608
3/4	14.576	3.736
1/2	15.676	4.175
1/4	18.297	5.363
1/8	20.599	6.501
0	24.000	8.235

b/a	¼ fRe	Nu (H1)
$\theta = 45^o$		
∞	13.153	2.982
8	13.301	3.030
4	13.323	3.048
2	13.364	3.081
4/3	13.541	3.155
1	13.827	3.268
¾	14.260	3.469
½	15.206	3.888
¼	17.397	4.943
1/8	19.743	6.034
0	24.000	8.235

$\theta = 75^o$		
∞	13.065	2.910
8	14.907	3.520
4	14.959	3.720
2	14.340	3.610
4/3	14.118	3.542
1	14.252	3.594
3/4	14.697	3.766
1/2	15.804	4.219
1/4	18.313	5.371
1/8	20.556	6.482
	24.000	8.235

$\theta = 30^o$		
∞	12.744	2.680
8	12.760	2.697
4	12.782	2.704
2	12.875	2.736
4/3	13.012	2.821
1	13.246	2.919
¾	13.599	3.077
½	14.323	3.436
¼	16.284	4.349
1/8	18.479	5.569
0	24.000	8.235

$\theta = 60^o$		
∞	13.333	3.111
8	13.867	3.284
4	13.916	3.348
2	13.804	3.350
4/3	13.888	3.390
1	14.151	3.495
3/4	14.637	3.691
1/2	15.693	4.140
1/4	18.053	5.247
1/8	20.304	6.341
0	24.000	8.235

- Methods to calculate Nusselt number and friction factor values have been discussed and published by Yuan *et al*. (2001:4052) for fully developed laminar flow in trapezoidal ducts (with aspect ratio equals to one) subjected to the H1 or T boundary condition. These values were obtained for a 60^o base angle and at different grid sizes by employing the finite volume method (see Table 2.2). Note that the corresponding values in Tables 2.1 and 2.2 are not exactly the same. These differences may be due to different computational methods. It can be seen from Table 2.2 that the results converge as the grid size increases, and also that the results are more accurate for a finer grid.

Table 2.2 Friction factors and Nusselt numbers for a trapezium with a 60^o base angle at different grid sizes, and $b/a = 1$ (Yuan *et al*., 2001:4052)

Grid	¼ *f*Re	*Nu* (H1)	*Nu* (T)
90×30	14.281	3.450	2.813
120×40	14.255	3.454	2.816
150×50	14.237	3.457	2.819
180×60	14.223	3.459	2.821
210×70	14.213	3.461	2.822

An extensive literature study revealed that up to date only a limited number of studies have been done on trapezoidal duct shapes and that they were only performed for certain base angles. During this literature study no textbook or article could be found where the finite element technique has been used to determine the Nusselt numbers or friction factors for trapezoidal duct shapes.

2.2. Fully developed laminar flow

The condition that is reached within a pipe when viscous action has spread through the flow of the entire cross section of the pipe, resulting in an invariant velocity profile in the flow direction and straight parallel streamlines, is called fully developed laminar flow. Laminar flow prevails when the appropriate Reynolds number is smaller or equal to 2300 (Shames, 2003:406-407).

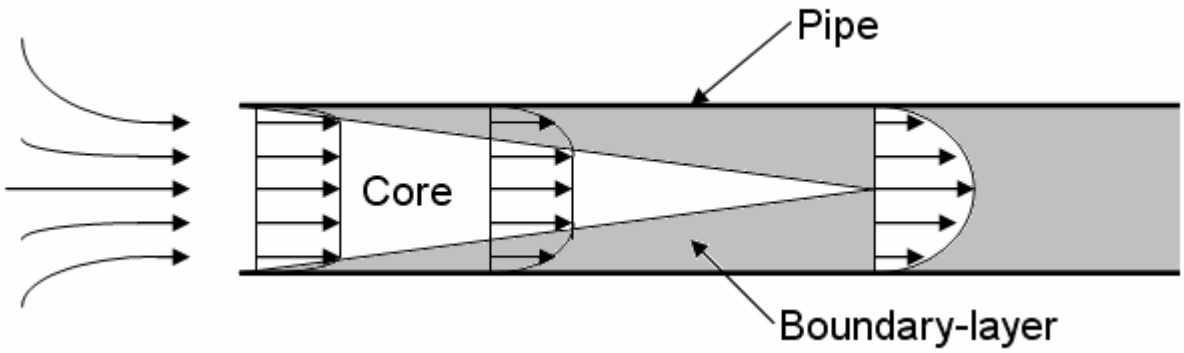

Figure 2.1. Boundary-layer growth at the entrance of a well-rounded pipe (Shames, 2003:406).

As illustrated in Figure 2.1, the flow in a pipe is initially inviscid and almost uniform, therefore, fully developed laminar flow is not present at the pipe entrance. This uniform region of the flow is called the core, and as can be seen in Figure 2.1 the core (the white area inside the pipe) shrinks as the viscous effects extend deeper into the flow. A laminar boundary layer (the grey area inside the pipe) begins to develop at the entrance of the pipe and it thickens downstream until the cross section consists entirely of this layer. Fully developed flow is achieved when the entire cross section is occupied by the laminar boundary layer (Shames, 2003:406-407). This study will only consider fully developed laminar flow in ducts.

2.3. The Galerkin weighted – residual method

The Galerkin method as described by Du Toit (1997:22-24).

The Galerkin method is used to find approximate solutions for differential equations from finite-dimensional subspaces of admissible functions. Consider the following differential equation:

$$u''(x) + u(x) = f(x) \qquad \text{for } 0 < x < L$$

with

$$u(0) = x_0, \qquad u''(L) = Q_0 \tag{2.1}$$

where x_0, Q_o and L refers to an essential boundary condition, a natural boundary condition and the domain length respectively.

The approximate solution $(\bar{u})$ must be of the form:

$$\bar{u} = \phi_0 + \sum_{j=1}^{n} c_j \phi_j \tag{2.2}$$

where ϕ_J represents the trail or basis functions and c_j the coefficients which are to be determined. The essential boundary conditions are satisfied with ϕ_0. The residual, which is the error (R) caused by the approximation, may be written as:

$$\bar{u}''(x) + \bar{u}(x) - f(x) = R \neq 0 \tag{2.3}$$

The residual will be equal to zero if $\bar{u} = u$. A set of arbitrary weighting functions (w) is used so that $R = 0$ in a weighted sense. For R to be equal to zero, it is necessary that the following should be true over the whole domain (Ω):

$$\int_{\Omega} wR \quad d\Omega = 0 \tag{2.4}$$

If the number of unknown parameters and the number of linear independent weighting functions are equal, then eq[2] (2.4) may be rewritten as:

$$\int_{\Omega} w_k R \; d\Omega = \int_{\Omega} w_k \left(\bar{u}''(x) + \bar{u}(x) - f(x)\right) d\Omega = 0 \qquad \text{k = 1, 2,....,s} \tag{2.5}$$

w_k (the arbitrary weighting function at point k) must be positive, single valued and finite. The Galerkin method is used in Du Toit's finite element formulation (see Section 2.6.2).

2.4. Stokes' viscosity law

Stokes' viscosity law as described by Du Toit (1997:20).

The Stokes' viscosity law is used to eliminate unknown viscous stress (τ_{ij}) components in any governing equation. For a Newtonian fluid it may be assumed that the viscous stresses are only proportional to the rate at which the deformation changes. The latter assumption simplifies the model to a great extent.

The Stokes' viscosity law for incompressible two-dimensional fluid flow is stated in Eqs (2.12), (2.13) and (2.14). By making use of these equations it would be possible to convert the momentum and energy equations (for fluid flow) into useful forms. The continuity, momentum and energy equations which will be discussed in Section 2.5 is referred to as the **Navier-Stokes equations**.

[2] The following abbreviations were used throughout this document: Eq for equation and Eqs for equations.

2.5. Conservation laws

The governing equations, namely conservation of mass, conservation of momentum and conservation of energy, that describe flow in a duct will now be discussed.

2.5.1. Conservation of mass

The conservation of mass as described by Van Zijl (1990:3-4).

According to the mass conservation law the increase in mass in an elemental area, over a certain time, is equal to the net flow of mass into the area during this period (t). A positive net flow results in an increase in density. Figure 2.2 illustrates the flow through an elemental area.

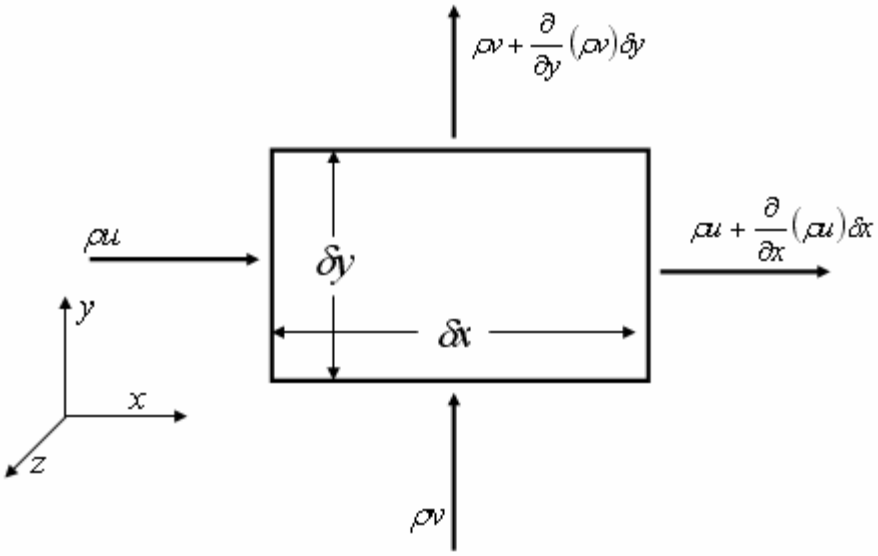

Figure 2.2. Elemental area with flow through it.

The governing equation of mass conservation for non-steady, compressible fluid flow can be obtained by equating the quantity of mass that enters and leaves the elemental area:

$$\frac{\partial \rho}{\partial t} = -\left[\frac{\partial}{\partial x}(\rho u) + \frac{\partial}{\partial y}(\rho v)\right] \tag{2.6}$$

where u, v, ρ, δx, and δy refers to the velocity in the x direction, velocity in the y direction, density, the width of the elemental, and the height of the elemental area respectively.

If the density is constant throughout the system, it means that the flow is incompressible and that Eq (2.6) will reduce to:

$$\frac{\partial u}{\partial x} + \frac{\partial v}{\partial y} = 0 \tag{2.7}$$

Eq (2.7) is referred to as the continuity equation. Note that this equation is only valid for incompressible two-dimensional flow.

2.5.2. Conservation of momentum

The conservation of momentum as described by Van Zijl (1990:4-6).

According to the conservation of momentum (Newton's second law) the time rate of change of the momentum is equal to the sum of all the forces acting on that system (see Figure 2.3).

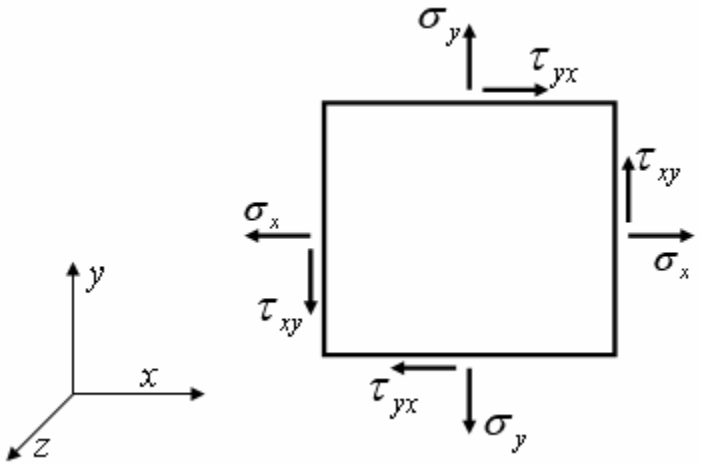

Figure 2.3. Stress notation on a two-dimensional elemental area.

Summing the forces on an elemental area and setting it equal to the rate of change, gives:

$$\rho \frac{du}{dt} = F_x - \frac{\partial p}{\partial x} + \frac{\partial \sigma_x}{\partial x} + \frac{\partial \tau_{yx}}{\partial y} \tag{2.8}$$

and

$$\rho \frac{dv}{dt} = F_y - \frac{\partial p}{\partial y} + \frac{\partial \sigma_y}{\partial y} + \frac{\partial \tau_{xy}}{\partial x} \tag{2.9}$$

where p, F_x, and F_y refers to the pressure, body force in the x direction and the body force in the y direction respectively. The acceleration in the x and y directions are given as:

$$\frac{du}{dt} = \frac{\partial u}{\partial t} + u\frac{\partial u}{\partial x} + v\frac{\partial u}{\partial y} \tag{2.10}$$

$$\frac{dv}{dt} = \frac{\partial v}{\partial t} + u\frac{\partial v}{\partial x} + v\frac{\partial v}{\partial y} \tag{2.11}$$

A linear relationship exists between the shear stress and the rate of deformation if a Newtonian fluid is incompressible. The stresses can now be written in terms of the rate of strain as:

$$\sigma_x = 2\mu\frac{\partial u}{\partial x} \tag{2.12}$$

$$\sigma_y = 2\mu\frac{\partial v}{\partial y} \tag{2.13}$$

$$\tau_{xy} = \tau_{yx} = \mu\left(\frac{\partial u}{\partial y} + \frac{\partial v}{\partial x}\right) \tag{2.14}$$

where μ, τ_{xy}, τ_{yx}, σ_x and σ_y respectively refers to the dynamic viscosity, shear stress in the y direction, shear stress in the x direction, compressive stress in the x direction and the compressive stress in the y direction.

Substituting Eqs (2.10), (2.11), (2.12), (2.13) and (2.14) into Eqs (2.8) and (2.9) give:

$$\rho\left(\frac{du}{dt} + u\frac{\partial u}{\partial x} + v\frac{\partial u}{\partial y}\right) = F_x - \frac{\partial p}{\partial x} + \mu\left(\frac{\partial^2 u}{\partial x^2} + \frac{\partial^2 u}{\partial y^2}\right) + \mu\frac{\partial}{\partial x}\left(\frac{\partial u}{\partial x} + \frac{\partial v}{\partial y}\right) \tag{2.15}$$

$$\rho\left(\frac{dv}{dt} + u\frac{\partial v}{\partial x} + v\frac{\partial v}{\partial y}\right) = F_y - \frac{\partial p}{\partial y} + \mu\left(\frac{\partial^2 v}{\partial x^2} + \frac{\partial^2 v}{\partial y^2}\right) + \mu\frac{\partial}{\partial y}\left(\frac{\partial u}{\partial x} + \frac{\partial v}{\partial y}\right) \tag{2.16}$$

Substituting eqs (2.7) into Eqs (2.15) and (2.16) give the following momentum equations:

$$\rho\left(\frac{du}{dt} + u\frac{\partial u}{\partial x} + v\frac{\partial u}{\partial y}\right) = F_x - \frac{\partial p}{\partial x} + \mu\left(\frac{\partial^2 u}{\partial x^2} + \frac{\partial^2 u}{\partial y^2}\right) \tag{2.17}$$

$$\rho\left(\frac{dv}{dt} + u\frac{\partial v}{\partial x} + v\frac{\partial v}{\partial y}\right) = F_y - \frac{\partial p}{\partial y} + \mu\left(\frac{\partial^2 v}{\partial x^2} + \frac{\partial^2 v}{\partial y^2}\right) \tag{2.18}$$

Eqs (2.17) and (2.18) are referred to as the Navier-Stokes equations. If a steady state situation prevails, Eqs (2.17) and (2.18) will reduce to:

$$\rho\left(u\frac{\partial u}{\partial x}+v\frac{\partial u}{\partial y}\right)=F_x-\frac{\partial p}{\partial x}+\mu\left(\frac{\partial^2 u}{\partial x^2}+\frac{\partial^2 u}{\partial y^2}\right) \tag{2.19}$$

$$\rho\left(u\frac{\partial v}{\partial x}+v\frac{\partial v}{\partial y}\right)=F_y-\frac{\partial p}{\partial y}+\mu\left(\frac{\partial^2 v}{\partial x^2}+\frac{\partial^2 v}{\partial y^2}\right) \tag{2.20}$$

Eqs (2.19) and (2.20) describe the conservation of momentum and is used in the numerical methods for solving the flow in a duct at steady state.

2.5.3. Conservation of energy

The conservation of energy as described by Du Toit (1997:18-20).

The conservation of energy (first law of thermodynamics) implies that the rate of change of the energy in a system is equal to the net rate of heat added plus the net rate of work done on the system:

$$\frac{DE}{Dt}=\frac{DQ}{Dt}-\frac{DW}{Dt} \tag{2.21}$$

with E, Q and W respectively the energy in the system, the heat added to the system and the work done on the system.

The following equation is obtained when inserting E into the Reynolds transport equation (Shames, 2003:144):

$$\frac{DE}{Dt}=\oiint_{CS}(e)\left(\rho\vec{V}\cdot d\vec{A}\right)+\frac{\partial}{\partial t}\iiint_{CV}(e)\rho\ dv \tag{2.22}$$

with CS, CV, $\vec{V}$, $d\vec{A}$, e and v respectively a closed surface, a control volume, the velocity vector, Area vector, the energy stored per unit mass and the volume. Energy stored per unit mass is the sum of the kinetic energy $\left(\frac{V^2}{2}\right)$, potential energy ($gz$) and the internal energy (u):

$$e=\frac{V^2}{2}+gz+u \tag{2.23}$$

The net work done on the system is a result of the total rate of flow work and the total rate of body force work:

$$\frac{dW}{dt} = \oiint_{CS} \vec{T}^* \cdot \vec{V} \; d\vec{A} + \oiiint_{CV} \vec{B} \cdot \vec{V} \rho \; dv \tag{2.24}$$

with $\vec{T}^*$ and $\vec{B}$ respectively the surface force distribution vector and the body force distribution vector.

The net heat added to the system is a result of the flux of energy through the CS and the source distribution inside the CV:

$$\frac{dQ}{dt} = -\oiint_{CS} q'' d\vec{A} + \oiiint_{CV} S\rho \; dv \tag{2.25}$$

with q'' and S respectively the heat-transfer per unit area and the source term.

Eq. (2.22) may now be rewritten as:

$$\oiint_{CS} (e)\left(\rho \; \vec{V} \cdot d\vec{A}\right) + \frac{\partial}{\partial t} \iiint_{CV} (e)\rho \; dv = -\oiint_{CS} q'' d\vec{A} + \oiiint_{CV} S\rho \; d + \oiint_{CS} \vec{T}^* \cdot \vec{V} \; d\vec{A} + \oiiint_{CV} \vec{B} \cdot \vec{V} \rho \; dv \tag{2.26}$$

After Eq (2.26) has been rewritten in index notation and gravity is included in the body force, the Cauchy equation is employed and the Gauss Law is used for the surface integrals. The resulting integrand may now be set equal to zero. After employing the continuity equation, Eq (2.7), and the Stokes' viscosity law the following energy equation is obtained:

$$\rho \; c_p \left(u \frac{\partial T}{\partial x} + v \frac{\partial T}{\partial y} \right) = k \left(\frac{\partial^2 T}{\partial x^2} + \frac{\partial^2 T}{\partial y^2} \right) + S + \mu \left(2 \left[\left(\frac{\partial u}{\partial x} \right)^2 + \left(\frac{\partial v}{\partial y} \right)^2 \right] + \left(\frac{\partial u}{\partial y} + \frac{\partial v}{\partial x} \right)^2 \right) \tag{2.27}$$

with c_p, k and T the specific heat, thermal conductivity and the temperature respectively. Eq (2.27) can be used to solve two-dimensional flow in a duct at steady state.

2.6. Computational fluid dynamics (CFD)

CFD is a computational technology used to predict heat transfer and fluid flow through computer simulations and it is, therefore, suitable for solving three-dimensional fluid flow problems. CFD works on the principal of solving the conservation (mass, momentum and energy) equations by means of numerical methods. The conservation equations are used to describe the fluid and physical dynamics,

of a specific situation, by employing coupled and partial differential equations. Since the finite volume method is inherently suitable to model fluid flow many commercial CFD codes use it for simulations, for example Star-CD, CFX and Fluent. The finite element and finite difference methods may also be used in CFD codes (Coetzee, 2005:1).

The finite volume CFD codes were originally based on structured orthogonal meshes that made use of straight forward indices as references to cells. The orthogonal meshes, however, have limited usefulness because they are limited to simple geometries. This problem was addressed by extending the finite volume method to include non-orthogonal structured meshes. With this inclusion it is now possible to solve the flow through complex geometries. Unfortunately, this modification came at a price: these meshes increased the complexity of the various discretised conservation equations. The next crucial development concerning the finite volume method was the development of solution algorithms for arbitrary unstructured meshes. Thus, it is now possible to create meshes with arbitrary cell location and topology that provides the necessary flexibility for creating complex meshes which are required for most problems. Algorithms based on arbitrary unstructured meshes are used to establish the connectivity between cells, whilst simple index systems are used for structured meshes (Coetzee, 2005:3).

In the current study it has been decided to only make use of the finite element method as described by Du Toit (2004a:2-30), because this method is converging very fast when used to determine the heat transfer and shear stress at the wall, which are used to calculate *Nu* and ¼*f*Re The finite difference method, finite element method and finite volume method will be discussed in the following section.

2.6.1. Finite difference method

The finite difference method is probably the best known and most widely used numerical method. The method is believed to have been introduced by Euler in the 18th century, making it probably the oldest known method for solving partial differential equations (Ferziger *et al*., 1997:35).

The finite difference method is usually only used for structured grids, where the grid lines are used as local coordinate lines. In this method the conservation equations is used in differential form. The differential equation is approximated at each grid point by replacing the partial derivatives with approximations which are in terms of the nodal values of the functions. This result is an algebraic equation for every grid node in which the variable at that node, as well as a certain number of neighbouring nodes, appear to be unknown.

The first and second derivatives of a variable, with respect to the coordinates, can be approximated by making use of a Taylor series expansion or a polynomial fitting. These methods may also be used at locations other than the grid nodes.

A finite difference method as described by Johnson and Riess (1982:441-443).

The following is a brief description of the finite difference method that was described by Johnson and Riess (1982:441-443).

A boundary-value problem was considered in which:

$$y'' = f(x, y, y') \tag{2.28}$$

$$y(a) = \alpha \tag{2.29}$$

$$y(b) = \beta \tag{2.30}$$

where the function $y(x)$ is unknown and the interval is given as $[a,b]$. Eqs (2.29) and (2.30) are referred to as the boundary conditions. It is possible that a particular problem may have no solution, a unique solution or an infinite number of solutions.

Finite difference methods can be used to solve Eqs (2.28), (2.29) and (2.30). The interval must firstly be divided into equally or irregularly spaced points:

$$a = x_0 < x_1 < x_2 < \cdots < x_{n-1} < x_n = b$$

with

$$x_i = x_0 + ih \tag{2.31}$$

where h represents the spacing between two consecutive points. It follows that the derivatives in Eq (2.28) must be replaced by suitable chosen difference quotients defined in terms of points x_i. A typical choice is to use the centred difference approximations:

$$y' = \frac{y(x_{i+1}) - y(x_{i-1})}{2h} \quad \text{and} \quad y'' = \frac{y(x_{i+1}) - 2y(x_i) + y(x_{i-1})}{h^2} \tag{2.32}$$

$$\frac{y_{i+1} - 2y_i + y_{i-1}}{h^2} = f\left(x_i, y_i, \frac{y_{i+1} - y_{i-1}}{2h}\right), \qquad \begin{cases} i = 1,2,\ldots,n-1 \\ y_0 = \alpha, \quad y_n = \beta \end{cases} \tag{2.33}$$

Note that $y_1, y_2, ..., y_{n-1}$ are unknowns and will probably not satisfy Eq (2.28) exactly, because Eq (2.33) is merely an approximation. It will hopefully be a good approximation when a sufficiently small spacing is used.

A nonlinear system of (n-1) equations in (n-1) unknowns must be solved if Eq (2.28) is a nonlinear function in y and y'. Newton's method for several variables may be used to determine $y_1, y_2, ..., y_{n-1}$. Newton's method takes the form of $\overline{Y}_{k+1} = \overline{Y_k} - \overline{J}\left(\overline{Y}_k\right)^{-1} \overline{G}\left(\overline{Y}_k\right)$ with $\overline{Y}_k = \left[y_1^{(k)}, y_2^{(k)}, ..., y_{n-1}^{(k)}\right]^T$ if it is applied to Eq (2.33). The i^{th} component for the vector function $\overline{G}\left(\overline{Y}\right)$ is given as:

$$g\left(\overline{Y}\right) = y_{i+1} - 2y_i + y_{i-1} - h^2 f\left(x_i, y_i, \frac{y_{i+1} - y_{i-1}}{2h}\right) \tag{2.34}$$

The $\left((n-1)\times(n-1)\right)$ Jacobian matrix $\overline{J}\left(\overline{Y}_k\right)$ is a tridiagonal matrix because $\frac{\partial g_i}{\partial y_i}$ is equal to zero for all values, except for ($j = i$-1), ($j = i$), and ($j = i$+1). The starting vector $\left(\overline{Y}_0\right)$ may incorporate components that are obtainable from a linear interpolation of the boundary conditions:

$$y_i^{(0)} = \frac{x_i - 1}{b - a}\beta + \frac{b - x_i}{b - a}\alpha \qquad 1 \le i \le n-1 \tag{2.35}$$

Eqs (2.31) – (2.35) can be used to solve the boundary-value problem (Eqs (2.28) - (2.30)).

The finite difference method has the following advantages and disadvantages (Ferziger *et al*., 1997:35):

- Advantages.
    - It is the easiest method to use for simple geometries.
    - It is very simple and effective on structured grids.
    - It is easy to obtain high-order schemes on regular grids.
- Disadvantages.
    - Special care must be taken to enforce conservation.
    - The restriction to simple geometries makes it very difficult to work with in complex flow.

2.6.2. Finite element method

The finite element method is a numerical method for solving boundary-value problems. Although it was originally developed by engineers for use in structural analysis, it was eventually realised that this method also has a rightful place in the development of numerical techniques that may be used for solving complex flow problems (Taylor & Hughes, 1981:1). The finite element method may also be used to solve problems originating from a variety of other fields such as electro-magnetic, electro-static, etc.

When using the finite element method the domain is divided into a set of discrete finite elements (or volumes) that are usually unstructured. A two-dimensional domain is usually discretised up into triangles or quadrilaterals, while a three-dimensional domain usually consists of tetrahedral or hexahedral elements. The equations of the finite element method are multiplied by a weight function before they are integrated over the domain. This multiplication by a weight function is the distinguishing difference between the finite element and the finite volume method. In the finite element method the solution is approximated by a shape function within each element. The latter procedure is performed in such a manner that it guarantees continuity of the solution across the boundaries (Ferziger *et al*., 1997:36-37).

The basic concepts used to solve problems with the finite element method, as described by Taylor and Hughes (1981:1-5), are summarised in Figure 2.4 and are explained in more detail in the following paragraphs.

The governing equations are usually subjected to some minimisation procedure. For this procedure a number of techniques may be employed, e.g. functional, collocation, least squares and the Galerkin weighted residuals approach. The Galerkin approach is usually used.

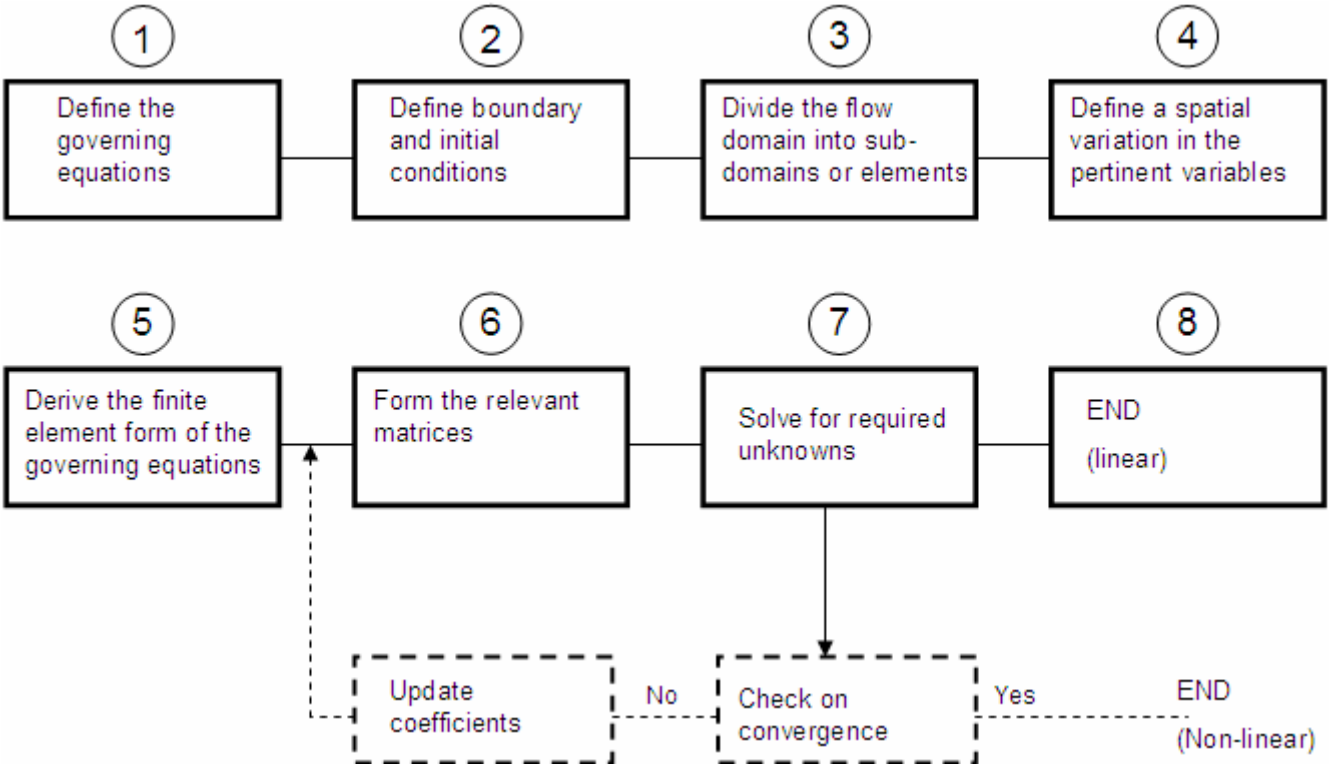

Figure 2.4. Basic concepts of the finite element method.

The basic equation in the Galerkin approach is weighted with appropriate discrete weighting functions, whilst the resulting equation is then integrated over the region of interest and equated to zero. If, for example, the Laplace equations are used as the governing equation, then:

$$\nabla^2 \varphi = 0 \tag{2.36}$$

where φ represents the velocity potential. The Galerkin approach now results in:

$$\int_{\Omega} w_k \left(\nabla^2 \varphi\right) d\Omega = 0 \qquad k=1,2,3....m \tag{2.37}$$

where *m* is the number of points in the domain.

To solve this equation the spatial variation of φ must firstly be defined and then the flow domain must be divided into smaller parts, called elements. Each element is defined by discrete points, called nodes, which is located within or on the element boundary. Within each element the spatial variation of φ is defined in terms of the values at the nodal points.

If an element is defined by n nodal points, with values $\varphi_1, \varphi_2, ..., \varphi_n$, then the φ value of the element is written as:

$$\varphi = \sum_{i=1}^{n} N_i \varphi_i \tag{2.38}$$

where N_i is a function of the nodal points. These polynomial functions are called shape functions and are interpolation functions. Figure 2.5 shows an element that is being defined by eight nodal points.

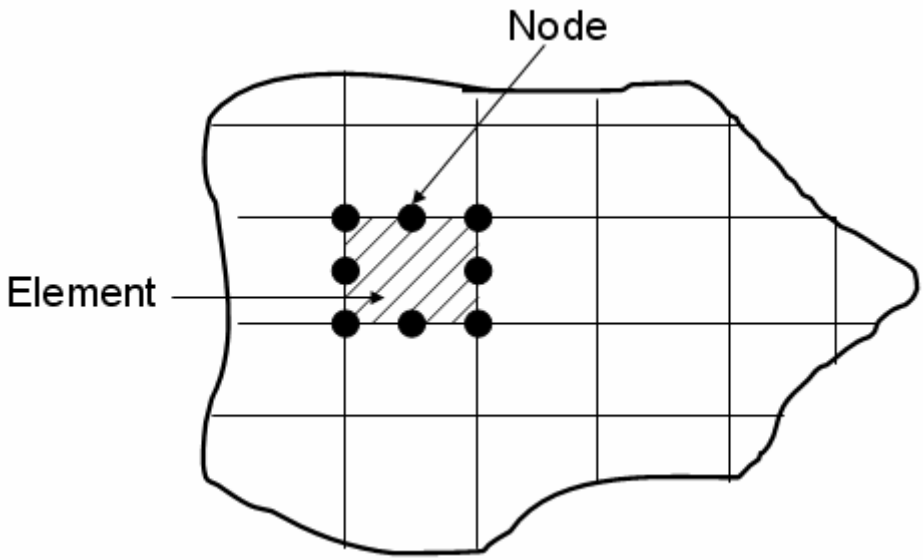

Figure 2.5. An element with eight nodal points.

After the domain has been divided into elements, and suitable shape functions have been allocated, Eq (2.37) must be integrated over each element and all the various contributions must be summed for each element. This is usually done by employing some kind of numerical integration that leads to the element contribution (h) in matrix form:

$$\left[\bar{h}\right] \cdot \begin{Bmatrix} \varphi_1 \\ . \\ . \\ . \\ \varphi_8 \end{Bmatrix} \tag{2.39}$$

After all the element contributions to the global system of equations have been summed, the final global system of equations in matrix form will be:

$$\left[\overline{H}\right]\cdot\begin{Bmatrix}\varphi_1\\ .\\ .\\ .\\ \varphi_n\end{Bmatrix}=0 \tag{2.40}$$

with n the number of nodal points in the domain and $\overline{H}$ the global coefficient matrix. After the appropriate boundary conditions have been applied the resulting equations must be solved for the nodal values of the variable.

The processes outlined above, leading to an explicit solution, must be modified if more complicated equations are to be solved. An equation for a simple form of steady state heat conduction in two dimensions is:

$$\frac{\partial}{\partial x}\left(K_x\frac{\partial T}{\partial x}\right)+\frac{\partial}{\partial y}\left(K_y\frac{\partial T}{\partial y}\right)=0 \tag{2.41}$$

with the material properties dependent on local temperature and space:

$$K_x=f_I(x,y,T) \tag{2.42}$$

$$K_y=f_{II}(x,y,T) \tag{2.43}$$

The same process that was followed for the Laplace equation may now be followed to set up the final matrix form of Eq (2.41). But, because the value of conductivity, K, is unknown, the solution technique must be iterative. Eq (2.41) is now rewritten as:

$$\frac{\partial}{\partial x}\left(K_x^{k-1}\frac{\partial T^k}{\partial x}\right)+\frac{\partial}{\partial y}\left(K_y^{k-1}\frac{\partial T^k}{\partial y}\right)=0 \tag{2.44}$$

with k the current iteration value. The iteration must continue until the solution has converged within a specified tolerance.

A finite element method as described by Du Toit (2004a:2-30).

Du Toit applied the following steps for solving flow in ducts by means of a finite element method.

- Formulate the problem.
    - Identify the problem and differential equation.
    - Define the approximate solution (see Eq (5.3)).
- Finite element formulation.
    - Determine the weak formulation for the problem, by writing the differential equation in a residual form, multiply it with an arbitrary suitable weighting function, and integrate it over the domain.
    - Determine the Galerkin weak formulation.
    - Divide the domain into elements, using nodal points to define the elements.
    - Define the interpolation functions and use it to rewrite the approximate solution.
- Determine the solution.
    - Set up the local equations.
    - Set up the global equations, by summing the contributions from each element.
    - Apply the boundary conditions to the global equations.
    - Solve the equations.

The difference between the finite element method as described by Du Toit and the method described in Figure 2.4 (by Taylor and Hughes), is that Du Toit's method defines the weak formulation and Galerkin formulation globally (over the entire domain). The domain is only discretised into elements to define the interpolation function and evaluate the integrals. Taylor and Hughes define the weak formulation and Galerkin formulation only over an element.

Application of the finite element method has advantages as well as disadvantages. The following advantages and disadvantages have been identified (Ferziger *et al*., 1997:36-37).

- Advantages.
    - It works excellent for arbitrary geometries.
    - Extensive literature is devoted to the construction of this method's grid.
    - It is easy to refine the grids, since the elements may simply be subdivided.

- It is easy to analyze mathematically.
- The method has optimality properties for certain types of equations.

- Disadvantages.
  - Any method that uses unstructured grids has the shortcoming that the matrices of the linearized equations are not as well structured as is the case for the regular grids. This factor makes it more difficult to find efficient solution methods.

2.6.3. The finite volume method

To employ the finite volume method to solve problems, the geometry is divided into a number of non-overlapping cells (control volumes). The conservation (of mass, momentum and energy) equations are then integrated over each cell using approximations. A finite volume method, as described by Leveque (2002:64-66), will now be discussed in the following section.

Leveque's finite volume method.

In Leveque's method the spatial domain is firstly divided into intervals (called grid cells), and then approximations are determined for the integrals of $q(x,t)$ over each of these grid cells. Let the i^{th} grid cell be defined as,

$$C_i = (x_{i-0.5}, x_{i+0.5}) \tag{2.45}$$

Let Q_i^n be the approximate value for $q(x,t)$ over the i^{th} interval (at time $t = t_n$),

$$Q_i^n \approx \frac{1}{\Delta x}\int_{x_{i-0.5}}^{x_{i+0.5}} q(x,t_n)dx \equiv \frac{1}{\Delta x}\int_{C_i} q(x,t_n)dx \tag{2.46}$$

where $\Delta x = x_{i+0.5} - x_{i-0.5}$ is the cell length. Note that it is not necessary for the grid to be uniform. If $q(x,t)$ is a smooth function, then Eq (2.43) agrees with the value of q at the midpoint of the interval.

The integral form of the conservation law is given as:

$$\frac{d}{dt}\int_{C_i} q(x,t)dx = f(q(x_{i-0.5},t)) - f(q(x_{i+0.5},t)) \tag{2.47}$$

Let t_{n+1} be the next time step after time t_n, with a step length of $\Delta t = t_{n+1} - t_n$. By using Eq (2.47), an approximation (Q_i^{n+1}) for cell i at time t_{n+1} can be determined. Integrate Eq (2.47) from time t_n to t_{n+1}:

$$\int_{C_i} q(x,t_{n+1})dx - \int_{C_i} q(x,t_n)dx = \int_{t_n}^{t_{n+1}} f\left(q(x_{i-0.5},t)\right)dt - \int_{t_n}^{t_{n+1}} f\left(q(x_{i+0.5},t)\right)dt \quad (2.48)$$

Rearranging Eq (2.48) and dividing it by Δx gives:

$$\frac{1}{\Delta x}\int_{C_i} q(x,t_{n+1})dx = \frac{1}{\Delta x}\int_{C_i} q(x,t_n)dx - \frac{1}{\Delta x}\left[\int_{t_n}^{t_{n+1}} f\left(q(x_{i+0.5},t)\right)dt - \int_{t_n}^{t_{n+1}} f\left(q(x_{i-0.5},t)\right)dt\right] \quad (2.49)$$

The exact solutions for $q(x_{i\pm0.5},t)$ are not known, because it vary in time along the edges for each cell. This implies that numerical methods which are to be used should be of the form:

$$Q_i^{n+1} = Q_i^n - \frac{\Delta t}{\Delta x}\left(F_{i+0.5}^n - F_{i-0.5}^n\right) \quad (2.50)$$

with $F_{i-0.5}^n$ the approximation for the average flux at $x = x_{i-0.5}$,

$$F_{i-0.5}^n \approx \frac{1}{\Delta t}\int_{t_n}^{t_{n+1}} f\left(q(x_{i-0.5},t)\right)dt \quad (2.51)$$

If it is now assumed that $F_{i-0.5}^n$ can be determined by using Q_{i-1}^n and Q_i^n, then the appropriate equation may be of the form:

$$F_{i-0.5}^n = Z\left(Q_{i-1}^n, Q_i^n\right) \quad (2.52)$$

where *Z* is a numerical flux function. Eq (2.50) may now be rewritten as:

$$Q_i^{n+1} = Q_i^n - \frac{\Delta t}{\Delta x}\left[Z\left(Q_i^n, Q_{i+1}^n\right) - Z\left(Q_{i-1}^n, Q_i^n\right)\right] \quad (2.53)$$

Note that Q_i^{n+1} depends only on three values, namely Q_{i-1}^n, Q_i^n and Q_{i+1}^n, from the previous time step. After some rearranging of Eq (2.53), this method may be seen as a direct finite difference approximation to the conservation law:

$$\frac{Q_i^{n+1} - Q_i^n}{\Delta t} + \frac{F_{i+0.5}^n - F_{i-0.5}^n}{\Delta x} = 0 \quad (2.54)$$

Many methods can be equally well viewed as finite difference approximations to this equation or as finite volume methods.

Application of this finite volume method has advantages as well as disadvantages. The following advantages and disadvantages have been identified (Ferziger *et al*., 1997:35-36).

- Advantages.
    - It is suitable for any type of grid, even for complex geometries.
    - The grid only defines the control volume boundaries. The coordinate system does not have to be related.
    - It is conservative by construction.
    - It is probably the simplest method to understand and to use (program).
    - Physical meanings are associated with all the terms that need to be approximated, and this is the reason why many engineers prefer to use this method.
- Disadvantages.
    - The disadvantage of finite volume methods compared to the finite difference methods is that methods of order higher than second are more difficult to develop in three-dimensions. This is due to the fact that the finite volume method requires two levels of approximation: interpolation and integration.

2.6.4. Properties of numerical solution methods

It is important to recognise that numerical methods have certain properties which cannot be analyzed directly. In these cases the components of the methods must be analyzed. If the components do not possess the desired properties, then neither will the complete method. The reverse is not necessarily true, even if the components actually possess the desired properties (Ferziger *et al*., 1997:31). The most important properties are discussed below.

Stability

A numerical method is considered to be stable if it does not magnify errors that appear during the course of the numerical solution processes. A stable method produces a bounded solution if the solution of the exact equation is bounded. When using iterative methods, a stable method will not diverge. It is difficult to investigate stability, especially in the presence of boundary conditions and non-linearities. Therefore, it is common practice to investigate the stability of a method for linear problems with constant coefficients without boundary conditions. Von Neumann's method is the most widely used approach to study the stability of a numerical scheme (Ferziger *et al*., 1997:31-32).

Consistency

The truncation error is the difference between the discretized equation and the exact equation. The truncation error is usually estimated by replacing the nodal values in the discrete approximation by a Taylor series expansion about a single point. This gives the original differential equation plus a residue that is the truncation error. If a method is consistent, the truncation error must become zero as the grid spacing tends to zero (Ferziger *et al*., 1997:31).

Accuracy

The numerical solutions of fluid flow and heat transfer problems are only approximate solutions. Except for the errors that may occur during programming, setting up of the boundary conditions, or during the course of developing of the solution algorithm, the following three kinds of systematic errors are always found in numerical solutions (Ferziger *et al*., 1997:34-35):

- modeling errors are the difference between the actual flow and the exact solution of the mathematical model;
- discretization errors are the difference between the exact solution of the algebraic system, which is obtained by discretizing these equations, and the exact solution of the conservation equations; and
- convergence errors are the difference between the exact and iterative solutions of the algebraic equation system.

Convergence

A numerical method is converging when the solution of the discretized equations becomes equal to the exact solution of the differential equation as the grid spacing decreases to zero. Stability is the necessary and sufficient condition for the convergence of a linear initial value problem. Note also, that a consistent scheme is only useful if the solution method converges (Ferziger *et al*., 1997:32).

Conservation

The equations for the laws of conservation are solved by employing numerical methods. These methods must respect the laws on a local as well as on a global basis. Thus, in the absence of a source at steady state the difference between the amount of a conserved quantity that enters and leaves a closed volume is zero. The conservation laws are guaranteed for each individual control volume, and for the solution domain as a whole, when the finite volume method is used. Other discretization

methods can also be made conservative if care is taken in the choice of approximations (Ferziger *et al*., 1997:32-33).

Boundedness

It is imperative that numerical solutions should make sense. For example, physically non-negative quantities (like density) must always be positive and the numerical solutions should always be located within proper bounds. In the absence of a source the minimum and maximum values of the equations should be located on the boundaries of the domain. For example, in the absence of a heat source the heat equations would require that the minimum and maximum temperature values are located on the boundaries of the domain (Ferziger *et al*., 1997:33).

Realizibility

A complex model that cannot be treated directly (like kinetic energy of turbulence) should be designed in such a manner that it is possible to acquire physically realistic solutions (Ferziger *et al*., 1997:33).

2.7. C++ programming language

Codes written in C++ will be used in this study to solve the fully developed laminar flow in one- and two-dimensional ducts by using the finite element method. After the flow has been solved C++ codes will also be used to determine the friction factors and Nusselt numbers for different duct shapes.

A programming language is the specific set of rules which are used for coding instructions to a computer. Many different programming languages are currently used by programmers, for example, C++, Fortran, Pascal, Basic, etc. In the late 70's a generally accepted version of the C language was created. But C is a rather low level programming language, which was designed for programmers who knew exactly what they were doing and who wanted to program at a low level. Since C is difficult to use the C++ language, which is an extension to C, was developed. C++ is a higher level programming language based on the concept of object-oriented programming and it is recognized by many professional programmers as the best vehicle available for object-oriented programming (Hahn, 1994:2-3).

2.8. Summary

In this chapter it was shown that a considerable amount work has been done on laminar and turbulent flow in ducts that is subjected to the H1 and/or T boundary conditions. The numerical methods that were used in these studies have proven themselves to be very elegant and accurate. It was also pointed

out that there exist discrepancies between Nusselt numbers and friction factors published by different authors.

Important properties used to analyze numerical methods were discussed.

- Stability: method does not magnify errors that appear during course of numerical solution processes.
- Consistency: truncation error must become zero as the grid spacing tents to zero.
- Accuracy: numerical solutions of fluid flow and heat transfer problems are only approximate solutions.
- Convergence: when the solution of the discretized equations become equal to the exact solution of the differential equation as the grid spacing decreases to zero.
- Conservation: the equations for the laws of conservation are solved.
- Boundedness: numerical solution should make sense.
- Realizibility: a complex model should acquire physically realistic solutions.

The three governing equations which are used to describe flow problems are:

- conservation of mass,
- conservation of momentum, and
- conservation of energy.

CFD is a computational technology used to predict heat transfer and fluid flow through computer simulations.

The numerical methods which are used to solve the governing equations are:

- finite difference method,
- finite element method, and
- finite volume method.

C++ is a programming language which is based on the concept of object-oriented programming.

In the next chapter one- and two-dimensional governing equations will be discussed. These are the equations that will be solved in this study by using a finite element method.

3. The governing equations

The literature study was discussed in the previous chapter. The current chapter deals with the one- and two-dimensional governing equations which will eventually be used in this study to solve the fully developed laminar flow in one- and two-dimensional ducts by using finite elements.

3.1. One-dimensional governing equations

The conservation of momentum may be used to calculate the radial distribution of axial velocity. The equation for the conservation of momentum in one-dimensional cylindrical coordinates for fully developed laminar flow in an annulus, or in a circular duct, is given as (Incropera & De Witt, 2005:489):

$$0 = -\frac{\partial p}{\partial z} + \frac{1}{r}\frac{\partial}{\partial r}\left(\mu r \frac{\partial w}{\partial r}\right) \quad \text{for } r_i < r < r_o \tag{3.1}$$

If Eq (3.1) is subjected to the non-slip velocity boundary conditions at the walls then the following holds for an annulus:

$$w(r_i) = w(r_o) = 0 \tag{3.2}$$

and for a circular duct:

$$w(r_o) = 0 \quad \text{and} \quad \left.\frac{\partial w}{\partial r}\right]_{r=0} = 0 \tag{3.3}$$

where w, r, and $\frac{\partial p}{\partial z}$ refers to the axial velocity, radius and the axial pressure gradient respectively.

The equation for the conservation of energy for thermally fully developed flow and negligible viscous dissipation can be expressed in one-dimensional cylindrical coordinates as (Bejan, 1993:222):

$$0 = -\rho\ c_p w \frac{\partial T}{\partial z} + \frac{1}{r}\frac{\partial}{\partial r}\left(kr\frac{\partial T}{\partial r}\right) \quad \text{for } r_i < r < r_o \tag{3.4}$$

where $\frac{\partial T}{\partial z}$ refers to the temperature gradient.

If Eq (3.3) is subjected to the heat flux boundary conditions then the following holds for an annulus:

$$-k\frac{\partial T}{\partial n}\Big]_{r=r_i} = q_i'' \quad \text{and} \quad -k\frac{\partial T}{\partial n}\Big]_{r=r_o} = q_o'' \tag{3.5}$$

and for a circular duct:

$$-k\frac{\partial T}{\partial n}\Big]_{r=0} = 0 \quad \text{and} \quad -k\frac{\partial T}{\partial n}\Big]_{r=r_o} = q_o'' \tag{3.6}$$

where q_i'' and q_o'' refer to the heat flux on the inner and outer wall respectively. Note that $r_i = 0$ for a circular duct in all of the above given equations.

The dimensionless temperature difference for thermally fully developed flow was given by Incropera and De Witt (2005:494) as:

$$\frac{\partial}{\partial z}\left[\frac{T_s(z) - T(r,z)}{T_s(z) - T_m(z)}\right] = 0 \tag{3.7}$$

where T_s and T_m respectively refers to the wall temperature and the bulk temperature.

3.2. Two-dimensional governing equations

The conservation of momentum for fully developed laminar flow in a duct in two-dimensional Cartesian coordinates is given as (Du Toit, 2002a:399):

$$0 = -\frac{\partial p}{\partial z} + \mu\left(\frac{\partial^2 w}{\partial x^2} + \frac{\partial^2 w}{\partial y^2}\right) \quad \text{in } \Omega \tag{3.8}$$

subjected to the Dirichlet boundary conditions:

$$w = \hat{w} \quad \text{on } \Gamma \tag{3.9}$$

with Γ the boundary of the problem domain Ω. The equation for the conservation of energy for thermally fully developed flow with negligible viscous dissipation in two-dimensional Cartesian coordinates, is given as (Du Toit, 2002a:399):

$$0 = -\rho\ c_p w\frac{\partial T}{\partial z} + k\left(\frac{\partial^2 T}{\partial x^2} + \frac{\partial^2 T}{\partial y^2}\right) \quad \text{in } \Omega \tag{3.10}$$

subjected to the Dirichlet boundary conditions:

$$T = \hat{T} \quad \text{on } \Gamma \tag{3.11}$$

Eqs (3.8) and (3.10) may now be used to solve the fully developed laminar flow in two-dimensional ducts.

3.3. Constant wall heat flux versus constant wall temperature

The axial variation of T_m was given by Incropera and De Witt (2005:495-498) as:

$$\frac{\partial T_m}{\partial z} = \frac{dT_m}{dz} = \frac{q_s^{"} P}{\dot{m} c_p} \tag{3.12}$$

with P the perimeter length. For the case of constant wall heat flux in the axial direction, Eq (3.12) is a constant that is independent of z. But for the case of constant wall temperature in the axial direction it is not as simple, and the axial variation of T_m is now given as (Incropera & De Witt, 2005: 495):

$$\frac{\partial T_m}{\partial z} = \left(\frac{\left(T_s - T\right)}{\left(T_s - T_m\right)} \right) \frac{dT_m}{dz} \tag{3.13}$$

The derivative of T_m with respect to z is thus a constant for the H1 boundary condition but not for the T boundary condition.

3.4. Summary

The equations for the conservation of momentum and energy, that will be used to solve the fully developed laminar flow in one- and two-dimensional ducts as well as the conditions that they are subjected to, were introduced in this chapter.

The difference between the formulations for constant wall heat flux in the axial direction and constant wall temperature in the axial direction were also pointed out.

In the next chapter analytical equations, to calculate Nusselt numbers and friction factors for fully developed laminar flow in annular and circular ducts, will be discussed.

4. Analytical equations for calculating Nusselt numbers and friction factors

In the previous chapter the governing equations which are used to describe the fully developed laminar flow in annular and circular ducts were introduced. In the current chapter the analytical solutions that may be used to calculate Nusselt numbers and friction factors for fully developed laminar flow in annular and circular ducts, subjected to the H1 or T boundary conditions, will be discussed.

4.1. Nusselt number for a circular duct (H1)

The analytical solution that may be used to calculate the Nusselt number for a circular duct subjected to the H1 boundary condition is discussed below.

The temperature gradient will be used as the starting point to derive an equation that furnishes the Nusselt number for a circular duct. For the special case when uniform surface heat flux prevails, it can be shown from Eq (3.7) that (Incropera & De Witt, 2005:495):

$$\frac{\partial T}{\partial z} = \frac{dT_m}{dz} \tag{4.1}$$

The mean velocity (w_m) is given by (Incropera & De Witt, 2005:488):

$$w_m = \frac{\int_{r_i}^{r_o} \rho w r dr}{\int_{r_i}^{r_o} \rho r dr} = \frac{\int_{A_c} \rho w(r,z) dA_c}{\rho A_c} = \frac{2}{r_0^2} \int_0^{r_o} w(r,z) r \, dr \tag{4.2}$$

Since the axial pressure gradient is independent of r, Eq (3.1) can be solved by integrating it twice and by using the boundary conditions given in Eq (3.3). It follows that (Incropera & De Witt, 2005:489):

$$w(r) = -\frac{1}{4\mu}\left(\frac{dp}{dz}\right) r_o^2 \left[1 - \left(\frac{r}{r_o}\right)^2\right] \tag{4.3}$$

Substituting Eq (4.3) into Eq (4.2) and integrating, gives (Incropera & De Witt, 2005:489):

$$w_m = -\frac{r_o^2}{8\mu}\left(\frac{dp}{dz}\right) \tag{4.4}$$

Substituting Eq (4.4) into Eq (4.3), gives (Incropera & De Witt, 2005:490):

$$\frac{w(r)}{w_m} = 2\left[1-\left(\frac{r}{r_o}\right)^2\right] \tag{4.5}$$

Now, by using $\alpha = \frac{k}{\rho c_p}$ and by substituting Eqs (4.1) and (4.5) into Eq (3.4) the following is obtained:

$$\frac{1}{r}\frac{\partial}{\partial r}\left(r\frac{\partial T}{\partial r}\right) = \frac{2w_m}{\alpha}\left(\frac{dT_m}{dz}\right)\left[1-\left(\frac{r}{r_o}\right)^2\right] \tag{4.6}$$

By integrating Eq (4.6) twice, and since the temperature remains finite at (r =0) and $T(r_o) = T_s$, it follows that:

$$T(r,z) = T_s(z) - \frac{2w_m r_o^2}{\alpha}\left(\frac{dT_m}{dz}\right)\left[\frac{3}{16}+\frac{1}{16}\left(\frac{r}{r_o}\right)^4-\frac{1}{4}\left(\frac{r}{r_o}\right)^2\right] \tag{4.7}$$

The bulk temperature is given as (Incropera & De Witt, 2005:493):

$$T_m = \frac{\int_{r_i}^{r_0}\rho c_p wTrdr}{\int_{r_i}^{r_o}\rho c_p wrdr} = \frac{2}{w_m r_o^2}\int_0^{r_o} wTr\,dr \tag{4.8}$$

Substituting Eqs (4.5) and (4.7) into Eq (4.8) and integrate over "r" gives (Incropera & De Witt, 2005:506):

$$T_m(z) = T_s(z) - \frac{11}{48}\left(\frac{w_m r_o^2}{\alpha}\right)\left(\frac{dT_m}{dz}\right) \tag{4.9}$$

It was shown by Incropera and De Witt (2005:498) that,

$$\frac{dT_m}{dz} = \frac{q_s'' P}{\dot{m} c_p} \tag{4.10}$$

where

$$\dot{m} = \rho w_m\left(\frac{\pi D^2}{4}\right) \tag{4.11}$$

and $$P = \pi D \tag{4.12}$$

with $\dot{m}$ and D the mass flow and the diameter respectively. Substituting Eqs (4.10), (4.11) and (4.12) into Eq (4.9) gives rise to (Incropera & De Witt, 2005:506):

$$T_m(z) - T_s(z) = -\frac{11}{48}\left(\frac{q_s'' D}{k}\right) \tag{4.13}$$

Combining Newton's law of cooling, namely $q_s'' = h(T_s - T_m)$, with Eq (4.13) gives (Incropera & De Witt, 2005:507):

$$Nu = \frac{hD}{k} = \frac{48}{11} = 4.36 \tag{4.14}$$

Where h and $Nu = \frac{hD}{k}$ respectively represents the heat transfer coefficient and the Nusselt number definition. Nusselt numbers determined in this study, by employing numerical methods, is in good agreement with the value given in Eq (4.14) (see Table. 7.1).

4.2. Nusselt number for a circular duct (T)

The analytical solution that may be used to calculate the Nusselt number for a circular duct subjected to the T boundary condition is discussed below.

For the special case when a constant surface temperature prevails in a circular duct it follows from Eq (3.7) that (Incropera & De Witt, 2005:495):

$$\frac{\partial T_m}{\partial z} = \left(\frac{(T_s - T)}{(T_s - T_m)}\right)\frac{dT_m}{dz} \tag{4.15}$$

Substituting Eq (4.15) into the energy equation, Eq (4.6), gives (Incropera & De Witt, 2005:507):

$$\frac{1}{r}\frac{\partial}{\partial r}\left(r\frac{\partial T}{\partial r}\right) = \frac{2w_m}{\alpha}\left(\frac{dT_m}{dz}\right)\left[1 - \left(\frac{r}{r_o}\right)^2\right]\frac{T_s - T}{T_s - T_m} \tag{4.16}$$

Eq (4.16) may now be solved by means of an iterative procedure to give the following Nusselt number (Incropera & De Witt, 2005:507), (Shah & London, 1978:286), (Kays, 1966:110):

$$Nu = 3.66 \tag{4.17}$$

An infinite series (Kays & Crawford, 1993:117) may also be employed to solve the last term on the right side of Eq (4.16):

$$\frac{T_s - T}{T_s - T_m} = \sum_{n=0}^{\infty} C_{2n} \left(\frac{r}{r_o} \right)^{2n} \tag{4.18}$$

where C_{2n} is defined as

$$C_{2n} = \frac{\lambda_o^2}{(2n)^2} \left(C_{2n-4} - C_{2n-2} \right)$$

with

$$C_o = 1, \quad C_2 = -\frac{1}{4}\lambda_o^2 = -1.828397 \quad \text{and} \quad \lambda_o = 2.704364 .$$

By employing the temperature distribution in Eq (4.18) the Nusselt number is calculated as:

$$Nu = \frac{1}{2}\lambda_o^2 = 3.657 \tag{4.19}$$

Nusselt numbers determined in this study, by employing numerical methods, is in good agreement with the value given in Eq (4.19) (see Table. 7.1).

4.3. Friction factor for a circular duct (H1 or T)

The analytical solution that may be used to calculate the friction factor for a circular duct subjected to the H1 or T boundary condition is discussed below.

The dimensionless Moody friction factor (f) will be used as the starting point to derive an equation that furnishes the friction factor for a circular duct. This friction factor is given as (Incropera & De Witt, 2005:490):

$$f \equiv \frac{-(dp/dz)D}{\rho w_m^2 / 2} \tag{4.20}$$

The Reynolds number (Re_D) for a circular duct is defined as (Incropera & De Witt, 2005:487):

$$\mathrm{Re}_D \equiv \frac{\rho w_m D}{\mu} \tag{4.21}$$

Substituting Eqs (4.21) and (4.4) into Eq (4.20) gives (Incropera & De Witt, 2005:490), (Shah & London, 1978:286) and (White, 1988:306):

$$f = \frac{64}{\mathrm{Re}_D}$$

Thus,

$$\frac{1}{4} f \,\mathrm{Re}_D = 16 \tag{4.22}$$

Friction factors determined in this study, by employing numerical methods, is in good agreement with the value given in Eq (4.22) (see Table. 7.1).

4.4. Nusselt number for an annular duct with constant heat transfer at the one wall whilst the other wall has no heat transfer

The analytical solution that may be used to calculate the Nusselt number for an annular duct subjected to constant heat transfer at one wall, whilst the other wall has no heat transfer, is discussed below.

The difference between the inner wall surface temperature (T_i) and the mean bulk temperature will be used as the starting point to derive an equation that gives the Nusselt number for an annular duct. This difference is given as (Dwyer, 1962:58):

$$T_i - T_m = \frac{\int_{r_i}^{r_o} (T_i - T) w 2\pi\, r\, dr}{\pi\left(r_o^2 - r_i^2\right) w_m} \tag{4.23}$$

The difference between the inner wall surface temperature and the temperature at any given radius, r, is (Dwyer, 1962:59):

$$T_i - T = \int_{r_i}^{r} -\frac{\partial T}{\partial r}\, dr \tag{4.24}$$

The heat transfer coefficient is defined as (Dwyer, 1962:58):

$$q_i^{'} = h\left(T_i - T_m\right) 2\pi\, r_i \tag{4.25}$$

The transport equation is given as (Dwyer, 1962:58):

$$q_i^{'} = \pi\left(r_o^2 - r_i^2\right)\left(w_m \rho\ c_p \frac{dT_m}{dz}\right) \tag{4.26}$$

Since the radial heat transfer rate must equal the axial heat transport rate it follows that (Dwyer, 1962:59):

$$-k_{eff}\, 2\pi\ r \frac{\partial T}{\partial r} = \int_r^{r_o} \pi\ rw\rho c_p \frac{dT_m}{dz}\ dr \tag{4.27}$$

By combining Eqs (4.23), (4.24) and (4.27), and substituting the newly obtained equation into Eq (4.25), the following is obtained (Dwyer, 1962:59):

$$\frac{1}{h_i} = \frac{4r_i}{\left(r_0^2 - r_i^2\right)^2 w_m^2} \int_{r_i}^{r_o} w \left[\int_{r_i}^{r} \frac{\int_r^{r_o} rwdr}{rk_{eff}} dr \right] r\ dr \tag{4.28}$$

with k_{eff} the effective thermal conductivity. Dwyer (1962:59) derived Eq (4.29) by using the definitions of the Nusselt number (Nu_{ii}) at the inner wall, with constant heat transfer at the inner wall and no heat transfer at the outer wall:

$$Nu_{ii} = \frac{h_i D_h}{k}$$

the Prandtl number (Pr):

$$Pr = \frac{c_p \mu}{k}$$

and

$$\psi = \frac{\varepsilon_H}{\varepsilon_M} = \frac{\left(\frac{k_e}{\rho\ c_p}\right)}{\left(\frac{\mu_e}{\rho}\right)}$$

D_h, ε_H, ε_M and k_e refer to the hydraulic diameter, the eddy diffusivity of heat, the eddy diffusivity of the momentum and the Eddy thermal conductivity of liquid metal respectively. The equation for $(Nu_{ii})^{-1}$ is given as:

$$\frac{1}{Nu_{ii}} = \frac{2r_i}{w_m^2\left(r_o + r_i\right)^2\left(r_o - r_i\right)^3}\int_{r_i}^{r_o} w\left[\int_{r_i}^{r}\frac{\int_{r}^{r_o} rwdr}{r\left[1+\left(\frac{\psi\varepsilon_M \,\mathrm{Pr}}{\upsilon}\right)\right]}dr\right]r\,dr \tag{4.29}$$

where $\upsilon = \dfrac{\mu}{\rho}$ represents the kinematic viscosity.

By rewriting Eq (4.29) and substituting Eq (4.2) into it the Nusselt number for the inner wall is obtained as (Dwyer, 1963b:337):

$$Nu_i = \frac{2(y-1)\left[\int_{r_i}^{r_o} rw\ dr\right]^2}{\int_{r_i}^{r_o}\left[\int_{r_i}^{r}\frac{\int_{r}^{r_o} rw\ dr}{r\left[1+\left(\frac{\psi\varepsilon_M \,\mathrm{Pr}}{\upsilon}\right)\right]}dr\right]wr\,dr} \tag{4.30}$$

where $$y = \frac{r_o}{r_i}$$

In an analogous manner, the Nusselt number (Nu_{oo}) at the outer wall, with constant heat transfer at the outer wall and no heat transfer at the inner wall, can be obtained (Dwyer, 1963b:337):

$$Nu_{oo} = \frac{2(1-\frac{1}{y})\left[\int_{r_i}^{r_o} wr\ dr\right]^2}{\int_{r_i}^{r_o}\left[\int_{r}^{r_o}\left\{\int_{r_i}^{r} rw\ dr\right\}\div\left\{r\left[1+\left(\frac{\psi\varepsilon_M \,\mathrm{Pr}}{\upsilon}\right)\right]\right\}dr\right]wr\,dr} \tag{4.31}$$

The linear velocity is given by Lamb's equation as (Dwyer, 1963b:337):

$$w = \frac{(\Delta p)}{4\mu L}\left[r_i^2 - r^2 + \frac{r_o^2 - r_i^2}{\ln(r_o / r_i)}\ln(r / r_i)\right] \tag{4.32}$$

By employing Eq (4.2) it can be shown that (Dwyer, 1963b:337):

$$\frac{(\Delta p)}{4\mu L} = \frac{2w_m}{r_i^2\left[y^2 + 1 - \dfrac{y^2-1}{\ln(y)}\right]} \tag{4.33}$$

Combining Eqs (4.32) and (4.33) gives (Dwyer, 1963b:337):

$$w = \frac{2w_m}{\left[y^2 + 1 - \dfrac{y^2-1}{\ln(y)}\right]} \times \left[1 - \frac{r^2}{r_i^2} + \frac{y^2-1}{\ln(y)}\ln(r/r_i)\right] \tag{4.34}$$

Substituting Eq (4.34) into Eq (4.30), and since $(\psi\varepsilon_M \,\mathrm{Pr}) \div \upsilon = 0$ (for laminar flow), gives (Dwyer, 1963b:337):

$$Nu_{ii} = \frac{(y-1)(y^2-1)^2\left[y^2+1-(y^2-1)/\ln y\right]^2 r_i^8}{8\zeta_i} \tag{4.35}$$

with

$$\zeta_i = \int_{r_i}^{r_o}\left[\int_{r_i}^{r}\left\{\frac{\int_{r}^{r_o} mr\,dr}{r}\right\}dr\right] mr\,dr \tag{4.36}$$

and

$$m = r_i^2 - r^2 + \frac{r_o^2 - r_i^2}{\ln(r_o/r_i)}\ln\frac{r}{r_i} \tag{4.37}$$

In an analogous manner, the Nusselt number for the outer wall can be obtained (Dwyer, 1963b:337):

$$Nu_{oo} = \frac{\left(1-\left(\dfrac{1}{y}\right)\right)(y^2-1)^2\left[y^2+1-(y^2-1)/\ln y\right]^2 r_i^8}{8\zeta_o} \tag{4.38}$$

with

$$\zeta_o = \int_{r_i}^{r_o}\left[\int_{r_o}^{r}\left\{\frac{\int_{r_i}^{r} mr\,dr}{r}\right\}dr\right] mr\,dr \tag{4.39}$$

Table 4.1 shows the values of inner and outer Nusselt numbers as calculated according to Eqs (4.35) and (4.39) (Dwyer, 1963b:337). Nusselt numbers determined in this study, by employing numerical methods, are in good agreement with the value given in Table 4.1 (see results in Table. 7.12)

Table 4.1. Inner and outer Nusselt numbers for annular ducts with constant heat transfer at one wall whilst the other wall has no heat transfer (Dwyer, 1963b:337).

r_i/r_o	Nu_{ii}	Nu_{oo}
0.00	-	4.364
0.10	11.90	4.83
0.13	10.57	4.84
0.17	9.22	4.88
0.25	7.78	4.92
0.50	6.17	5.03
0.67	5.78	5.15
0.80	5.60	5.26
1.00	5.385	5.385

4.5. Nusselt number for an annular duct (H1)

No analytical solution could be been found in the literature for an annular duct that is subjected to constant heat flux at both walls. However, 6th order polynomial equations that may be used to calculate these Nusselt numbers are available. Du Toit (2004b:1-16) used the finite element method and a least squares approach to derive the following influence coefficient equations:

$$Nu_{ii} = 0.00340\left[\ln\left(\frac{r_i}{r_o}\right)\right]^6 + 0.018685\left[\ln\left(\frac{r_i}{r_o}\right)\right]^5 + 0.083965\left[\ln\left(\frac{r_i}{r_o}\right)\right]^4 - 0.022861\left[\ln\left(\frac{r_i}{r_o}\right)\right]^3 + 0.545818\left[\ln\left(\frac{r_i}{r_o}\right)\right]^2 - 0.734224\left[\ln\left(\frac{r_i}{r_o}\right)\right]^1 + 5.386236 \quad (4.40)$$

$$Nu_{oo} = 0.000038\left[\ln\left(\frac{r_i}{r_o}\right)\right]^6 + 0.002055\left[\ln\left(\frac{r_i}{r_o}\right)\right]^5 + 0.027243\left[\ln\left(\frac{r_i}{r_o}\right)\right]^4 + 0.160059\left[\ln\left(\frac{r_i}{r_o}\right)\right]^3 + 0.47620\left[\ln\left(\frac{r_i}{r_o}\right)\right]^2 + 0.764235\left[\ln\left(\frac{r_i}{r_o}\right)\right]^1 + 5.38494 \quad (4.41)$$

$$\theta_i^* = 0.000512\left[\ln\left(\frac{r_i}{r_o}\right)\right]^6 + 0.003322\left[\ln\left(\frac{r_i}{r_o}\right)\right]^5 + 0.016507\left[\ln\left(\frac{r_i}{r_o}\right)\right]^4 + 0.011277\left[\ln\left(\frac{r_i}{r_o}\right)\right]^3 + 0.065535\left[\ln\left(\frac{r_i}{r_o}\right)\right]^2 - 0.218175\left[\ln\left(\frac{r_i}{r_o}\right)\right]^1 + 0.346377 \quad (4.42)$$

$$\theta_o^* = 0.000005\left[\ln\left(\frac{r_i}{r_o}\right)\right]^6 - 0.000044\left[\ln\left(\frac{r_i}{r_o}\right)\right]^5 - 0.000765\left[\ln\left(\frac{r_i}{r_o}\right)\right]^4 + 0.001228\left[\ln\left(\frac{r_i}{r_o}\right)\right]^3 + 0.047348\left[\ln\left(\frac{r_i}{r_o}\right)\right]^2 + 0.220635\left[\ln\left(\frac{r_i}{r_o}\right)\right]^1 + 0.346075 \quad (4.43)$$

where θ_i^* is an influence coefficient that is employed to adjust the Nusselt number Nu_{ii} and θ_o^* is an influence coefficient that is employed to adjust the Nusselt number Nu_{oo}.

The Nusselt number on the inner and outer walls may now be calculated according to the following equations:

$$Nu_i = \frac{Nu_{ii}}{1 - \left(\frac{q_o''}{q_i''}\right)\theta_i^*} \quad (4.44)$$

and

$$Nu_o = \frac{Nu_{oo}}{1 - \left(\frac{q_i''}{q_o''}\right)\theta_o^*} \quad (4.44)$$

It has been shown by Du Toit (2004b:21-25) that the results obtained by means of Eqs (4.40), (4.41), (4.42), (4.43) and (4.44) are in excellent agreement with results that were reported by Kays and Crawford (1993:108-126).

4.6. Nusselt number for an annular duct (T)

No analytical solution has been found in the literature for an annular duct that is subjected to constant surface temperatures at both walls. It was pointed out by Dwyer (1963a:55) that at least one of the variables must be solved by making use of a trial and error approach.

4.7. Friction factor for an annular duct (H1 or T)

The analytical solution for calculating the friction factor for an annular duct that is subjected to the H1 or T boundary condition will be discussed in this section.

The mean velocity equation will be used as the starting point to derive an equation that gives the friction factor for an annular duct. It follows from Eq (4.2) that the mean velocity is given by:

$$w_m = \frac{\int_{r_i}^{r_o} \rho w r \; dr}{\int_{r_i}^{r_o} \rho r \; dr} \tag{4.45}$$

By expanding Eq (4.45) and by substituting $k = \frac{r_i}{r_o}$ into this equation, the following is obtained:

$$w_m = \frac{r_o^2}{8\mu}\frac{\partial p}{\partial z}\left[\left(1+k^2\right) - \frac{1-k^2}{\ln\left(\frac{1}{k}\right)}\right] \tag{4.46}$$

Substitute Eq (4.46) into Eq (4.20), whilst remembering that $D_h = 2(r_o - r_i)$ for an annular duct. Substituting the resulting equation and Eq (4.21) into Eq (4.22), gives:

$$\frac{1}{4} f \,\mathrm{Re}_D = \frac{1}{4}\frac{-(dp/dz)(2(r_o - r_i))}{\rho w_m^2 / 2} \times \frac{\rho w_m (2(r_o - r_i))}{\mu} = \frac{-2(dp/dz)(r_o - r_i)^2}{w_m \mu} \tag{4.47}$$

The friction factor remains the same for the H1 or T boundary conditions; therefore, Eq (4.47) is applicable for both of these conditions.

4.8. Summary

In this chapter analytical solutions were presented for calculating the:

- Nusselt number and friction factors for a circular duct subjected to the H1 boundary condition,
- friction factors for circular and annular ducts subjected to the H1 or T boundary condition,

- Nusselt numbers for an annular duct with one wall subjected to constant heat transfer whilst the other wall has no heat transfer.

Note that the Nusselt number for a circular duct that is subjected to the T boundary condition must be determined iteratively. No analytical solutions could be found in the literature for annular ducts that are subjected to the H1 or T boundary conditions at both walls. However, it was shown in this section that the Nusselt numbers for an annular duct subjected to the H1 boundary condition may be calculated with a set of 6^{th} order polynomial equations.

In the next chapter a one-dimensional finite element formulation is discussed that may be employed to determine the Nusselt numbers and friction factors for fully developed laminar flow in circular and annular ducts.

5. One-dimensional numerical solution: finite element formulation

In the previous chapter analytical equations for calculating Nusselt numbers and friction factors for fully developed laminar flow in circular and annular ducts were discussed. In the current chapter the one-dimensional finite element formulations to calculate the Nusselt numbers and friction factors, for fully developed laminar flow in annular and circular ducts subjected to the H1 or T boundary conditions, will be introduced and discussed.

5.1. Finite element formulation

The finite element formulation that may be used to solve the one-dimensional fully developed laminar flow in circular and annular ducts will be discussed in this section.

The finite element formulation was developed by assuming that changes in fluid properties with temperature over a cross-section are negligible. Firstly, Eq (3.1) is rewritten in the residual form and multiplied with a suitable weighting function (ν) where after it is integrated. The weak formulation for the conservation of momentum is now given by (Du Toit, 2004b:7):

$$\int_{r_i}^{r_o} \mu\ r \frac{\partial \nu}{\partial r}\frac{\partial w}{\partial r} dr = \int_{r_i}^{r_o} \nu\ r\left(-\frac{\partial p}{\partial z}\right) dr - \nu_{r_i} r_i \tau_i - \nu_{r_o} r_o \tau_o \tag{5.1}$$

with τ_i and τ_o respectively the inner and outer wall shear stresses.

In an analogous manner Eq (3.4) may be rewritten to yield the weak formulation for the conservation of energy (Du Toit, 2004b:7):

$$\int_{r_i}^{r_o} kr \frac{\partial \nu}{\partial r}\frac{\partial T}{\partial r} dr = \int_{r_i}^{r_o} \nu\ r\rho\ c_p w\left(-\frac{\partial T}{\partial z}\right) dr - \nu_{r_i} r_i q_i'' - \nu_{r_o} r_o q_o'' \tag{5.2}$$

Note that $r_i = 0$ for a circular duct. The finite element approximation for the axial velocity distribution $\left(w^N\right)$ is (Du Toit, 2004b:7):

$$w^N = \sum_{J=1}^{N} w_J \Phi_J = \sum_{e=1}^{E}\left[\sum_{j=1}^{NE} w_j^e \psi_j^e\right] \tag{5.3}$$

and the finite element approximation for the temperature distribution $\left(T^N\right)$ is (Du Toit, 2004b:7):

$$T^N = \sum_{J=1}^{N} T_J \Phi_J = \sum_{e=1}^{E} \left[\sum_{j=1}^{NE} T_j^e \psi_j^e \right] \tag{5.4}$$

where N, E , NE, Φ_J and ψ_j^e are the number of global nodes, the number of elements in the mesh, the number of nodal points associated with an element, the global interpolation function associated with global node J and the element interpolation function associated with the element node j respectively.

Substitute Eq (5.3) into Eq (5.1) and substitute Eq (5.4) into Eq (5.2). Apply the Galerkin method to these two newly obtained equations and integrate them. This leads to two sets of coupled linear algebraic equations. Both sets of linear algebraic equations are of the following matrix form (Du Toit, 2004b:7):

$$[K]\{U\} = \{F\} \tag{5.5}$$

where $[K]$, $\{U\}$ $\{F\}$ are respectively the coefficient matrix, the solution vector and the source vector. In the case of the momentum linear algebraic equations it follows that:

$$K_{IJ} = \sum_{e=1}^{E} \left[\int_e \mu \; r \frac{\partial \Phi_I}{\partial r} \frac{\partial \Phi_J}{\partial r} dr \right] \quad \text{for } 1 \le I \le N \text{ and } 2 \le J \le N-1 \tag{5.6}$$

$$F_I = \sum_{e=1}^{E} \left[\int_e \Phi_I r \left(\frac{\partial p}{\partial z} \right) dr \right] - \Phi_I\left(r_i\right) r_i \tau_i - \Phi_I\left(r_o\right) r_o \tau_o \quad \text{for } 1 \le I \le N \tag{5.7}$$

In this case the solution vector incorporates the axial velocities values. By using Gauss quadrature to evaluate the integrals in Eqs (5.6) and (5.7), the equations can be rewritten in numerical format as:

$$K_{IJ} = \sum_{e}^{RE} \sum_{i=1}^{NG} \left[\mu \left(\sum_{p=1}^{NE} \psi_p r_p \right) \frac{\partial \psi_I}{\partial \xi} \frac{1}{J_e} \frac{\partial \psi_J}{\partial \xi} \frac{1}{J_e} a_i J_e \right] \quad \text{for } 1 \le I \le N \text{ and } 2 \le J \le N-1 \tag{5.8}$$

$$F_I = \sum_{e}^{RE} \sum_{i=1}^{NG} \left[\psi_I \left(\sum_{p=1}^{NE} \psi_p r_p \right) \left(\frac{\partial p}{\partial z} \right) a_i J_e \right] + \psi_I\left(r_i\right) \; r_i \vec{\tau}_i + \psi_I\left(r_o\right) \; r_o \vec{\tau}_o \quad \text{for } 1 \le I \le N \tag{5.9}$$

with RE the relevant elements associated with node I, NG the number of Gauss integration points, J_e is the Jacobian of the relevant element and J is one of the nodal points associated with node I. Define $\vec{\tau}_i = -\tau_i$ and $\vec{\tau}_o = -\tau_o$. The Jacobian is the ratio between the lengths dr and $d\xi$, and is defined as:

$$J_e = \frac{element\ \ length}{2} \tag{5.10}$$

In this study the quadratic interpolation (shape) functions are used for the one-dimensional finite element formulations. The quadratic interpolation functions at the given Gauss points are (ψ_i) (Becker *et al*., 1981:197):

$$\psi_1 = 0.5\left(\xi^2 - \xi\right) \qquad \psi_2 = 1 - \xi^2 \qquad \psi_3 = 0.5\left(\xi^2 + \xi\right) \tag{5.11}$$

The third order Gaussian integration points (or natural coordinates) (ξ) are defined as (Taylor & Hughes, 1981:46):

$$\xi_1 = -\sqrt{0.6} \qquad \xi_2 = 0 \qquad \xi_3 = \sqrt{0.6} \tag{5.12}$$

and the Gaussian weighting factors (a_i) are defined as:

$$a_1 = \frac{5}{9} \qquad a_2 = \frac{8}{9} \qquad a_3 = \frac{5}{9} \tag{5.13}$$

Substituting Eqs (5.6) and (5.7) into Eq (5.5) gives the following matrix:

$$\begin{bmatrix} K_{11} & . & . & . & K_{1N} \\ . & . & . & . & . \\ . & . & . & . & . \\ . & . & . & . & . \\ K_{N1} & . & . & . & K_{NN} \end{bmatrix} \begin{bmatrix} w_1 \\ . \\ . \\ . \\ w_N \end{bmatrix} = \begin{bmatrix} F_1 + r_i \bar{\tau}_i \\ F_2 \\ . \\ F_{N-1} \\ F_N + r_o \bar{\tau}_o \end{bmatrix} \tag{5.14}$$

In the case of the energy linear algebraic equations the following prevail:

$$K_{IJ} = \sum_{e=1}^{E} \left[\int_e kr \frac{\partial \Phi_I}{\partial r} \frac{\partial \Phi_J}{\partial r} dr \right] \quad \text{for } 1 \le I \le N \text{ and } 1 \le J \le N-1 \tag{5.15}$$

$$F_I = \sum_{e=1}^{E} \left[\int_e \Phi_I r \rho\ c_p w \left(-\frac{\partial T}{\partial z} \right) dr \right] - \Phi_I(r_i) r_i q_i'' - \Phi_I(r_o) r_o q_o'' \quad \text{for } 1 \le I \le N \tag{5.16}$$

In this case the solution vector incorporates the temperature values. By using Gauss quadrature to evaluate the integrals in Eqs (5.15) and (5.16), the equations can be rewritten in numerical format as:

$$K_{IJ} = \sum_{e=1}^{E}\sum_{i=1}^{NE}\left[k\left(\sum_{p=1}^{NE}\psi_p r_p\right)\frac{\partial\psi_I}{\partial\xi}\frac{1}{J_e}\frac{\partial\psi_J}{\partial\xi}\frac{1}{J_e}a_i J_e \right] \text{ for } 1\le I\le N \text{ and } 2\le J\le N-1 \tag{5.17}$$

$$F_I = \sum_{e=1}^{E}\sum_{i=1}^{NE}\left[\psi_I\left(\sum_{p=1}^{NE}\psi_p r_p\right)\rho\ c_p w\left(-\frac{\partial T}{\partial z}\right)a_i J_e \right] + \psi_I(r_i)\ r_i\bar{q}_i'' + \psi_I(r_o)\ r_o\bar{q}_o'' \text{ for } 1\le I\le N \tag{5.18}$$

Define $\bar{q}_i'' = -q_i''$ and $\bar{q}_o'' = -q_o''$. Substituting Eqs (5.15) and (5.16) into Eq (5.5) gives the following matrix:

$$\begin{bmatrix} K_{11} & . & . & . & K_{1N} \\ . & . & . & . & . \\ . & . & . & . & . \\ . & . & . & . & . \\ K_{N1} & . & . & . & K_{NN} \end{bmatrix}\begin{bmatrix} T_1 \\ . \\ . \\ . \\ T_N \end{bmatrix} = \begin{bmatrix} F_1 + r_i\bar{q}_i'' \\ F_2 \\ . \\ F_{N-1} \\ F_N + r_o\bar{q}_o'' \end{bmatrix} \tag{5.19}$$

Note that the direct Gaussian elimination method (see Section 6.3) is now employed to solve all the equations mentioned in this section.

If the velocity values are known, the temperature values can be determined directly. Also, if the temperature values are known, the heat flux at the walls can be determined. Thus, after solving equations, Eqs (5.14) and (5.19), the velocity and temperature values will be known for all the nodes, as well as the heat flux and shear stress at the walls. This means that all the necessary information needed to determine the friction factor and Nusselt number are now known.

5.2. Nusselt number for a circular duct (H1)

A finite element formulation that may be used to determine the Nusselt numbers for fully developed laminar flow in circular ducts subjected to the H1 boundary condition and different sets of input data will be discussed in this section.

5.2.1. Wall temperature (T_o) and the temperature gradient $\left(\frac{\partial T}{\partial z}\right)$ are known

The finite element formulation that is used to solve an one-dimensional fully developed laminar flow, in a circular duct subjected to the H1 boundary condition, will be discussed when $\left(\frac{\partial T}{\partial z}\right)$ and the outer wall surface temperature (T_o) are known.

Firstly, rewrite Eq (5.14) in order to solve for $\bar{\tau}_o$ and the remaining axial velocities:

$$\begin{bmatrix} K_{11} & . & . & K_{1,N-1} & 0 \\ . & . & . & . & . \\ . & . & . & . & . \\ . & . & . & . & 0 \\ K_{N1} & . & . & K_{N,N-1} & -r_N \end{bmatrix} \begin{bmatrix} w_1 \\ . \\ . \\ w_{N-1} \\ \bar{\tau}_o \end{bmatrix} = \begin{bmatrix} F_1 - K_{1N} w_N + \bar{\tau}_i \, r_1 \\ F_2 - K_{2N} w_N \\ . \\ F_{N-1} - K_{N-1,N} w_N \\ F_N - K_{NN} w_N \end{bmatrix} \tag{5.20}$$

For a circular duct $\bar{\tau}_i = 0$ and $w_o = w_N = 0$. Note that $r_i = r_1 = 0$ and $r_o = r_N$.

Eq (5.19) should now be rewritten in order to solve $\bar{q}_o^{"}$ and the remaining temperatures:

$$\begin{bmatrix} K_{11} & . & . & K_{1,N-1} & 0 \\ . & . & . & . & . \\ . & . & . & . & . \\ . & . & . & . & 0 \\ K_{N1} & . & . & K_{N,N-1} & -r_N \end{bmatrix} \begin{bmatrix} T_1 \\ . \\ . \\ T_{N-1} \\ \bar{q}_o^{"} \end{bmatrix} = \begin{bmatrix} F_1 - K_{1N} T_N + \bar{q}_i^{"} r_1 \\ F_2 - K_{2N} T_N \\ . \\ F_{N-1} - K_{N-1,N} T_N \\ F_N - K_{NN} T_N \end{bmatrix} \tag{5.21}$$

Note that $\bar{q}_i^{"} = 0$ and $T_N = T_0$ for a circular duct.

By using the definition of the Nusselt number, it follows that:

$$Nu = \frac{hD_h}{k} = \frac{2hr_o}{k} \tag{5.22}$$

Eqs (5.20) - (5.22) were programmed into the one-dimensional C++ program for the computation of the Nusselt number under specified conditions.

5.2.2. The uniform heat flux $\left(\overline{q}_o^{"}\right)$ and reference temperature (T_o) at the wall are known

The finite element formulation for solving the one-dimensional fully developed laminar flow in a circular duct subjected to the H1 boundary condition, for the situation where $\overline{q}_o^{"}$ and T_o are known, will be discussed in this section.

The computations for $\overline{\tau}_o$ and the remaining axial velocities are performed in analogous manner as was described in Section 5.2.1. Since $\frac{\partial T}{\partial z}$ is unknown, whilst $\overline{q}_o^{"}$ is known, the matrices given in Section 5.2.1 can be rewritten in such a manner that $\frac{\partial T}{\partial z}$ is part of the solution vector $\{U\}$. After rewriting these matrices, the newly obtained source vector $\{F\}$ is given by the following:

$$F_I = \sum_{e=1}^{E}\sum_{i=1}^{NG}\left[\psi_I\left(\sum_{p=1}^{NE}\psi_p r_p\right)\rho\ c_p w a_i J_e\right] + r_i\overline{q}_i^{"} + r_o\overline{q}_o^{"} \qquad \text{for } 1 \le I \le N \tag{5.23}$$

In order to solve $\frac{\partial T}{\partial z}$ and the remaining temperatures, Eq (5.23) is used to rewrite Eq (5.19):

$$\begin{bmatrix} K_{11} & . & . & K_{1,N-1} & -F_1 \\ . & . & . & . & . \\ . & . & . & . & . \\ . & . & . & . & . \\ K_{N1} & . & . & K_{N,N-1} & -F_N \end{bmatrix}\begin{bmatrix} T_1 \\ . \\ . \\ T_N - 1 \\ \frac{\partial T}{\partial z} \end{bmatrix} = \begin{bmatrix} -K_{1N}T_N + \overline{q}_i^{"} r_1 \\ -K_{2N}T_N \\ . \\ -K_{N-1,N}T_N \\ -K_{NN}T_N + r_N\overline{q}_o^{"} \end{bmatrix} \tag{5.24}$$

Note that $r_i = 0$, $T_N = T_0$ and $\overline{q}_i^{"} = 0$. Also note that the last column of the coefficient matrix is an adapted form of F_I devoid of $\frac{\partial T}{\partial z}$. Eqs (4.8) and (4.10) may now be employed to determine the bulk temperature. It is also important to note that although $\overline{q}_i^{"}$ and $\overline{q}_o^{"}$ were defined as part of F_i and F_o in Eqs (5.18), they are separated in Eq (5.24) and are thus not part of F_i and F_o in this case. Eq (5.24) was programmed into the one-dimensional C++ program for the eventual computation of the Nusselt number under specified conditions.

5.3. Nusselt number for a circular duct (T)

The finite element formulation for solving the one-dimensional fully developed laminar flow in a circular duct subjected to the T boundary condition will be discussed in this section.

The computations for $\bar{\tau}_o$ and the remaining axial velocities are performed in an analogous manner as was described in Section 5.2.1. Eq. (4.15) can now, however, be substituted into the source vector of the energy equations to give:

$$F_I = \sum_{e=1}^{E}\sum_{i=1}^{NE}\left[\psi_I\left(\sum_{p=1}^{NE}\psi_p r_p\right)\rho\ c_p w\left(-\frac{\partial T_m}{\partial z}\right)\left(\frac{T_s - \sum_{p=1}^{NE}\psi_p T_p}{T_s - T_m}\right)a_i J_e\right] + r_i\bar{q}_i'' + r_o\bar{q}_o'' \text{ for } 1 \le I \le N \quad (5.25)$$

Unfortunately, the temperature values at some nodes as well as the bulk temperature are unknowns in this newly obtained source vector. It is, thus, necessary that an iterative procedure should be employed to solve the energy equations. Guessed values are, however, needed to initiate this iterative procedure. To obtain the desired guessed values, the energy equations of the circular duct are solved for the H1 boundary condition. Now, substitute Eq (5.25), instead of Eq (5.16), into the matrix from Eq (5.19) and determine T_m iteratively (by employing Eqs (4.8) and (4.10)). Use the newly obtained T_m value to determine the next T_m value and so forth, until the difference between two consecutive T_m values is less than 0.000 001. Note that $T_s = T_o$. Substitute the final T_m value into Newton's law of cooling and then use Newton's law of cooling together with Eq (5.22) to determine the Nusselt number.

Eq (5.25) and the process discussed above were programmed into the one-dimensional C++ program for the eventual computation of the Nusselt number under specified conditions.

5.4. Friction factor for a circular duct (H1 or T)

The computation of the friction factor for a one-dimensional flow in a circular duct subjected to the H1 or T boundary conditions will be discussed in this section.

The friction factor is defined as (White, 1988:306):

$$\frac{1}{4} f \,\mathrm{Re} = \frac{1}{4}\left(\frac{8\bar{\tau}}{\rho w_m^2} \times \frac{\rho w_m D_h}{\mu}\right) \quad (5.26)$$

Substitute the solutions given in Sections 5.1, or 5.2, into Eq (4.2) and determine w_m. Eq (5.26) may now be used to determine the friction factor.

Eq (5.26) was programmed into the one-dimensional C++ program for the computation of the friction factor.

5.5. Nusselt numbers for an annular duct (H1)

A finite element formulation that may be used to determine the Nusselt numbers for annular ducts subjected to the H1 boundary condition and different sets of input data will be discussed in this section. The different sets of input data used in the various computations are the following.

- When T_i, T_o and $\left(\frac{\partial T}{\partial z}\right)$ are known.
- When $\overline{q}_i^{"}$, $\overline{q}_o^{"}$ and T_o are known.
- When $\overline{q}_i^{"}$, T_o and $\left(\frac{\partial T}{\partial z}\right)$ are known.
- When $\overline{q}_o^{"}$, T_i and $\left(\frac{\partial T}{\partial z}\right)$ are known.

5.5.1. Inner (T_i) wall temperatures, outer (T_o) wall temperatures and the temperature gradient $\left(\frac{\partial T}{\partial z}\right)$ known

The finite element formulation for the one-dimensional fully developed laminar flow in an annular duct subjected to the H1 boundary condition when the values of T_i, T_o and $\left(\frac{\partial T}{\partial z}\right)$ are known will now be discussed.

Rewrite the matrix from Eq (5.14) in order to solve $\overline{\tau}_o$, $\overline{\tau}_i$ and the remaining axial velocities:

$$\begin{bmatrix} -r_1 & K_{12} & . & K_{1,N-1} & 0 \\ 0 & . & . & . & . \\ . & . & . & . & . \\ . & . & . & . & 0 \\ 0 & K_{N2} & . & K_{N,N-1} & -r_N \end{bmatrix} \begin{bmatrix} \bar{\tau}_i \\ w_2 \\ . \\ w_{N-1} \\ \bar{\tau}_o \end{bmatrix} = \begin{bmatrix} F_1 - K_{11}w_1 - K_{1N}w_N \\ F_2 - K_{21}w_1 - K_{2N}w_N \\ . \\ F_{N-1} - K_{N-1,1}w_1 - K_{N-1,N}w_N \\ F_N - K_{N,1}w_1 - K_{NN}w_N \end{bmatrix} \tag{5.27}$$

Remember that $w_o = w_N = 0$ and $w_i = w_1 = 0$ for an annulus, and also note that $r_i = r_1$ and $r_o = r_N$.

Rewrite the matrix from Eq (5.19) in order to solve for $\bar{q}_o''$, $\bar{q}_i''$ and the remaining temperatures:

$$\begin{bmatrix} -r_1 & K_{1,2} & . & K_{1,N-1} & 0 \\ 0 & . & . & . & . \\ . & . & . & . & . \\ . & . & . & . & 0 \\ 0 & K_{N,2} & . & K_{N,N-1} & -r_N \end{bmatrix} \begin{bmatrix} \bar{q}_i'' \\ . \\ . \\ T_{N-1} \\ \bar{q}_o'' \end{bmatrix} = \begin{bmatrix} F_1 - K_{11}T_1 - K_{1N}T_N \\ F_2 - K_{21}T_1 - K_{2N}T_N \\ . \\ F_{N-1} - K_{N-1,1}T_1 - K_{N-1,N}T_N \\ F_N - K_{N1}T_1 - K_{NN}T_N \end{bmatrix} \tag{5.28}$$

Note that $T_1 = T_i$ and $T_N = T_0$. Eqs (4.8) and (4.10) may now be used to determine the bulk temperature. The heat transfer coefficient at any wall (with wall temperature = T_s) is given as (Incropera & De Witt, 2005:493):

$$h = \frac{\bar{q}''}{T_s - T_m} \tag{5.29}$$

Substitute Eq (5.29) into Eq (5.22) and rewrite the Nusselt number equations so that:

$$Nu_i = \frac{\bar{q}_i''(2(r_o - r_i))}{(T_i - T_m)k} \tag{5.30}$$

and

$$Nu_o = \frac{\bar{q}_o''(2(r_o - r_i))}{(T_o - T_m)k} \tag{5.31}$$

Eqs (5.27) - (5.31) were programmed into the one-dimensional C++ program for the computation of the Nusselt numbers under specified conditions.

5.5.2. Inner $\left(\overline{q}_i^{"}\right)$ wall heat flux, outer wall heat flux $\left(\overline{q}_o^{"}\right)$ and the outer wall temperature (T_o) known

The finite element formulation for the one-dimensional fully developed laminar flow in an annular duct subjected to the H1 boundary condition, when the values of $\overline{q}_i^{"}$, $\overline{q}_o^{"}$ and T_o are known, will now be discussed.

The computation of $\overline{\tau}_i$, $\overline{\tau}_o$ and the remaining axial velocities are performed in an analogous manner as was described in Section 5.4.1. Rewrite the matrix in Eq (5.24) in order to solve for $\frac{dT}{dz}$ and the remaining temperatures:

$$\begin{bmatrix} K_{11} & . & . & K_{1,N-1} & -F_1 \\ . & . & . & . & . \\ . & . & . & . & . \\ . & . & . & . & -F_{N-1} \\ K_{N1} & . & . & K_{N,N-1} & -F_N \end{bmatrix} \begin{bmatrix} T_1 \\ . \\ . \\ T_{N-1} \\ \frac{dT}{dz} \end{bmatrix} = \begin{bmatrix} -K_{1N}T_N + \overline{q}_i^{"} r_1 \\ -K_{2N}T_N \\ . \\ -K_{N-1,N}T_N \\ -K_{NN}T_N + \overline{q}_o^{"} r_N \end{bmatrix} \tag{5.32}$$

Note that $T_N = T_0$. Eqs (4.8) and (4.10) may now be used to determine the bulk temperature, which can then be used together with Newton's law of cooling to determine the Nusselt numbers according to Eqs (5.30) and (5.31). Also note that although $\overline{q}_i^{"}$ and $\overline{q}_o^{"}$ were defined as part of F_i and F_o in Eqs (5.18), they are separated in Eq (5.32) and are thus not part of F_i and F_o in this case.

Eq (5.32) was programmed into the one-dimensional C++ program for the eventual computation of the Nusselt numbers under specified conditions.

5.5.3. Inner $\left(\overline{q}_i^{"}\right)$ wall heat flux, outer wall temperature (T_o) and the temperature gradient $\left(\frac{\partial T}{\partial z}\right)$ known

The finite element formulation for solving the one-dimensional fully developed laminar flow in an annular duct subjected to the H1 boundary condition, when the values of $\overline{q}_i^{"}$, T_o and $\left(\frac{\partial T}{\partial z}\right)$ are known, will now be discussed.

The computation of $\overline{\tau}_i$, $\overline{\tau}_o$ and the remaining axial velocities, are performed in an analogous manner as was described in Section 5.4.1. Rewrite the matrix in Eq (5.19) in order to solve for $\left(\overline{q}_o^{"}\right)$ and for the remaining temperatures:

$$\begin{bmatrix} K_{11} & . & . & K_{1,N-1} & 0 \\ . & . & . & . & . \\ . & . & . & . & . \\ . & . & . & . & 0 \\ K_{N1} & . & . & K_{N,N-1} & -r_N \end{bmatrix} \begin{bmatrix} T_1 \\ . \\ . \\ T_N - 1 \\ \overline{q}_o^{"} \end{bmatrix} = \begin{bmatrix} F_1 - K_{1N}T_N + \overline{q}_i^{"} r_1 \\ F_2 - K_{2N}T_N \\ . \\ F_{N-1} - K_{N-1,N}T_N \\ F_N - K_{NN}T_N \end{bmatrix} \tag{5.33}$$

Note that $T_N = T_0$. Eqs (4.8) and (4.10) may now be used to determine the bulk temperature, which can then be used together with Newton's law of cooling to determine the Nusselt numbers according to Eqs (5.30) and (5.31).

Eq (5.33) was programmed into the one-dimensional C++ program for the eventual computation of the Nusselt numbers under specified conditions.

5.5.4. Outer $\left(\overline{q}_o^{"}\right)$ wall heat flux, inner wall temperature (T_i) and the temperature gradient $\left(\frac{\partial T}{\partial z}\right)$ are known

The finite element formulation for solving the one-dimensional fully developed laminar flow in an annular duct subjected to the H1 boundary condition, when the values of $\overline{q}_o^{"}$, T_i and $\left(\frac{\partial T}{\partial z}\right)$ are known, will now be discussed.

The computation of $\overline{\tau}_i$, $\overline{\tau}_o$ and the remaining axial velocities are performed in an analogous manner as was described in Section 5.4.1. Rewrite Eq (5.19) in order to solve for $\left(\overline{q}_i^{"}\right)$ and for the remaining temperatures:

$$\begin{bmatrix} -r_1 & K_{12} & . & . & K_{1,N} \\ 0 & . & . & . & . \\ . & . & . & . & . \\ . & . & . & . & . \\ 0 & K_{N2} & . & . & K_{N,N} \end{bmatrix} \begin{bmatrix} \overline{q}_i^{"} \\ T_2 \\ . \\ . \\ T_o \end{bmatrix} = \begin{bmatrix} F_1 - K_{11}T_1 \\ F_2 - K_{21}T_1 \\ . \\ F_{N-1} - K_{N-1,1}T_1 \\ F_N - K_{N1}T_1 + \overline{q}_o^{"} r_N \end{bmatrix} \tag{5.34}$$

Note that $T_1 = T_i$. Eqs (4.8) and (4.10) may now be used to determine the bulk temperature, which can then be used together with Newton's law of cooling to determine the Nusselt numbers by employing Eqs (5.30) and (5.31).

Eq (5.34) was programmed into the one-dimensional C++ program for the eventual computation of the Nusselt numbers under specified conditions.

5.6. Friction factor for an annular duct (H1 or T)

The computation of the friction factor for the one-dimensional flow in an annular duct subjected to the H1 or T boundary conditions will be discussed in this section.

The perimeter average Fanning friction factor, f, for an annular duct, is given by the following equation (Shah & London, 1978:285):

$$f = \frac{f_i r_i + f_o r_o}{r_i + r_o} \tag{5.35}$$

Combining Eqs (5.35) and (5.26) gives rise to:

$$\frac{1}{4} f \,\mathrm{Re} = \frac{8(r_i \bar{\tau}_i + r_o \bar{\tau}_o)}{\rho w_m^2 (r_i + r_o)} \frac{\rho w_m D_h}{\mu} \tag{5.36}$$

Substitute the axial velocities (as determined in Sections 5.5.1, 5.5.2, 5.5.3 or 5.5.4) into Eq (4.2) in order to determine w_m. Eq (5.36) may now be used to determine the friction factor (¼fRe).

Eqs (5.35) and (5.36) were programmed into the one-dimensional C++ program for the computation of the friction factor.

5.7. Influence coefficients (Nu_{ii}, Nu_{oo}, θ_i^* and $\theta_o^{"}$) for an annulus with constant heat flux at both walls (with $\bar{q}_i^{"}$, $\bar{q}_o^{"}$ and T_o known)

The finite element formulation to calculate the influence coefficients in an annular duct subjected to the H1 boundary condition will be discussed in this section.

The following steps are used for calculating the influence coefficients.

1. Computation of $\overline{\tau}_i$, $\overline{\tau}_o$ and the remaining axial velocities are the same as were described in Section 5.4.1.
2. $\frac{\partial T}{\partial z}$ and the unknown temperatures are determined by solving Eq (5.32).
3. The bulk temperature may now be determined according to Eqs (4.8) and (4.10).
4. The bulk temperature may now be used to determine Nu_i and Nu_o according to Eqs (5.30) and (5.31).

After Nu_i and Nu_o are determined, the value of $\overline{q}_o^{"}$ is set equal to zero and the first three (above mentioned) steps are repeated to determine the influence coefficient Nu_{ii} according to Eq (5.30).In the next step $\overline{q}_i^{"}$ is set equal to zero and the first three steps are again repeated. The latter obtained results are now used to determine the influence coefficient Nu_{oo} according to Eq (5.31).

Equations for the remaining two influence coefficients, namely θ_i^* and θ_o^*, are obtained by rewriting the equations for Nu_i and Nu_o that was published by Incropera and De Witt (2005:520):

$$\theta_i^* = \left(1 - \frac{Nu_{ii}}{Nu_i}\right)\left(\frac{\overline{q}_i^{"}}{\overline{q}_o^{"}}\right) \tag{5.37}$$

$$\theta_o^* = \left(1 - \frac{Nu_{oo}}{Nu_o}\right)\left(\frac{\overline{q}_o^{"}}{\overline{q}_i^{"}}\right) \tag{5.38}$$

By using the above determined influence coefficients (Nu_{ii}, Nu_{oo}, θ_i^* and θ_o^*), the Nusselt number may be determined for annular ducts subjected to a constant heat flux on the inner wall as well as a different (or the same) constant heat flux on the outer wall.

5.8. A list of Nu_i and Nu_o at different radius ratios, with constant surface temperature at one wall whilst the other wall has no heat transfer (with T_i, T_o and $\left(\frac{\partial T_m}{\partial z}\right)$ known)

The process of creating a list of various annular Nusselt numbers (at different annular radius ratios) subjected to the T boundary condition at one wall, whilst the other wall has no heat transfer, will be discussed in this section. This list of annular Nusselt numbers was created for the situation when T_i, T_o and $\left(\frac{\partial T_m}{\partial z}\right)$ are known.

The computation of $\overline{\tau}_i$, $\overline{\tau}_o$ and the unknown axial velocities are performed in an analogous manner as was described in Section 5.4.1.

The temperatures $\overline{q}_o^{"}$ and $\overline{q}_i^{"}$ are determined by solving Eq (5.28). These determined temperatures may now be used as the required guessed values in the iteration process (see Section 5.2).

Eqs (4.8) and (4.10) are now used to determine the bulk temperature guessed value.

Iteration for Nu_i:

To determine Nu_i the source vector is defined by Eq (5.25) and the energy equations are rewritten in the same manner as was done for Eq (5.34).

Let $\overline{q}_o^{"} = 0$, use the guessed values (determined above) and Eq (5.34) to determine T_m iteratively. Repeat the iteration process until the difference between two consecutive bulk temperatures is less than 0.000 001. Note that $T_s = T_i$. in Eq (5.25). Eq (5.30) may now be used to determine Nu_i.

Iteration for Nu_o:

To determine Nu_o the source vector is defined by Eq (5.25) and the energy equations are rewritten in the same manner as was done for Eq (5.33).

Let $\overline{q}_i^{"} = 0$, use the guess values (determined above) and Eq (5.33) to determine T_m iteratively. Repeat the iteration process until the difference between two consecutive bulk temperatures is less 0.000 001. Note that $T_s = T_o$ in Eq (5.25). Eq (5.31) may now be used to determine Nu_o.

The processes described above were programmed into the one-dimensional C++ program for the computation of Nu_o.

5.9. Explicit and implicit computations for a T boundary condition

The choice between explicit or implicit computations for solving a flow problem subjected to the T boundary condition will be discussed in this section.

Eq (4.15) may be incorporated explicitly, or implicitly, in the governing equations for a fluid flow problem. In this study Eq (4.15) was employed implicitly as in Eq (5.25). To employ Eq (4.15) explicitly, Eq (5.25) must be rewritten as:

$$F_I = \sum_{e=1}^{E}\sum_{i=1}^{NE}\left[X_1 - X_2\right] + r_i\bar{q}_i'' + r_o\bar{q}_o'' \quad \text{for } 1 \le I \le N \tag{5.39}$$

where

$$X_1 = \psi_I\left(\sum_{p=1}^{NE}\psi_p r_p\right)\rho\ c_p w\left(-\frac{\partial T_m}{\partial z}\right)\left(\frac{T_s}{T_s - T_m}\right)a_i J_e$$

and

$$X_2 = \psi_I\left(\sum_{p=1}^{NE}\psi_p r_p\right)\rho\ c_p w\left(-\frac{\partial T_m}{\partial z}\right)\left(\frac{\sum_{p=1}^{NE}\psi_p T_p}{T_s - T_m}\right)a_i J_e$$

If X_2 is removed from eq (5.39) and then added to the K-values in the coefficient matrix, an explicit solution is obtained. The K-values equation may be written as:

$$K_{IJ} = \sum_{e=1}^{E}\sum_{i=1}^{NE}\left[\left(\sum_{p=1}^{NE}\psi_p r_p\right)\left(k\frac{\partial\psi_I}{\partial\xi}\frac{1}{J_e}\frac{\partial\psi_J}{\partial\xi}\frac{1}{J_e} + \psi_I\rho\ c_p w\left(-\frac{\partial T_m}{\partial z}\right)\left(\frac{1}{T_s - T_m}\right)\right)a_i J_e\right] \tag{5.40}$$

$$\text{for} \quad 1 \le I \le N \quad \text{and} \quad 2 \le J \le N-1$$

Although the explicit computations are theoretically correct, it was not suitable for this study. It was found that the extra addition to the K-values is practically infinitely small (i.e. 10 000 to 100 000 times smaller than the original coefficients), and the contribution of the newly added term is thus unfortunately negligible. This gives rise to inaccurate results if the explicit method is employed.

5.10. Summary

In this chapter the finite element formulation, that was used in the one-dimensional C++ program to solve the one-dimensional fully develop laminar flow in a duct, was introduced and discussed. Equations for the computation of the following were given.

- Nusselt number and friction factor for a circular duct subjected to a constant heat flux at the wall for different sets of input data.
- Nusselt number and friction factor for a circular duct subjected to a constant surface temperature at the wall.
- Nusselt numbers and friction factor for an annular duct subjected to a constant heat flux at the walls for different sets of input data.
- Nusselt numbers and friction factor for an annular duct with one wall subjected to a constant surface temperature whilst the other wall has no heat transfer.
- The influence coefficients that may be used to determine the Nusselt numbers for an annular duct subjected to constant heat fluxes at the walls.

The process that was used to generate a list of annular Nusselt numbers (for different annular radius ratios) subjected to a constant surface temperature was discussed. A reason was also given why only an implicit formulation was used for one-dimensional ducts that are subjected to the T boundary condition.

In the next chapter a finite element formulation is discussed that may be used to determine the Nusselt numbers and friction factors for two-dimensional fully developed laminar flow in ducts.

6. Two-dimensional numerical solution: finite element formulation

In the previous chapter the one-dimensional finite element formulations for calculating the Nusselt numbers and friction factors for fully developed laminar flow in annular and circular ducts were discussed. In this chapter the mesh creation for two-dimensional domains and the finite element formulation for calculating the friction factors and Nusselt numbers for two-dimensional fully developed laminar flow in ducts subjected to the H1, or T boundary, conditions will be discussed.

6.1. Finite element formulation

The finite element formulation that may be used to solve the two-dimensional fully developed laminar flow in ducts will be discussed in this section.

Firstly, Eq (3.8) is rewritten in the residual form and multiplied with a suitable weighting function where after it is integrated. The weak formulation for the conservation of momentum is now given by (Du Toit, 2002a:400):

$$\int_{\Omega} \mu \nabla \cdot \nabla w d\Omega = \int_{\Omega} v \left(-\frac{\partial p}{\partial z} \right) d\Omega - \int_{\Gamma} v \tau_w d\Gamma \tag{6.1}$$

with τ_w the wall shear stress.

In an analogous manner Eq (3.10) may be rewritten to yield the weak formulation for the conservation of energy (Du Toit, 2002a:401):

$$\int_{\Omega} k \nabla v \cdot \nabla T d\Omega = \int_{\Omega} v \rho c_p w \left(-\frac{\partial T}{\partial z} \right) d\Omega - \int_{\Gamma} v q_w^{"} d\Gamma \tag{6.2}$$

with $q_w^{"}$ the heat flux at the wall.

The finite element approximation for the axial velocity distribution $\left(w^N\right)$ and the temperature distribution $\left(T^N\right)$ is the same as in Eqs (5.3) and (5.4). Substitute Eq (5.3) into Eq (6.1) and substitute Eq (5.4) into Eq (6.2). Apply the Galerkin method to these two newly obtained equations and integrate them. This leads to two sets of coupled linear algebraic equations. The linear algebraic momentum equations can now be defined as (Du Toit, 2004b:7):

$$[K]\{U\} = \{F\} + \{\bar{\tau}\} \tag{6.3}$$

where $\{\bar{\tau}\}$ is a vector that incorporates the unknown shear stress values (τ) multiplied by the associated lengths (ds) for all the boundary nodal points and multiplied with (-1). The Jacobian is defined as the ratios between the various lengths *dx*, *dy*, $d\xi$ and $d\eta$. The Jacobian matrix at the i^{th} gauss integration point in the j^{th} element is given as (Du Toit, 2007:15):

$$\left[J_i^j\right] = \begin{bmatrix} \frac{\partial x_i^j}{\partial \xi} & \frac{\partial y_i^j}{\partial \xi} \\ \frac{\partial x_i^j}{\partial \eta} & \frac{\partial y_i^j}{\partial \eta} \end{bmatrix} = \begin{bmatrix} \sum_{k=1}^{NE} \frac{\partial \psi_k}{\partial \xi} x_i^j & \sum_{k=1}^{NE} \frac{\partial \psi_k}{\partial \xi} y_i^j \\ \sum_{k=1}^{NE} \frac{\partial \psi_k}{\partial \eta} x_i^j & \sum_{k=1}^{NE} \frac{\partial \psi_k}{\partial \eta} y_i^j \end{bmatrix} \tag{6.4}$$

with the coordinates of the integration points given as x_i^j and y_i^j. Use Eq (6.4) to compute the determinant for the Jacobian matrix of the integration point:

$$\det\left[J_i^j\right] = J_i^j[1;1] \times J_i^j[2;2] - J_i^j[1;2] \times J_i^j[2;1] \tag{6.5}$$

The adjoint of Eq (6.4) is defined as:

$$\text{Adjoint}_i^j = \begin{bmatrix} \frac{\partial y_i^j}{\partial \eta} & -\frac{\partial y_i^j}{\partial \xi} \\ -\frac{\partial x_i^j}{\partial \eta} & \frac{\partial x_i^j}{\partial \xi} \end{bmatrix} \tag{6.6}$$

Dividing Eq (6.6) by Eq (6.5) gives the inverse of the integration points' Jacobian matrix:

$$\left[J_i^j\right]^{-1} = \frac{1}{\det\left[J_i^j\right]} \begin{bmatrix} \frac{\partial y_i^j}{\partial \eta} & -\frac{\partial y_i^j}{\partial \xi} \\ -\frac{\partial x_i^j}{\partial \eta} & \frac{\partial x_i^j}{\partial \xi} \end{bmatrix} \tag{6.7}$$

The interpolation functions and Eq (6.7) may be used to determine the derivatives of the integration points:

$$\frac{\partial \psi_i^j}{\partial x} = \frac{\partial \psi_i}{\partial \xi} J_i^j[1;1]^{-1} + \frac{\partial \psi_i}{\partial \eta} J_i^j[1;2]^{-1} = \frac{\partial \psi_i}{\partial \xi}\frac{\partial y_i^j}{\partial \eta} - \frac{\partial \psi_i}{\partial \eta}\frac{\partial y_i^j}{\partial \xi} \tag{6.8}$$

$$\frac{\partial \psi_i^j}{\partial y} = \frac{\partial \psi_i}{\partial \xi} J_i^j[2;1]^{-1} + \frac{\partial \psi_i}{\partial \eta} J_i^j[2;2]^{-1} = -\frac{\partial \psi_i}{\partial \xi}\frac{\partial x_i^j}{\partial \eta} + \frac{\partial \psi_i}{\partial \eta}\frac{\partial x_i^j}{\partial \xi} \tag{6.9}$$

Use Eqs (6.5) and the Gaussian weighting factors to define the integration area factor (A_i^j) for the i^{th} gauss integration point in the j^{th} element as (Du Toit, 2007:16):

$$A_i^j = \det\left[J_i^j\right] a_i \quad \text{with} \quad 1 \le i \le 9 \tag{6.10}$$

Use Eqs (6.8), (6.9), (6.10) and the interpolation functions to define the source vector for the conservation of momentum (see Eqs (6.1) and (6.3)):

$$F_I = \sum_{e}^{RE}\sum_{n=1}^{NG} A_n^e \psi_I \frac{\partial p}{\partial z} \tag{6.11}$$

where ψ_I is the interpolation function for node I at the n^{th} integration point. Note that Eq (6.11) does not include any boundary information. Next, Eqs (6.8), (6.9), and (6.10) are used to define the coefficients matrix for the conservation of momentum as (see Eqs (6.1) and (6.3)):

$$K_{IJ} = \sum_{e}^{RE}\sum_{n=1}^{NG} \mu A_n^e \left(\frac{\partial \psi_I^e}{\partial x}\frac{\partial \psi_J^e}{\partial x} + \frac{\partial \psi_I^e}{\partial y}\frac{\partial \psi_J^e}{\partial y} \right) \tag{6.12}$$

Eq (6.3) can now be written in matrix format, to get for example:

$$\begin{bmatrix} K_{11} & \cdot & \cdot & \cdot & K_{1N} \\ \cdot & \cdot & \cdot & \cdot & \cdot \\ \cdot & \cdot & \cdot & \cdot & \cdot \\ \cdot & \cdot & \cdot & \cdot & \cdot \\ \cdot & \cdot & \cdot & \cdot & \cdot \\ \cdot & \cdot & \cdot & \cdot & \cdot \\ K_{N1} & \cdot & \cdot & \cdot & K_{NN} \end{bmatrix} \begin{bmatrix} w_1 \\ w_2 \\ w_3 \\ \cdot \\ w_{N-2} \\ w_{N-1} \\ w_N \end{bmatrix} = \begin{bmatrix} F_1 \\ F_2 \\ F_3 \\ \cdot \\ F_{N-2} \\ F_{N-1} \\ F_N \end{bmatrix} + \begin{bmatrix} ds_1\bar{\tau}_1 \\ ds_2\bar{\tau}_2 \\ 0 \\ \cdot \\ 0 \\ ds_{N-1}\bar{\tau}_{N-1} \\ ds_N\bar{\tau}_N \end{bmatrix} \tag{6.13}$$

Note that Eqs (6.13) is only an example, since Eq (6.13) has no specific number of inner or outer boundary nodes, also note that the boundary nodes can be positioned anywhere in the matrix, it does not have to be positioned at the end points. After solving Eq (6.13) the velocity values at all the nodes will be known. The axial velocity for the i^{th} gauss integration point in the j^{th} element is given by the following:

$$w_{ji} = \sum_{n=1}^{NE} \psi_n w_n^j \tag{6.14}$$

The linear algebraic energy equations may now be defined as (Du Toit, 2004b:7):

$$[K]\{U\} = \{F\} + \{\overline{q}^{"}\} \tag{6.15}$$

where $\{\overline{q}^{"}\}$ is a vector that incorporates the unknown heat flux values multiplied by associated lengths (ds) for all the boundary nodal points and multiplied with (-1). Now, by using density, specific heat, temperature gradient, interpolation functions and Eqs (6.10) and (6.14) to define the source vector for the conservation of energy, it follows that (see Eqs (6.2) and (6.15)):

$$F_I = \sum_{e}^{RE} \sum_{n=1}^{NG} \left[\rho \; c_p \psi_I \left(\sum_{p=1}^{NE} \psi_p w_p^e \right) \frac{\partial T}{\partial z} A_n^e \right] \tag{6.16}$$

By using Eqs (6.8) - (6.10), the *K*-values may be written for the conservation of energy as (see Eqs (6.2) and (6.15)):

$$K_{IJ} = \sum_{e}^{RE} \sum_{n=1}^{NG} k A_n^e \left(\frac{\partial \psi_I^e}{\partial x} \frac{\partial \psi_J^e}{\partial x} + \frac{\partial \psi_I^e}{\partial y} \frac{\partial \psi_J^e}{\partial y} \right) \tag{6.17}$$

Eq (6.15) can now be written in matrix format, to get for example:

$$\begin{bmatrix} K_{11} & \cdot & \cdot & \cdot & K_{1N} \\ \cdot & \cdot & \cdot & \cdot & \cdot \\ \cdot & \cdot & \cdot & \cdot & \cdot \\ \cdot & \cdot & \cdot & \cdot & \cdot \\ \cdot & \cdot & \cdot & \cdot & \cdot \\ \cdot & \cdot & \cdot & \cdot & \cdot \\ K_{N1} & \cdot & \cdot & \cdot & K_{NN} \end{bmatrix} \begin{bmatrix} T_1 \\ T_2 \\ T_3 \\ \cdot \\ T_{N-2} \\ T_{N-1} \\ T_N \end{bmatrix} = \begin{bmatrix} F_1 \\ F_2 \\ F_3 \\ \cdot \\ F_{N-2} \\ F_{N-1} \\ F_N \end{bmatrix} + \begin{bmatrix} ds_1 \overline{q}_1^{"} \\ ds_2 \overline{q}_2^{"} \\ 0 \\ \cdot \\ 0 \\ ds_{N-1} \overline{q}_{N-1}^{"} \\ ds_N \overline{q}_N^{"} \end{bmatrix} \tag{6.18}$$

Note that Eqs (6.18) is only an example, since Eq (6.18) has no specific number of inner or outer boundary nodes. Also note that the boundary nodes can be positioned anywhere in the matrix, it does not have to be positioned at the end points. After solving Eq (6.18) the temperature values at all the nodes will be known.

6.2. Create the mesh of the domain

The creation of the mesh of a two-dimensional domain will now be discussed.

The two-dimensional domain that will be analysed is firstly defined by blocks (for an example, see Figure 6.1), boundary lines and nodal points that may now be used to determine the final mesh with a C++ mesh program. The C++ mesh program requires the following initial information.

- Number of blocks.
- Number of outer boundary lines (these are the lines that define the outer boundary of the domain).
- Number of inner boundary lines (these are the lines that define the inner boundary of the domain).
- Total number of key nodal points used to define all the blocks (each block is defined by eight nodal points).
- The x- and y-coordinates of each nodal point.
- Which key nodal points define which block.
- Which key nodal points define which outer boundary line.
- Which key nodal points define which inner boundary line.
- The number of x- and y-divisions for each block (needed to create the final mesh).
- The number of line divisions for each boundary line (needed to create the final mesh).

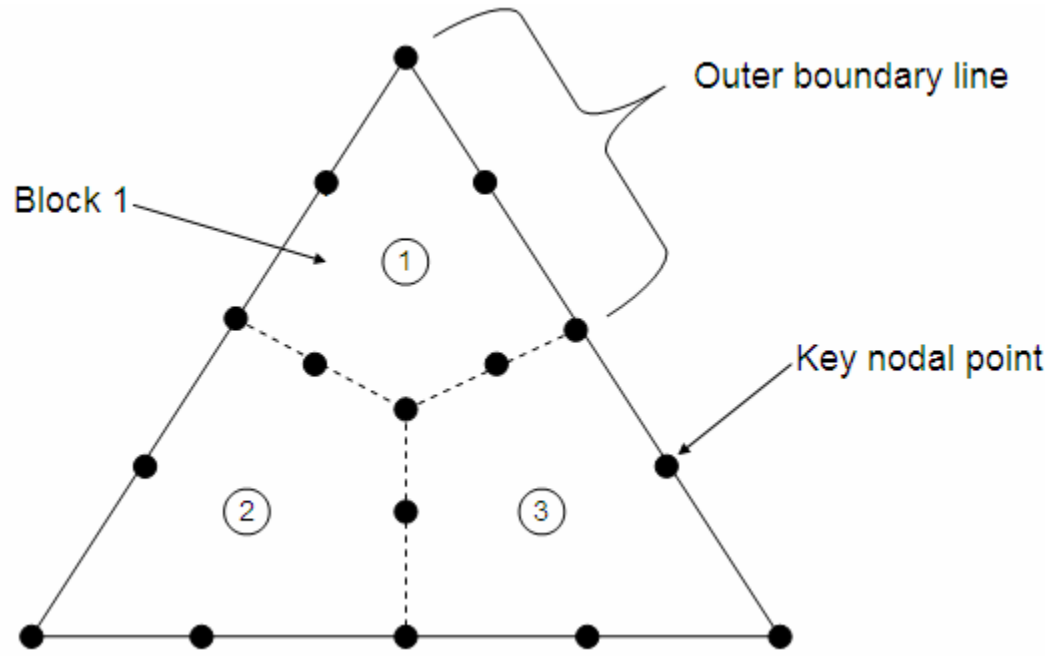

Figure 6.1. Triangle divided into three blocks.

The following steps are used to create the final mesh.

1. Use the specified *x*- and *y*-divisions to define new nodal points which will at a later stage be used to divide each block into a number of elements. Each of these elements is defined by nine nodal points. In order to define the natural coordinates of the nodes in a block, the block should be defined from (-1;-1) to (1;1), as is illustrated in Figure 6.2.

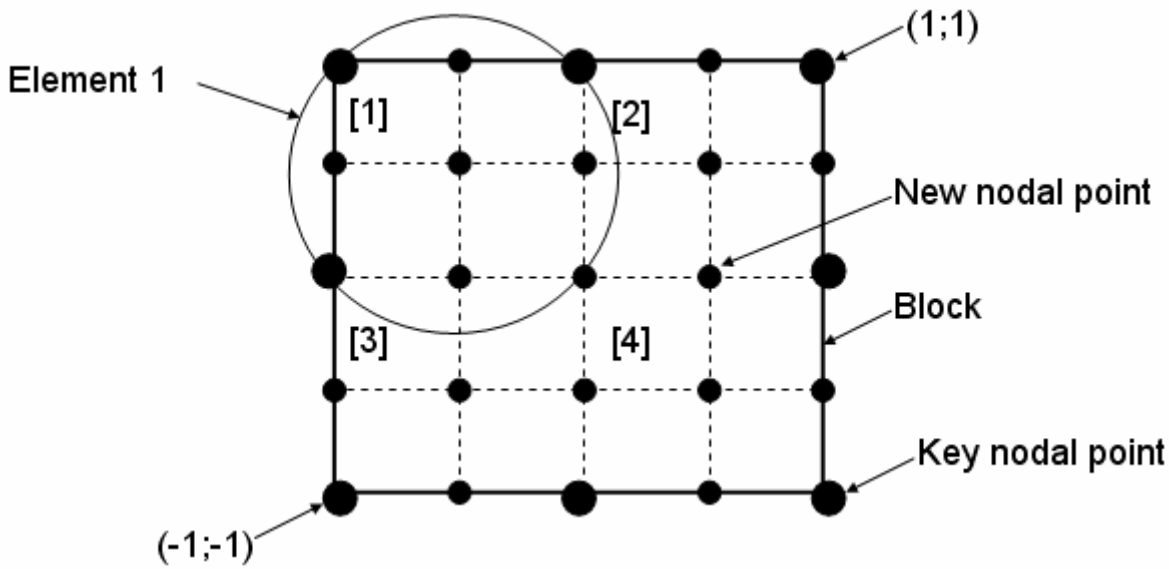

Figure 6.2. A block divided into four elements by using natural coordinates.

2. Use the specified line divisions to define new nodal points which will at a later stage be used to divide each boundary line into line elements, using three nodal points to define an element line. In order to define the natural coordinates of the nodes on a line, the line must be defined from (-1) to (1) as is illustrated in Figure 6.3.

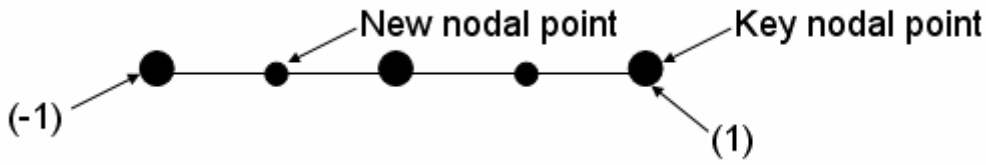

Figure 6.3. Boundary line divide into two element lines.

3. Define the interpolation (shape) functions for each nodal point by using the eight-node quadrilateral interpolation functions for finite elements (Becker *et al*., 1981:198):

$$\begin{aligned}
\psi_1 &= \frac{1}{4}(1-\xi)(1-\eta)(-1-\xi-\eta) & \psi_2 &= \frac{1}{2}(1-\xi^2)(1-\eta) \\
\psi_3 &= \frac{1}{4}(1+\xi)(1-\eta)(-1+\xi-\eta) & \psi_4 &= \frac{1}{2}(1+\xi)(1-\eta^2) \\
\psi_5 &= \frac{1}{4}(1+\xi)(1+\eta)(-1+\xi+\eta) & \psi_6 &= \frac{1}{2}(1-\xi^2)(1+\eta) \\
\psi_7 &= \frac{1}{4}(1-\xi)(1+\eta)(-1-\xi+\eta) & \psi_8 &= \frac{1}{2}(1-\xi)(1-\eta^2)
\end{aligned} \tag{6.19}$$

where ξ and η are respectively the natural *x*- and *y*-coordinates for each nodal point.

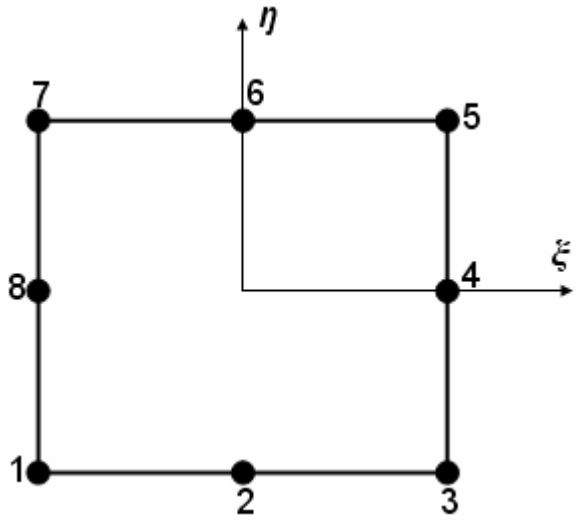

Figure 6.4. A block with nodal point numbering for an eight-node quadrilateral finite element.

4. Eq (6.19) is used to define the coordinates of each nodal point as:

$$x = \sum_{j=1}^{8} x_j \psi_j \qquad\qquad y = \sum_{j=1}^{8} y_j \psi_j \tag{6.20}$$

where x_j and y_j respectively represents the coordinates of the key nodal points in the block that incorporates x and y (see Figure 6.4).

5. Define the coordinates for the nodal points on the lines (boundaries) by using the coordinates of the three key nodal points which define the boundary line together with Eq (6.19):

$$x = \sum_{j=1}^{3} x_j \psi_j \qquad\qquad y = \sum_{j=1}^{3} y_j \psi_j \tag{6.21}$$

Note that $\eta = -1$ in Eq (6.19) for the line nodes.

6. Use the specified x- and y-divisions to define which nodal points define which element.
7. Use the specified line divisions to define which nodal points define which line element
8. Since each block and boundary line was treated separately when their new nodal points were defined, there may be identical nodal points with different numbers. For example, two neighbouring elements which are part of two different blocks will share a line (and thus nodal points), whilst each element may have different numbers for the same nodal points. This may also be the case for an element and a line element that share the same line (and thus nodal points). A specific procedure is now followed to check which nodal points have more than one number. This is done by comparing the coordinates of each node with the coordinates of all the other nodes.
9. A procedure is now used to renumber each nodal point so that each nodal point will only have one number.

The following information is now written to an ".inp" file which will at a later stage be used as input for the two-dimensional C++ program.

- Number of elements.
- Number of boundary (line) elements.
- Number of nodal points.

- Number of dimensions.
- Number of essential boundary conditions for velocity.
- Number of essential boundary conditions for temperature.
- Viscosity.
- Axial pressure gradient.
- Density.
- Conductivity.
- Specific heat.
- Axial temperature gradient.
- Number of inner boundary elements.
- Each nodal point number together with its x- and y-coordinates.
- Each element number as well as the numbers of all nine nodal points that define that element.
- The element numbers of each inner boundary as well as the numbers of all three the nodal points that define that inner boundary element and an inner boundary flag variable.
- The element numbers of each outer boundary as well as the numbers of all three the nodal points that define that outer boundary element and an outer boundary flag variable.
- The number of each boundary nodal point, a velocity flag variable and the velocity at the specific nodal point.
- The number of each boundary nodal point, a temperature flag variable and the temperature at the specific nodal point.

A flag variable is used to classify the data in a program. For example, if the flag variable of a boundary element is equal to one, then it means that the element is an outer boundary element. On the other hand, if the flag variable is equal to two, then it means that the element is an inner boundary element.

After the mesh has been created the finite element method may be used to solve the fully developed laminar flow in the domain.

6.3. Two-dimensional finite element program

A finite element formulation that may be used in the two-dimensional C++ program to solve the two-dimensional fully developed laminar flow in a duct will be further discussed in this section. All the input needed for the two-dimensional C++ program is provided by the C++ mesh program.

In the approach being followed the velocities were first solved and then the temperatures. During each solution step there was one variable per nodal point that had to be solved. A direct relationship was employed between the variable number and the nodal point number.

The following steps are used in the program to process the input data.

- Create a local matrix (called LTEMP[ ]) that counts the number of off-diagonal coefficients in each row and extracts the column numbers of the coefficients. This matrix is then used to create the LGCOL[ ] and LGROW vectors (see next bullet point). The first row in each column of LTEMP[ ] gives the off-diagonal coefficients count for the corresponding row (in the global coefficient matrix), whilst the rest of the rows are the off-diagonal column numbers. For example: LTEMP[1;2] = 9 in Eq (6.22), which means that row 2 in the global coefficient matrix has 9 off-diagonal coefficients, and LTEMP[2,...,10;2] are the column numbers of the off-diagonal coefficients.

$$\text{LTEMP}[\,] = \begin{bmatrix} 8 & 9 & 8 & .. \\ 1 & 3 & 16 & .. \\ 2 & 4 & 14 & .. \\ 3 & 5 & 7 & .. \\ 13 & 6 & 8 & .. \\ 16 & 7 & 9 & .. \\ 15 & 14 & 10 & .. \\ 11 & 16 & 11 & .. \\ 12 & 13 & 15 & .. \\ & 18 & & .. \end{bmatrix} \tag{6.22}$$

  Note that the values inside each column are not sorted.

- Use LTEMP[ ] to create two vectors, namely (LGCOL [ ] and LGROW [ ]). LGCOL[ ] is a vector that incorporates the column numbers of the off-diagonal coefficients in the global coefficient matrix; the column numbers of the off-diagonal coefficients for the first row (in the global coefficient matrix) are written in the first LGCOL [ ] columns, then the column numbers

of the second row are written in the next LGCOL [ ] columns , and so forth (as can be seen in Eq (6.23)).

$$\text{LGCOL}[] = [1 \;\; 2 \;\; 3 \;\; 11 \;\; 13 \;\; 15 \;\; 16 \;\; 17 \;\; 3 \;\; 4 \;\; 5 \;\; 6 \;\; 7 \;\; 13 \;\; 14 \;\; 16 \;\; 18 \;\; 7 \;\; 8 \;\; 9 \;\; 10 \;\; .....] \tag{6.23}$$

Note that the column numbers of each row are now sorted; for example, the column numbers of row number 2 are now given as 3; 4; 5; 6; 7; 13; 14; 16; 18 (and they are to be found in LGCOL[9,.....,17]). Vector LGROW[ ] is an address vector and it is employed to indicate which row's column numbers begins in which column (in LGROW[ ]). For example, LGROW [2] = 9, in Eq (6.24), implies that the column numbers of the second row begins in LGCOL[9]).

$$\text{LGROW}[\,] = [1 \quad 10 \quad 19 \quad ....] \tag{6.24}$$

LGCOL [ ] and LGROW [ ] are used to locate all the coefficients that are associated with any specific node.

Create a matrix (called LADRES[ ]) for each element. Each row in LADRES[ ] represents a part of a global equation and contains the addresses (numbers) of the diagonal and off-diagonal terms associated with the element.

The nine-node quadrilateral interpolation (shape) functions are being used for the two-dimensional finite element formulations in this program. The interpolation functions for a nine-node quadrilateral finite element are (Becker *et al*., 1981:198):

$$\begin{aligned}
\psi_1 &= \frac{1}{4}\left(\xi^2 - \xi\right)\left(\eta^2 - \eta\right) & \psi_6 &= \frac{1}{2}\left(\xi^2 + \xi\right)\left(1 - \eta^2\right) \\
\psi_2 &= \frac{1}{4}\left(\xi^2 + \xi\right)\left(\eta^2 - \eta\right) & \psi_7 &= \frac{1}{2}\left(1 - \xi^2\right)\left(\eta^2 + \eta\right) \\
\psi_3 &= \frac{1}{4}\left(\xi^2 + \xi\right)\left(\eta^2 + \eta\right) & \psi_8 &= \frac{1}{2}\left(\xi^2 - \xi\right)\left(1 - \eta^2\right) \\
\psi_4 &= \frac{1}{4}\left(\xi^2 - \xi\right)\left(\eta^2 + \eta\right) & \psi_9 &= \left(1 - \xi^2\right)\left(1 - \eta^2\right) \\
\psi_5 &= \frac{1}{2}\left(1 - \xi^2\right)\left(\eta^2 - \eta\right)
\end{aligned} \tag{6.25}$$

The derivatives of Eq (6.25) with respect to the natural coordinates are given by the following:

$$
\begin{aligned}
\frac{\partial \psi_1}{\partial \xi} &= \frac{1}{4}(2\xi - 1)(\eta^2 - \eta) & \frac{\partial \psi_1}{\partial \eta} &= \frac{1}{4}(\xi^2 - \xi)(2\eta - 1) \\
\frac{\partial \psi_2}{\partial \xi} &= \frac{1}{4}(2\xi + 1)(\eta^2 - \eta) & \frac{\partial \psi_2}{\partial \eta} &= \frac{1}{4}(\xi^2 + \xi)(2\eta - 1) \\
\frac{\partial \psi_3}{\partial \xi} &= \frac{1}{4}(2\xi + 1)(\eta^2 + \eta) & \frac{\partial \psi_3}{\partial \eta} &= \frac{1}{4}(\xi^2 + \xi)(2\eta + 1) \\
\frac{\partial \psi_4}{\partial \xi} &= \frac{1}{4}(2\xi - 1)(\eta^2 + \eta) & \frac{\partial \psi_4}{\partial \eta} &= \frac{1}{4}(\xi^2 - \xi)(\eta + 1) \\
\frac{\partial \psi_5}{\partial \xi} &= -2\xi(\eta^2 - \eta) & \frac{\partial \psi_5}{\partial \eta} &= \frac{1}{2}(1 - \xi^2)(\eta - 1) \\
\frac{\partial \psi_6}{\partial \xi} &= \frac{1}{2}(2\xi + 1)(1 - \eta^2) & \frac{\partial \psi_6}{\partial \eta} &= \frac{1}{2}(\xi^2 + \xi)(-2\eta) \\
\frac{\partial \psi_7}{\partial \xi} &= -\xi(\eta^2 + \eta) & \frac{\partial \psi_7}{\partial \eta} &= \frac{1}{2}(1 - \xi^2)(2\eta + 1) \\
\frac{\partial \psi_8}{\partial \xi} &= \frac{1}{2}(2\xi - 1)(1 - \eta^2) & \frac{\partial \psi_8}{\partial \eta} &= \frac{1}{2}(\xi^2 - \xi)(-2\eta) \\
\frac{\partial \psi_9}{\partial \xi} &= -2\xi(1 - \eta^2) & \frac{\partial \psi_9}{\partial \eta} &= (1 - \xi^2)(-2\eta)
\end{aligned}
\tag{6.26}
$$

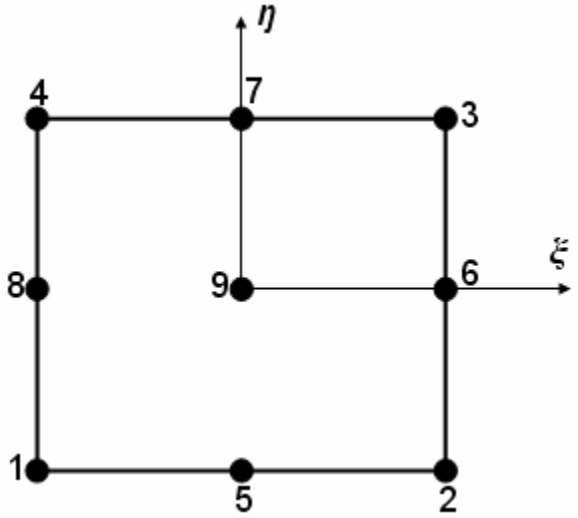

Figure 6.5. A Block with nodal point numbering for a nine-node quadrilateral finite element.

The ninth order Gaussian integration points (natural coordinates) and weights (a_i) are defined as (Becker *et al*., 1981:199):

$$\begin{aligned}
&\xi_1 = -\sqrt{0.6} \qquad \xi_4 = -\sqrt{0.6} \qquad \xi_7 = 0 \\
&\xi_2 = \sqrt{0.6} \qquad \xi_5 = 0 \qquad \xi_8 = -\sqrt{0.6} \\
&\xi_3 = \sqrt{0.6} \qquad \xi_6 = \sqrt{0.6} \qquad \xi_9 = 0 \\
&\eta_1 = -\sqrt{0.6} \qquad \eta_4 = \sqrt{0.6} \qquad \eta_7 = \sqrt{0.6} \\
&\eta_2 = -\sqrt{0.6} \qquad \eta_5 = -\sqrt{0.6} \qquad \eta_8 = 0 \\
&\eta_3 = \sqrt{0.6} \qquad \eta_6 = 0 \qquad \eta_9 = 0
\end{aligned} \tag{6.27}$$

and

$$\begin{aligned}
&a_1 = \frac{25}{81} \qquad a_4 = \frac{25}{81} \qquad a_7 = \frac{40}{81} \\
&a_2 = \frac{25}{81} \qquad a_5 = \frac{40}{81} \qquad a_8 = \frac{40}{81} \\
&a_3 = \frac{25}{81} \qquad a_6 = \frac{40}{81} \qquad a_9 = \frac{64}{81}
\end{aligned} \tag{6.28}$$

The source vector for the conservation of momentum was given in Eq (6.11) as:

$$F_I = \sum_{e}^{RE} \sum_{n=1}^{NG} A_n^e \psi_I \frac{\partial p}{\partial z} \tag{6.29}$$

where $NG = 9$ is the number of integration points. The LADRES[ ] matrices of the relevant elements are used to locate the nodal points associated with node *I*. The coefficients matrix for the conservation of momentum was given in Eq (6.12) as:

$$K_{IJ} = \sum_{e}^{RE} \sum_{n=1}^{NG} \mu A_n^e \left(\frac{\partial \psi_I^e}{\partial x} \frac{\partial \psi_J^e}{\partial x} + \frac{\partial \psi_I^e}{\partial y} \frac{\partial \psi_J^e}{\partial y} \right) \tag{6.30}$$

In the two-dimensional C++ program the coefficient matrix is divided into two vectors, namely (GDIAG[ ] and GCOEF[ ]): GDIAG[ ] is a vector that incorporates all the diagonal values for the coefficient matrix, for example, the third value of GDIAG[ ] is also the third diagonal value of the coefficient matrix. GCOEF[ ] consists of the *K*-values associated with the column numbers in LGCOL[ ],and the value of GCOEF[4] is, for example, the K-value for LGCOL[4]. Note that GDIAG[] and GCOEF[] is a sparse compact row storage scheme and therefore represent the coefficient matrix [*K*]. An example of the linear algebraic momentum equations in matrix format was given in Eq (6.13) as:

$$\begin{bmatrix} K_{11} & \cdot & \cdot & \cdot & K_{1N} \\ \cdot & \cdot & \cdot & \cdot & \cdot \\ \cdot & \cdot & \cdot & \cdot & \cdot \\ \cdot & \cdot & \cdot & \cdot & \cdot \\ \cdot & \cdot & \cdot & \cdot & \cdot \\ \cdot & \cdot & \cdot & \cdot & \cdot \\ K_{N1} & \cdot & \cdot & \cdot & K_{NN} \end{bmatrix} \begin{bmatrix} w_1 \\ w_2 \\ w_3 \\ \cdot \\ w_{N-2} \\ w_{N-1} \\ w_N \end{bmatrix} = \begin{bmatrix} F_1 \\ F_2 \\ F_3 \\ \cdot \\ F_{N-2} \\ F_{N-1} \\ F_N \end{bmatrix} + \begin{bmatrix} ds_1\bar{\tau}_1 \\ ds_2\bar{\tau}_2 \\ 0 \\ \cdot \\ 0 \\ ds_{N-1}\bar{\tau}_{N-1} \\ ds_N\bar{\tau}_N \end{bmatrix} \tag{6.31}$$

GDIAG[] and GCOEF[] are now used to locate the relevant *K* values so that the Dirichlet boundary conditions may be subtracted from the *F*-vector (Eq (6.29)). It follows now that Eq (6.31) can be rewritten as:

$$\begin{bmatrix} 1 & 0 & K_{13} & \cdots & K_{1,N-2} & 0 & 0 \\ 0 & 1 & K_{23} & \cdots & K_{2,N-2} & 0 & 0 \\ 0 & 0 & K_{33} & \cdots & K_{3,N-2} & 0 & 0 \\ \cdots & \cdots & \cdots & \cdots & \cdots & \cdots & \cdots \\ 0 & 0 & K_{N-2,3} & \cdots & K_{N-2,N-2} & 0 & 0 \\ 0 & 0 & K_{N-1,3} & \cdots & K_{N-1,N-2} & 1 & 0 \\ 0 & 0 & K_{N3} & \cdots & K_{N,N-2} & 0 & 1 \end{bmatrix} \begin{bmatrix} -ds_1\bar{\tau}_1 \\ -ds_2\bar{\tau}_2 \\ w_3 \\ \cdots \\ w_{N-2} \\ -ds_{N-1}\bar{\tau}_{N-1} \\ -ds_N\bar{\tau}_N \end{bmatrix} = \begin{bmatrix} F_1 - K_{11}w_1 - K_{12}w_2 - K_{1,N-1}w_{N-1} - K_{1N}w_N \\ F_2 - K_{21}w_1 - K_{22}w_2 - K_{2,N-1}w_{N-1} - K_{2N}w_N \\ F_3 - K_{31}w_1 - K_{32}w_2 - K_{3,N-1}w_{N-1} - K_{3N}w_N \\ \cdots \\ F_{N-2} - K_{N-2,1}w_1 - K_{N-2,2}w_2 - K_{N-2,N-1}w_{N-1} - K_{N-2,N}w_N \\ F_{N-1} - K_{N-1,1}w_1 - K_{N-1,2}w_2 - K_{N-1,N-1}w_{N-1} - K_{N-1,N}w_N \\ F_N - K_{N1}w_1 - K_{N2}w_2 - K_{N,N-1}w_{N-1} - K_{NN}w_N \end{bmatrix} \tag{6.32}$$

Gaussian elimination is now used to solve the solution vector (which contains all the unknown variables). Note, however, that the axial pressure gradient as well as the axial boundary velocities $\left(w_1 = w_1 = w_{N-1} = w_N = 0\right)$ is known. After Forward reduction was applied, Eq (6.32) becomes:

$$\begin{bmatrix} 1 & K^*_{12} & K^*_{13} & .... & K^*_{1,N-2} & K^*_{1,N-1} & K^*_{1N} \\ 0 & 1 & K^*_{23} & .... & K^*_{2,N-2} & K^*_{2,N-1} & K^*_{2N} \\ 0 & 0 & 1 & .... & K^*_{3,N-2} & K^*_{3,N-1} & K^*_{3N} \\ .... & .... & .... & .... & .... & .... & .... \\ 0 & 0 & 0 & .... & 1 & K^*_{N-2,N}-1 & K^*_{N-2,N} \\ 0 & 0 & 0 & .... & 0 & 1 & K^*_{N-1,N} \\ 0 & 0 & 0 & .... & 0 & 0 & 1 \end{bmatrix} \begin{bmatrix} -ds_1\bar{\tau}_1 \\ -ds_2\bar{\tau}_2 \\ w_3 \\ .... \\ w_{N-2} \\ -ds_{N-1}\bar{\tau}_{N-1} \\ -ds_N\bar{\tau}_N \end{bmatrix} = \begin{bmatrix} F^*_1 \\ F^*_2 \\ F^*_3 \\ .... \\ F^*_{N-2} \\ F^*_{N-1} \\ F^*_N \end{bmatrix} \tag{6.33}$$

Note that all the diagonal values are equal to one and that all the lower triangle values are zero. The *F*-vector values and the upper triangle values in the *K*-matrix have changed due to the Forward reduction and are now denoted as K^*_{ij} and F^*_i. In this specific case $K^*_{iN}=0$, for $1 \le i \le N-1$, due to the applied Dirichlet boundary conditions. After Backward substitution Eq (6.33) becomes:

$$\begin{bmatrix} 1 & 0 & 0 & .... & 0 & 0 & 0 \\ 0 & 1 & 0 & .... & 0 & 0 & 0 \\ 0 & 0 & 1 & .... & 0 & 0 & 0 \\ .... & .... & .... & .... & .... & .... & .... \\ 0 & 0 & 0 & .... & 1 & 0 & 0 \\ 0 & 0 & 0 & .... & 0 & 1 & 0 \\ 0 & 0 & 0 & .... & 0 & 0 & 1 \end{bmatrix} \begin{bmatrix} -ds_1\bar{\tau}_1 \\ -ds_2\bar{\tau}_2 \\ w_3 \\ .... \\ w_{N-2} \\ -ds_{N-1}\bar{\tau}_{N-1} \\ -ds_N\bar{\tau}_N \end{bmatrix} = \begin{bmatrix} F^{**}_1 \\ F^{**}_2 \\ F^{**}_3 \\ .... \\ F^{**}_{N-2} \\ F^{**}_{N-1} \\ F^{**}_N \end{bmatrix} = \begin{bmatrix} -ds_1\bar{\tau}_i \\ -ds_2\bar{\tau}_2 \\ w_3 \\ .... \\ w_{N-2} \\ -ds_{N-1}\bar{\tau}_{N-1} \\ -ds_N\bar{\tau}_N \end{bmatrix} \tag{6.34}$$

The new source vector (of which the values are now denoted as F^{**}_i) is equal to the solution vector. This means that all the unknown variables have been solved and that all the velocity values at the nodal points, as well as the shear stress values at all the boundary nodal points multiplied by their lengths are now known.

To decrease the solution time of the program the *K*-values are written into a new matrix (called GDMAT[ ]) which is much smaller that the normal *K*-matrix. The reason for this is that space matrices are used: if the first column value is zero for a specific row, then the other column values of the row are moved to the left until the value of the first column is non-zero. To ensure that the Gaussian elimination process can still be carried out, two other vectors have been created, namely (LFRST[ ] and LLAST[ ]). LFRST[ ] is used to denote the number of columns, in each row with zero *K*-values, before the first non-zero *K*-value and LLAST[ ] is used to denote in which column the non-zero *K*-values of each row ends. Therefore, a computation such as *K*[6;5] – *K*[5;5] may now be rewritten as

GDMAT [6;(5-LFRST[6])] – *GDMAT* [5; (5-LFRST[5])]. Eq (6.35) is an example of a coefficient matrix whilst Eq (6.36) is it's GDMAT[ ] matrix.

$$[\mathrm{K}] = \begin{bmatrix} 12 & 5 & 8 & 0 & 0 & 0 & 0 \\ 4 & 16 & 7 & 0 & 0 & 0 & 0 \\ 3 & 6 & 4 & 5 & 9 & 0 & 0 \\ 0 & 0 & 11 & 0 & 16 & 0 & 0 \\ 0 & 0 & 12 & 7 & 9 & 10 & 13 \\ 0 & 0 & 0 & 0 & 13 & 11 & 16 \\ 0 & 0 & 0 & 0 & 15 & 13 & 9 \end{bmatrix} \tag{6.35}$$

$$[\mathrm{GDMAT}] = \begin{bmatrix} 12 & 5 & 8 & 0 & 0 \\ 4 & 16 & 7 & 0 & 0 \\ 3 & 6 & 4 & 5 & 9 \\ 11 & 0 & 16 & 0 & 0 \\ 12 & 7 & 9 & 10 & 13 \\ 13 & 11 & 16 & 0 & 0 \\ 15 & 13 & 9 & 0 & 0 \end{bmatrix} \tag{6.36}$$

By inspecting row 4 in Eq (6.35), it can be seen that the first two *K*-values are zero and that the third *K*-value is non-zero. It follows now that LFRST[4] = 2 and that the last non-zero values are located in column 5, thus, LLAST[4]= 5.

Note that Eqs (6.31) - (6.34) are the matrices for an object with an inner and outer boundary. If the object has only an outer boundary, then these equations would have the same appearance as Eq (6.37) – (6.40):

$$\begin{bmatrix} K_{11} & \cdot & \cdot & \cdot & K_{1N} \\ \cdot & \cdot & \cdot & \cdot & \cdot \\ \cdot & \cdot & \cdot & \cdot & \cdot \\ \cdot & \cdot & \cdot & \cdot & \cdot \\ \cdot & \cdot & \cdot & \cdot & \cdot \\ \cdot & \cdot & \cdot & \cdot & \cdot \\ K_{N1} & \cdot & \cdot & \cdot & K_{NN} \end{bmatrix} \begin{bmatrix} w_1 \\ w_2 \\ w_3 \\ \cdot \\ w_{N-2} \\ w_{N-1} \\ w_N \end{bmatrix} = \begin{bmatrix} F_1 \\ F_2 \\ F_3 \\ \cdot \\ F_{N-2} \\ F_{N-1} \\ F_N \end{bmatrix} + \begin{bmatrix} 0 \\ 0 \\ 0 \\ \cdot \\ 0 \\ ds_{N-1}\bar{\tau}_{N-1} \\ ds_N\bar{\tau}_N \end{bmatrix} \tag{6.37}$$

$$\begin{bmatrix} K_{11} & \cdots & K_{1,N-2} & 0 & 0 \\ K_{21} & \cdots & K_{2,N-2} & 0 & 0 \\ K_{31} & \cdots & K_{3,N-2} & 0 & 0 \\ \cdots & \cdots & \cdots & \cdots & \cdots \\ K_{N-2,1} & \cdots & K_{N-2,N-2} & 0 & 0 \\ K_{N-1,1} & \cdots & K_{N-1,N-2} & 1 & 0 \\ K_{N1} & \cdots & K_{N,N-2} & 0 & 1 \end{bmatrix} \begin{bmatrix} w_1 \\ w_2 \\ w_3 \\ \cdots \\ w_{N-2} \\ -ds_{N-1}\bar{\tau}_{N-1} \\ -ds_N\bar{\tau}_N \end{bmatrix} = \begin{bmatrix} F_1 - K_{1,N-1}w_{N-1} - K_{1N}w_N \\ F_2 - K_{2,N-1}w_{N-1} - K_{2N}w_N \\ F_3 - K_{3,N-1}w_{N-1} - K_{3N}w_N \\ \cdots \\ F_{N-2} - K_{N-2,N-1}w_{N-1} - K_{N-2,N}w_N \\ F_{N-1} - K_{N-1,N-1}w_{N-1} - K_{N-1,N}w_N \\ F_N - K_{N,N-1}w_{N-1} - K_{NN}w_N \end{bmatrix} \tag{6.38}$$

$$\begin{bmatrix} 1 & K^*_{12} & K^*_{13} & .... & K^*_{1,N-2} & K^*_{1,N-1} & K^*_{1N} \\ 0 & 1 & K^*_{23} & .... & K^*_{2,N-2} & K^*_{2,N-1} & K^*_{2N} \\ 0 & 0 & 1 & .... & K^*_{3,N-2} & K^*_{3,N-1} & K^*_{3N} \\ .... & .... & .... & .... & .... & .... & .... \\ 0 & 0 & 0 & .... & 1 & K^*_{N-2,N}-1 & K^*_{N-2,N} \\ 0 & 0 & 0 & .... & 0 & 1 & K^*_{N-1,N} \\ 0 & 0 & 0 & .... & 0 & 0 & 1 \end{bmatrix} \begin{bmatrix} w_1 \\ w_2 \\ w_3 \\ .... \\ w_{N-2} \\ -ds_{N-1}\bar{\tau}_{N-1} \\ -ds_N\bar{\tau}_N \end{bmatrix} = \begin{bmatrix} F^*_1 \\ F^*_2 \\ F^*_3 \\ .... \\ F^*_{N-2} \\ F^*_{N-1} \\ F^*_N \end{bmatrix} \tag{6.39}$$

$$\begin{bmatrix} 1 & 0 & 0 & .... & 0 & 0 & 0 \\ 0 & 1 & 0 & .... & 0 & 0 & 0 \\ 0 & 0 & 1 & .... & 0 & 0 & 0 \\ .... & .... & .... & .... & .... & .... & .... \\ 0 & 0 & 0 & .... & 1 & 0 & 0 \\ 0 & 0 & 0 & .... & 0 & 1 & 0 \\ 0 & 0 & 0 & .... & 0 & 0 & 1 \end{bmatrix} \begin{bmatrix} w_1 \\ w_2 \\ w_3 \\ .... \\ w_{N-2} \\ -ds_{N-1}\tau_{N-1} \\ -ds_N\tau_N \end{bmatrix} = \begin{bmatrix} F^{**}_1 \\ F^{**}_2 \\ F^{**}_3 \\ .... \\ F^{**}_{N-2} \\ F^{**}_{N-1} \\ F^{**}_N \end{bmatrix} = \begin{bmatrix} w_1 \\ w_2 \\ w_3 \\ .... \\ w_{N-2} \\ -ds_{N-1}\bar{\tau}_{N-1} \\ -ds_N\bar{\tau}_N \end{bmatrix} \tag{6.40}$$

Since the velocity values at all the nodes are now known the axial velocity for the i^{th} gauss integration point in the j^{th} element may now be determined with Eq (6.14). The source vector for the conservation of energy was given in Eq (6.16) as:

$$F_I = \sum_e^{RE}\sum_{n=1}^{NG}\left[\rho\ c_p\psi_I\left(\sum_{p=1}^{NE}\psi_p w_p^e\right)\frac{\partial T}{\partial z}A_n^e\right] \tag{6.41}$$

The LADRES[ ] matrices of the relevant elements are again used to locate the nodal points associated with node *I*. The *K*-values for the conservation of energy was given in Eq (6.17) as:

$$K_{IJ} = \sum_e^{RE}\sum_{n=1}^{NG} kA_n^e\left(\frac{\partial\psi_I^e}{\partial x}\frac{\partial\psi_J^e}{\partial x} + \frac{\partial\psi_I^e}{\partial y}\frac{\partial\psi_J^e}{\partial y}\right) \tag{6.42}$$

In the two-dimensional C++ program the coefficient matrix is again divided into two vectors, namely (GDIAG[] and GCOEF[ ]). An example of the linear algebraic energy equations in matrix format was given in Eq (6.18) as:

$$\begin{bmatrix} K_{11} & \cdot & \cdot & \cdot & K_{1N} \\ \cdot & \cdot & \cdot & \cdot & \cdot \\ \cdot & \cdot & \cdot & \cdot & \cdot \\ \cdot & \cdot & \cdot & \cdot & \cdot \\ \cdot & \cdot & \cdot & \cdot & \cdot \\ \cdot & \cdot & \cdot & \cdot & \cdot \\ K_{N1} & \cdot & \cdot & \cdot & K_{NN} \end{bmatrix} \begin{bmatrix} T_1 \\ T_2 \\ T_3 \\ \cdot \\ T_{N-2} \\ T_{N-1} \\ T_N \end{bmatrix} = \begin{bmatrix} F_1 \\ F_2 \\ F_3 \\ \cdot \\ F_{N-2} \\ F_{N-1} \\ F_N \end{bmatrix} + \begin{bmatrix} ds_1 \overline{q}_1'' \\ ds_2 \overline{q}_2'' \\ 0 \\ \cdot \\ 0 \\ ds_{N-1} \overline{q}_{N-1}'' \\ ds_N \overline{q}_N'' \end{bmatrix} \tag{6.43}$$

If the object only has an outer boundary, then Eq (6.43) may be rewritten as:

$$\begin{bmatrix} K_{11} & \cdot & \cdot & \cdot & K_{1N} \\ \cdot & \cdot & \cdot & \cdot & \cdot \\ \cdot & \cdot & \cdot & \cdot & \cdot \\ \cdot & \cdot & \cdot & \cdot & \cdot \\ \cdot & \cdot & \cdot & \cdot & \cdot \\ \cdot & \cdot & \cdot & \cdot & \cdot \\ K_{N1} & \cdot & \cdot & \cdot & K_{NN} \end{bmatrix} \begin{bmatrix} T_1 \\ T_2 \\ T_3 \\ \cdot \\ T_{N-2} \\ T_{N-1} \\ T_N \end{bmatrix} = \begin{bmatrix} F_1 \\ F_2 \\ F_3 \\ \cdot \\ F_{N-2} \\ F_{N-1} \\ F_N \end{bmatrix} + \begin{bmatrix} 0 \\ 0 \\ 0 \\ \cdot \\ 0 \\ ds_{N-1} \overline{q}_{N-1}'' \\ ds_N \overline{q}_N'' \end{bmatrix} \tag{6.44}$$

Note that Eqs (6.43) and (6.44) are only examples, since Eq (6.15) has no specific number of inner or outer boundary nodes. Also note that the boundary nodes can be positioned anywhere in the matrix, it does not have to be positioned at the end points. GDIAG[ ] and GCOEF[ ] are now used to locate the relevant *K*-values so that the Dirichlet boundary conditions may be subtracted from the source vector (Eq (6.41)). The newly modified energy equations depend on the geometry and boundary conditions of the object.

Eqs (6.22) – (6.44) were programmed into the two-dimensional C++ program for solving two-dimensional fully developed laminar flow in ducts.

6.4. Friction factor and Nusselt numbers for a duct that has an inner and outer boundary (H1)

A finite element formulation that may be used to determine the friction factor and Nusselt numbers for two-dimensional fully developed laminar flow in a duct that has an outer as well as an inner boundary,

where both of these boundaries are subjected to the H1 boundary condition, will be discussed in this section.

After the momentum equations (Eq (6.3)) have been solved, the next step is to solve the energy equations (Eq (6.15)). Since the axial temperature gradient as well as the boundary temperatures are known, the energy equations must be rewritten in such a manner that the remaining temperature values and boundary heat flux values (multiplied with length – see Section 6.3) may be solved. Eq (6.43) should thus be rewritten as:

$$\begin{bmatrix} 1 & 0 & K_{13} & \cdots & K_{1,N-2} & 0 & 0 \\ 0 & 1 & K_{23} & \cdots & K_{2,N-2} & 0 & 0 \\ 0 & 0 & K_{33} & \cdots & K_{3,N-2} & 0 & 0 \\ \cdots & \cdots & \cdots & \cdots & \cdots & \cdots & \cdots \\ 0 & 0 & K_{N-2,3} & \cdots & K_{N-2,N-2} & 0 & 0 \\ 0 & 0 & K_{N-1,3} & \cdots & K_{N-1,N-2} & 1 & 0 \\ 0 & 0 & K_{N,3} & \cdots & K_{N,N-2} & 0 & 1 \end{bmatrix} \begin{bmatrix} -ds_1\bar{q}_1'' \\ -ds_2\bar{q}_2'' \\ T_3 \\ \cdots \\ T_{N-2} \\ -ds_{N-1}\bar{q}_{N-1}'' \\ -ds_N\bar{q}_N'' \end{bmatrix} = \begin{bmatrix} F_1 - K_{11}T_1 - K_{12}T_2 - K_{1,N-1}T_{N-1} - K_{1N}T_N \\ F_2 - K_{21}T_1 - K_{22}T_2 - K_{2,N-1}T_{N-1} - K_{2N}T_N \\ F_3 - K_{31}T_1 - K_{32}T_2 - K_{3,N-1}T_{N-1} - K_{3N}T_N \\ \cdots \\ F_{N-2} - K_{N-2,1}T_1 - K_{N-2,2}T_2 - K_{N-2,N-1}T_{N-1} - K_{N-2,N}T_N \\ F_{N-1} - K_{N-1,1}T_1 - K_{N-1,2}T_2 - K_{N-1,N-1}T_{N-1} - K_{N-1,N}T_N \\ F_N - K_{N1}T_1 - K_{N2}T_2 - K_{N,N-1}T_{N-1} - K_{NN}T_N \end{bmatrix} \tag{6.45}$$

Gaussian elimination may now be used to solve the solution vector (which contains all the unknown variables).

Define the total boundary shear stress multiplied with the associated length $\left(s\bar{\tau}_{tot}\right)$, the total inner boundary heat flux multiplied with the associated length $\left(s\bar{q}''_{tot_i}\right)$, and the total outer boundary heat flux multiplied with the associated length $\left(s\bar{q}''_{tot_o}\right)$ as:

$$s\bar{\tau}_{BTot} = \sum_{i}^{NB} ds_i \bar{\tau}_i \tag{6.46}$$

$$s\bar{q}''_{BTot_i} = \sum_{i}^{NBi} ds_i \bar{q}_i'' \tag{6.47}$$

$$s\bar{q}''_{BTot_o} = \sum_{i}^{NBo} ds_i \bar{q}_i'' \tag{6.48}$$

with *NB* the number of nodal points on the boundary, *NBi* the number of nodal points on the inner boundary and *NBo* the number of nodal points on the outer boundary. After the momentum equations

(in Eq (6.3)) have been solved, the temperature value for the i^{th} gauss integration point in the j^{th} element can be determined by means of:

$$T_{ji} = \sum_{n=1}^{Np} T_n^j \psi_n \tag{6.49}$$

Eqs (6.10), (6.14) and (6.49) may now be used to determine the mean axial velocity (see Eq (4.2)) and the bulk temperature (see Eq (4.8)):

$$w_m = \frac{\sum_{e=1}^{E}\sum_{i}^{NG} \rho \left(\sum_{p=1}^{NE} w_p^e \right) A_i^e}{\sum_{e=1}^{E}\sum_{i}^{NG} \rho A_i^e} \tag{6.50}$$

$$T_m = \frac{\sum_{e=1}^{E}\sum_{i}^{NG} \rho \; c_p \left(\sum_{p=1}^{NE} \psi_p w_p^e \right) \left(\sum_{p=1}^{NE} \psi_p T_p^e \right) A_i^e}{\sum_{e=1}^{E}\sum_{i}^{NG} \rho \; c_p \left(\sum_{p=1}^{NE} \psi_p w_p^e \right) A_i^n} \tag{6.51}$$

Make use of Eq (5.13) to define the length associated with the i^{th} gauss integration point in the j^{th} boundary element as:

$$s_i^j = \sqrt{\left(x_i^j\right)^2 + \left(y_i^j\right)^2}\, a_i \tag{6.52}$$

The total inner $\left(s_{BTot_i}\right)$ and outer $\left(s_{BTot_o}\right)$ boundary length is now defined as:

$$s_{BTot_i} = \sum_{j=1}^{NBi}\sum_{i=1}^{NG} s_i^j \tag{6.53}$$

$$s_{BTot_o} = \sum_{j=1}^{NBo}\sum_{i=1}^{NG} s_i^j \tag{6.54}$$

Note that $NG = 3$, because the boundary length of an element is defined by only three nodal points. The sum of all the temperature values multiplied by the associated lengths for the inner $\left(sT_{BTot_i}\right)$ and outer $\left(sT_{BTot_o}\right)$ boundary nodes may be written as:

$$sT_{BTot_i} = \sum_{j=1}^{NBi} \sum_{i=1}^{NG} \sum_{n=1}^{NE} \left(\psi_n T_n^j \right) s_i^j \tag{6.55}$$

$$sT_{BTot_o} = \sum_{j=1}^{NBo} \sum_{i=1}^{NG} \sum_{n=1}^{NE} \left(\psi_n T_n^j \right) s_i^j \tag{6.56}$$

The total object area is defined as:

$$A_{Tot} = \sum_{j=1}^{N} \sum_{i=1}^{NG} A_i^j \tag{6.57}$$

whilst the mean inner $\left(T_{m_i} \right)$ and outer $\left(T_{m_o} \right)$ boundary temperatures are defined as:

$$T_{m_i} = \frac{sT_{BTot_i}}{s_{BTot_i}} \tag{6.58}$$

$$T_{m_o} = \frac{sT_{BTot_o}}{s_{BTot_o}} \tag{6.59}$$

The hydraulic diameter for a two-dimensional object is defined as (Incropera & De Witt, 2005:518):

$$D_h \equiv \frac{4A_{Tot}}{s_{BTot_i} + s_{BTot_o}} \tag{6.60}$$

According to Eq (5.26) the friction factor will now be given by:

$$\frac{1}{4} f \,\mathrm{Re} = \frac{1}{4} \left(\frac{8 \left(\dfrac{s\bar{\tau}_{BTot}}{sT_{BTot_i} + sT_{BTot_o}} \right)}{\rho \; w_m^2} \times \frac{\rho \; w_m D_h}{\mu} \right) \tag{6.61}$$

After substituting Eq (5.29) into Eq (5.22) the inner and outer Nusselt numbers may respectively be written as:

$$Nu_i = \frac{\left(\dfrac{s\bar{q}''_{BTot_i}}{s_{BTot_i}} \right) D_h}{\left(T_{m_i} - T_m \right) k} \tag{6.62}$$

and

$$Nu_o = \frac{\left(\dfrac{s\overline{q}''_{BTot_o}}{s_{BTot_o}}\right)D_h}{\left(T_{m_o} - T_m\right)k} \tag{6.63}$$

Eqs (6.45) – (6.63) can be used in the two-dimensional C++ program to solve the two-dimensional fully developed laminar flow in ducts and to determine the friction factors and Nusselt numbers under specified conditions.

6.5. Friction factor and Nusselt number for a duct that has only an outer boundary (H1)

A finite element formulation that may be used to determine the friction factor and Nusselt numbers for two-dimensional fully developed laminar flow in a duct that has only an outer boundary, where this boundary is subjected to the H1 boundary condition, will be discussed in this section.

Finite element formulations that can be used to determine Nusselt numbers and friction factors for ducts, that only have an outer boundary (H1), are identical to the computations previously described in Section 6.4. The obvious difference between the current computations, and the previous computations, is that Nu_i is not determined now and that the variables $s\overline{q}''_{BTot_i}$, NBi, s_{BTot_i} and T_{m_i} are all equal to zero.

Eq (6.37) is an example of the new momentum equations, whilst Eq (6.44) is an example of the new energy equations. Since the axial temperature gradient as well as the boundary temperatures is known, Eq (6.44) may be rewritten as:

$$\begin{bmatrix} K_{11} & \cdots & K_{1,N-2} & 0 & 0 \\ K_{21} & \cdots & K_{2,N-2} & 0 & 0 \\ K_{31} & \cdots & K_{3,N-2} & 0 & 0 \\ \cdots & \cdots & \cdots & \cdots & \cdots \\ K_{N-2,1} & \cdots & K_{N-2,N-2} & 0 & 0 \\ K_{N-1,1} & \cdots & K_{N-1,N-2} & 1 & 0 \\ K_{N1} & \cdots & K_{N,N-2} & 0 & 1 \end{bmatrix} \begin{bmatrix} T_1 \\ T_2 \\ T_3 \\ \cdots \\ T_{N-2} \\ -ds_{N-1}\overline{q}''_{N-1} \\ -ds_N\overline{q}''_N \end{bmatrix} = \begin{bmatrix} F_1 - K_{1,N-1}T_{N-1} - K_{1N}T_N \\ F_2 - K_{2,N-1}T_{N-1} - K_{2N}T_N \\ F_3 - K_{3,N-1}T_{N-1} - K_{3N}T_N \\ \cdots \\ F_{N-2} - K_{N-2,N-1}T_{N-1} - K_{N-2,N}T_N \\ F_{N-1} - K_{N-1,N-1}T_{N-1} - K_{N-1,N}T_N \\ F_N - K_{N,N-1}T_{N-1} - K_{NN}T_N \end{bmatrix} \tag{6.64}$$

The friction factor and Nusselt number of the duct are determined with the equations given in Section 6.4. Eq (6.64) was programmed into the two-dimensional C++ program for the eventual computation of the friction factor and the Nusselt numbers under specified conditions.

6.6. Friction factor and Nusselt numbers for a duct that has an inner and outer boundary (T)

A finite element formulation that may be used to determine the friction factor and Nusselt numbers for two-dimensional fully developed laminar flow in a duct that has an outer as well as an inner boundary, where both these boundaries are subjected to the T boundary condition, will be discussed in this section.

After the momentum equations (Eq (6.3)) have been solved, the next step is to solve the energy equations (Eq (6.15)). Since the initial axial temperature gradient and the boundary temperatures are known, the energy equations must be rewritten in such a manner that the remaining temperature values and boundary heat flux values (multiplied with length – see Section 6.3) may be solved. Eq (6.43) should thus be rewritten as Eq (6.45). Note that the *F*-values of the source vectors are determined by employing Eq 6.58.

Substituting Eq (4.15) into Eq (6.41) gives:

$$F_I = \sum_{e}^{RE} \sum_{n=1}^{NG} \left[\rho \; c_p \psi_I \left(\sum_{p=1}^{NE} \psi_p w_p^e \right) \left(\frac{T_s - \sum_{p=1}^{NE} \psi_p T_p^e}{\left(T_s - T_m \right)} \right) \frac{\partial T_m}{\partial z} A_n^e \right] \tag{6.65}$$

The latter equation poses a problem, because the temperature values at all the nodal points (which are not all known) as well as the unknown bulk temperature (from Eq (6.51)) are required as input. Therefore, it is necessary that an iterative procedure must be used to solve the energy equations. Guessed values will, however, be needed to initiate this iterative process. To obtain the guessed values it is necessary that the energy equations must be solved by using Eq (6.41) instead of Eq (6.65), which is not applicable for this situation. Eq (6.41) can produce results, for the H1 boundary condition (as was described in Section 6.4), which is a good starting point for the iteration. The computed guessed values may now be used in two iteration procedures, i.e. to determine outer- and inner Nusselt numbers.

1. Computation of the outer Nusselt number

To determine the outer Nusselt number it is firstly necessary to rewrite Eq (6.65) as:

$$F_I = \sum_{e}^{RE}\sum_{n=1}^{NG}\left[\rho\ c_p\psi_I\left(\sum_{p=1}^{NE}\psi_p w_p^e\right)\left(\frac{T_{m_o}-\sum_{p=1}^{NE}\psi_p T_p^e}{\left(T_{m_o}-T_m\right)}\right)\frac{\partial T_m}{\partial z}A_n^e\right] \tag{6.66}$$

Insert the H1 guessed values T_m, T_{m_o} and T into Eq (6.66) and determine the next set of iterative values. Except for the difference in the source vector, the computations are exactly the same as were described in Section 6.4. Repeat the iteration process until two consecutive bulk temperatures have a difference of less than 0.000 001. The friction factor and outer Nusselt number can now be determined by employing Eqs (6.61) and (6.63).

2. Computation of the inner Nusselt number

To determine the inner Nusselt number it is firstly necessary to rewrite Eq (6.65) as:

$$F_I = \sum_{e}^{RE}\sum_{n=1}^{NG}\left[\rho\ c_p\psi_I\left(\sum_{p=1}^{NE}\psi_p w_p^e\right)\left(\frac{T_{m_i}-\sum_{p=1}^{NE}\psi_p T_p^e}{\left(T_{m_i}-T_m\right)}\right)\frac{\partial T_m}{\partial z}A_n^e\right] \tag{6.67}$$

Insert the H1 guess values T_m, T_{m_i} and T into Eq (6.67) and compute the next set of iterative values. Except for the difference in the source vector, the computations are exactly the same as were described in Section 6.4. Repeat the iteration process until two consecutive bulk temperatures have a difference of less than 0.000 001. The friction factor and inner Nusselt number respectively may now be determined by employing Eqs (6.61) and (6.62).

6.7. Friction factor and Nusselt number for a duct that has only an outer boundary (T)

A finite element formulation that may be used to determine the friction factor and Nusselt numbers for two-dimensional fully developed laminar flow in a duct that has only an outer boundary, where this boundary is subjected to the T boundary condition, will be discussed in this section.

Finite element formulations that may be used to determine Nusselt numbers and friction factors for ducts, that only have an outer boundary (T), are identical to the computations previously described in

Section 6.6. The obvious difference between the current computations, and the previous computations, is that Nu_i is not applicable in this case and that the variables $s\bar{q}''_{BTot_i}$, NBi, s_{BTot_i} and T_{m_i} are all equal to zero. Eq (6.37) is an example of the new momentum equations, whilst Eq (6.44) is an example of the new energy equations. Note, however, that Eq (6.66) is again used to substitute the source vector in Eq (6.44).

6.8. Friction factor and Nusselt numbers for a duct with one boundary at constant surface temperature whilst the other boundary has no heat transfer

A finite element formulation that may be used to determine the friction factor and Nusselt numbers for two-dimensional fully developed laminar flow in a duct with an inner and outer boundary, where one boundary is subjected to the T boundary condition whilst the other boundary has no heat transfer, will be discussed in this section.

The methods for calculating these friction factors and Nusselt numbers are the same as the methods described in Section 6.6. The only difference is that one boundary has no heat transfer $\left(\bar{q}''_s = 0\right)$ and has an unknown boundary temperature. Thus, for the first simulation procedure where fRe and $\underline{Nu_o}$ are determined, Eq (6.43) may be rewritten as:

$$\begin{bmatrix} K_{11} & \cdots & K_{1,N-2} & 0 & 0 \\ K_{21} & \cdots & K_{2,N-2} & 0 & 0 \\ K_{31} & \cdots & K_{3,N-2} & 0 & 0 \\ \cdots & \cdots & \cdots & \cdots & \cdots \\ K_{N-2,1} & \cdots & K_{N-2,N-2} & 0 & 0 \\ K_{N-1,1} & \cdots & K_{N-1,N-2} & 1 & 0 \\ K_{N1} & \cdots & K_{N,N-2} & 0 & 1 \end{bmatrix} \begin{bmatrix} T_1 \\ T_2 \\ T_3 \\ \cdots \\ T_{N-2} \\ -ds_{N-1}\bar{q}''_{N-1} \\ -ds_N\bar{q}''_N \end{bmatrix} = \begin{bmatrix} F_1 - K_{1,N-1}T_{N-1} - K_{1N}T_N + \bar{q}''_1 \\ F_2 - K_{2,N-1}T_{N-1} - K_{2N}T_N + \bar{q}''_2 \\ F_3 - K_{3,N-1}T_{N-1} - K_{3N}T_N \\ \cdots \\ F_{N-2} - K_{N-2,N-1}T_{N-1} - K_{N-2,N}T_N \\ F_{N-1} - K_{N-1,N-1}T_{N-1} - K_{N-1,N}T_N \\ F_N - K_{N,N-1}T_{N-1} - K_{NN}T_N \end{bmatrix} = \begin{bmatrix} F_1 - K_{1,N-1}T_{N-1} - K_{1N}T_N \\ F_2 - K_{2,N-1}T_{N-1} - K_{2N}T_N \\ F_3 - K_{3,N-1}T_{N-1} - K_{3N}T_N \\ \cdots \\ F_{N-2} - K_{N-2,N-1}T_{N-1} - K_{N-2,N}T_N \\ F_{N-1} - K_{N-1,N-1}T_{N-1} - K_{N-1,N}T_N \\ F_N - K_{N,N-1}T_{N-1} - K_{NN}T_N \end{bmatrix} \quad (6.68)$$

Note that the inner boundary has no heat transfer. For the second simulation procedure where fRe and $\underline{Nu_i}$ are determined, the example from Eq (6.43) may be rewritten as:

$$\begin{bmatrix} 1 & 0 & K_{13} & \cdots & K_{1N} \\ 0 & 1 & K_{23} & \cdots & K_{2N} \\ 0 & 0 & K_{33} & \cdots & K_{3N} \\ \cdots & \cdots & \cdots & \cdots & \cdots \\ 0 & 0 & K_{N-2,3} & \cdots & K_{N-2,N} \\ 0 & 0 & K_{N-1,3} & \cdots & K_{N-1,N} \\ 0 & 0 & K_{N3} & \cdots & K_{NN} \end{bmatrix} \begin{bmatrix} -ds_1\bar{q}_1'' \\ -ds_2\bar{q}_2'' \\ T_3 \\ \cdots \\ T_{N-2} \\ T_{N-1} \\ T_N \end{bmatrix} = \begin{bmatrix} F_1 - K_{11}T_1 - K_{12}T_2 \\ F_2 - K_{21}T_1 - K_{22}T_2 \\ F_3 - K_{31}T_1 - K_{32}T_2 \\ \cdots \\ F_{N-2} - K_{N-2,1}T_1 - K_{N-2,2}T_2 \\ F_{N-1} - K_{N-1,1}T_1 - K_{N-1,2}T_2 + \bar{q}_{N-1}'' \\ F_N - K_{N1}T_1 - K_{N2}T_2 + \bar{q}_N'' \end{bmatrix} = \begin{bmatrix} F_1 - K_{11}T_1 - K_{12}T_2 \\ F_2 - K_{21}T_1 - K_{22}T_2 \\ F_3 - K_{31}T_1 - K_{32}T_2 \\ \cdots \\ F_{N-2} - K_{N-2,1}T_1 - K_{N-2,2}T_2 \\ F_{N-1} - K_{N-1,1}T_1 - K_{N-1,2}T_2 \\ F_N - K_{N1}T_1 - K_{N2}T_2 \end{bmatrix} \quad (6.69)$$

Note that the outer boundary is not subjected to any heat transfer. The friction factor and Nusselt numbers of the duct may now be computed by employing the equations given in Section 6.4. Eqs (6.68) and (6.69) were programmed into the two-dimensional C++ program for the eventual computation of the friction factor and the Nusselt numbers under specified conditions.

6.9. Summary

In this chapter the following were discussed: 1) finite element formulation that was used in the two-dimensional C++ program to solve two-dimensional fully develop laminar flow in a duct, and 2) the creation of a two-dimensional domain. It was also shown how to determine the friction factors and Nusselt numbers for a duct that has:

- an inner and outer boundary and where each of these boundaries are subjected to a constant heat flux,
- only an outer boundary and where this outer boundary is subjected to a constant heat flux,
- an inner and outer boundary and where each of these boundaries are subjected to a constant surface temperature, and
- only an outer boundary and where this outer boundary is subjected to a constant surface temperature.

In the next chapter the one- and two-dimensional results from the C++ programs are compared with results reported in the literature.

7. Comparing the one- and two-dimensional results with known values

The finite element formulation that was used to compute the Nusselt numbers and friction factors for two-dimensional fully developed laminar flow in ducts was discussed in the previous chapter. In the current chapter the one- and two-dimensional C++ results determined in this study are discussed and compared with values reported in the literature. Tabulated friction factors and Nusselt numbers, for annular- and trapezoidal ducts, that had been subjected to various scenarios have also been included.

Note that in this section the computed results for Nusselt numbers and friction factors are compared[3] with the values published by Shah & London (1978:200-394). The values of Shah and London were arbitrarily chosen as 'standard' values and will in this study be referred to as Shah-London values. It is not implied that the values of Shah and London are the 'correct' or 'most correct' values. These values are simply chosen because they are available and referred to in all the tables included in this study (see Tables 7.1 – 7.9).

In this study the number of elements used to compute the various values (namely friction factors and Nusselt numbers) was increased until the obtained values tended to stabilise. It was thus assumed that further grid dependants studies will be unnecessary.

7.1. Comparisons for a circular duct

The Nusselt numbers (*Nu* (H1) and *Nu* (T)) and friction factors, for fully developed laminar flow in a circular duct, were determined with the one- and two-dimensional C++ programs that were discussed in Chapters 5 & 6. The results, obtained with the one-dimensional program and two-dimensional program (20, 108 or 192 elements), are tabulated in Table 7.1 and compared with each other as well as with the values reported in the literature. The domain consisting of 20 elements was obtained by first creating a mesh consisting of 5 blocks as shown in Figure 7.1, thereafter the C++ mesh program was used to further divide the mesh into 20 elements, as is shown in Figure 7.2. The two domains that

[3] The following are used when comparing different values:
- excellent: differences between 0 and 0.0009;
- good: differences between 0.001 and 0.009;
- reasonable: differences between 0.01 and 0.09; and
- poor: differences of more than 0.9.

consist respectively of 108 and 192 elements were both initially divided into 12 blocks and hereafter the C++ mesh program was used to divide them respectively into the final 108 and 192 elements.

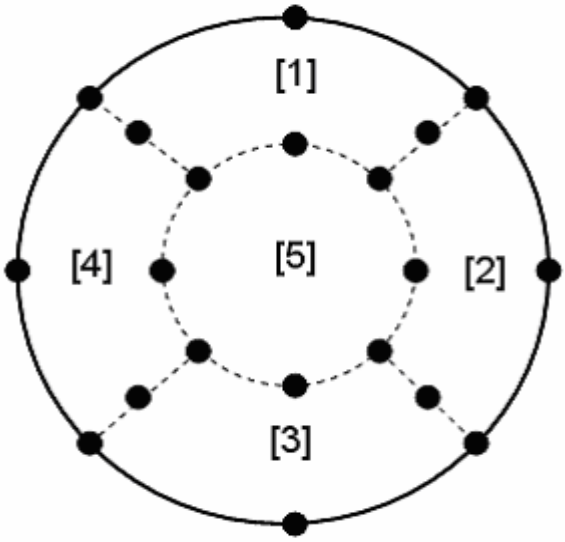

Figure 7.1. Circular duct divided into five blocks.

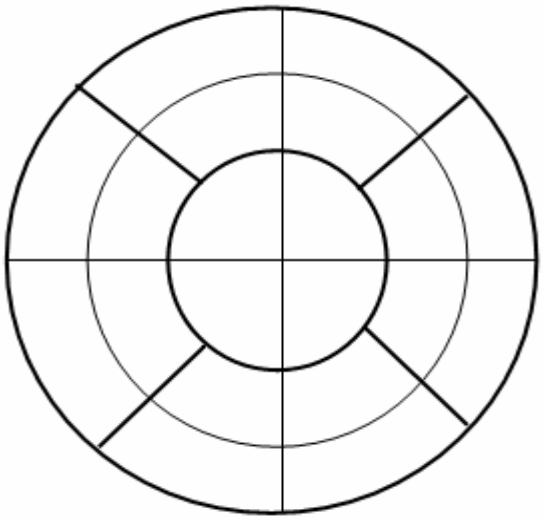

Figure 7.2. Circular duct divided into 20 elements.

In Table 7.1 the values of Nu (H1), Nu (T) and ¼ *f*Re computed for circular ducts by employing one-dimensional and two-dimensional are compared with the Shah-London values, as well as with other values reported by various authors in the literature.

Table 7.1. Comparing the computed Nusselt numbers (*Nu* (H1) and *Nu* (T)) and friction factors with published values for circular ducts.

Source	*Nu* (H1)	*Nu* (H1) - 4.364*	*Nu* (T)	*Nu* (T) - 3.657*	¼ *f*Re	¼ *f*Re - 16.000*
Du Toit *et al*. (2000:158)	4.395	+0.031	-	-	16.06	+0.06
Incropera and De Witt (2005:519)	4.36	-0.004	3.66	+0.003	16.00	0
Kays (1966:117)	4.364	0	3.66	+0.003	-	-
Kays and Crawford (1993:125)	4.364	0	3.66	+0.003	-	-
Kays and London (1984:120)	4.364	0	3.66	+0.003	16.00	0
Shah and London (1978:259)	4.364	0	3.657	0	16.000	0
One-dimensional C++ program	4.3636	-0.0004	3.6568	-0.0002	16.0000	0
Two-dimensional C++ program (20 elements)	4.3617	-0.0023	3.6580	+0.001	15.9942	-0.0058
Two-dimensional C++ program (108 elements)	4.3636	-0.0004	3.6567	-0.0003	15.9997	-0.0003
Two-dimensional C++ program (192 elements)	4.3636	-0.0004	3.6567	-0.0003	15.9997	-0.0003

*Shah-London values: *Nu* (H1) = 4.364; *Nu* (T) = 3.657; ¼ *f*Re = 16.000.

Nu (H1), *Nu* (T) and ¼ *f*Re values computed by means of the one- and two-dimensional (108 and 192 elements) programs compare excellently with the Shah-London values and only differ in the forth decimal. The values computed with the two-dimensional program (20 elements) compared somewhat less favourably with the Shah-London values (and other reported values)

It seems therefore that the best results, as compared to the Shah-London values, are obtained with the one- and two-dimensional (108+ elements) programs.

7.2. Comparisons for annular ducts

The Nusselt numbers (Nu_i and Nu_o) and friction factors, for fully developed laminar flow in annular ducts, were determined with the one- and two-dimensional C++ programs that were discussed in Chapters 5 & 6. The results obtained for an annulus (see Figure 7.3) are tabulated in Tables 7.2, 7.3 and 7.4 and compared with each other as well as with the values reported in the literature. Table 7.2 shows the results that are obtained when one wall of the annulus is adiabatic, whilst the other wall is at

a constant surface temperature (T). Table 7.3 shows the results that are obtained for constant heat flux at both walls of the annulus. Table 7.4 shows the results when both annulus walls are at a constant surface temperature. Note that the two-dimensional results are obtained for four separate domains which were initially divided into 4, 8, 8 and 8 blocks respectively. These domains were then, respectively, further divided into 16, 72, 128 and 200 elements by the C++ mesh program.

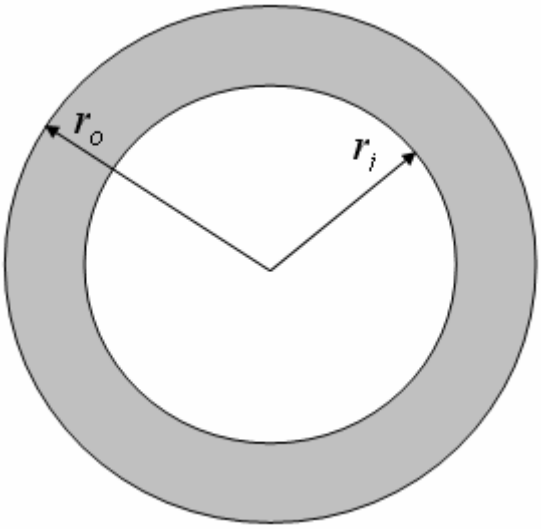

Figure 7.3. An annulus with its inner and outer radius.

It can be seen in Table 7.2 that the values of Nu_i (T), Nu_o (T) and ¼ fRe computed for annular ducts (r_i/r_o = 0.5) by employing one- and two-dimensional (128 and 200 elements) programs generally compares excellent with the Shah-London values, as well as with other values reported by various authors in the literature. However, Nu_i (T), Nu_o (T) and ¼ fRe computed by means of the

Table 7.2. Comparing the computed Nusselt numbers and friction factors to published values. All these values were obtained for annular ducts with one wall at constant surface temperature, whilst the other wall was adiabatic and $r_i/r_o = 0.5$.

Source	Nu_i (T)	Nu_i (T) - 5.7382*	Nu_o (T)	Nu_o (T) - 4.4293*	¼ fRe	¼ fRe - 23.813*
Incropera and De Witt (2005:519)	5.74	+0.0018	4.43	+0.0007	-	-
Shah and London (1978:259)	5.7382	0	4.4293	0	23.813	0
One-dimensional C++ program	5.7381	-0.0001	4.4293	0	23.8125	-0.0005
Two-dimensional C++ program (16 elements)	5.7564	+0.0182	4.4345	+0.0052	23.8238	+0.0108
Two-dimensional C++ program (72 elements)	5.7421	+0.0039	4.4306	+0.0013	23.8156	+0.0026
Two-dimensional C++ program (128 elements)	5.7393	+0.0011	4.4297	+0.0004	23.8133	+0.0003
Two-dimensional C++ program (200 elements)	5.7386	+0.0004	4.4294	+0.0001	23.8127	-0.0003

*Shah-London values: Nu_i (T) = 5.738; Nu_o (T) = 4.4293; ¼ fRe = 23.813.
Nu_i was obtained for a constant surface temperature at the inner wall, whilst outer wall was not subjected to heat flux.
Nu_o was obtained for a constant surface temperature at the outer wall, whilst inner wall was not subjected to heat flux.

two-dimensional (72 and 16 elements) program compares less favourably with the Shah-London values. It follows that the one- and two-dimensional (200 elements) programs yielded the best values, whilst the two-dimensional (16 elements) program produced the least acceptable values, as compared to the Shah-London values.

It can be seen in Table 7.3 that the values of Nu_i (H1), Nu_o (H1) computed for annular ducts (r_i/r_o = 0.6) by employing the one- and two-dimensional (200 elements) programs compares respectively excellent and good with the Shah-London values, whilst the two-dimensional (16 and 72 elements) programs produced reasonable to good Nu_i (H1) and Nu_o (H1) values.

Table 7.3. Comparing the computed Nusselt numbers (Nui and Nuo) and friction factors with published values. All these values were obtained for annular ducts subjected to a constant heat flux at the walls, and $r_i/r_o = 0.6$.

Source	Nu_i **(H1)**	Nu_i **(H1) - 9.429***	Nu_o **(H1)**	Nu_o **(H1) - 7.414***	¼ f**Re**	¼ f**Re - 23.897***
Du Toit *et al*. (2000:158)	9.408	-0.021	7.398	-0.016	23.977	+0.08
Incropera and De Witt (2005:519)	9.413	-0.016	7.414	0	-	-
Shah and London (1978:259)	9.429	0	7.414	0	23.897	0
One-dimensional C++ program	9.4291	+0.0001	7.4143	+0.0003	23.8970	0
Two-dimensional C++ program (16 elements)	9.4637	+0.0347	7.4597	+0.0457	23.9013	+0.0043
Two-dimensional C++ program (72 elements)	9.4377	+0.0087	7.4247	+0.0107	23.8984	+0.0014
Two-dimensional C++ program (128 elements)	9.4319	+0.0029	7.4176	+0.0036	23.8973	+0.0003
Two-dimensional C++ program (200 elements)	9.4302	+0.0012	7.4156	+0.0016	23.8969	-0.0001

*****Shah-London values: Nu_i (H1) = 9.429; Nu_o (H1) = 7.414; ¼ fRe = 23.897.

The ¼ fRe values obtained with the one- and two-dimensional (128 and 200 elements) programs also agrees excellently to the Shah-London values, whilst the values produced by the two-dimensional (16 and 72 elements) programs compares good.

It follows from Table 7.4 that Nu_i (T), Nu_o (T) values computed, for annular ducts ($r_i/r_o = 0.5$), with the two-dimensional program (200 elements) compare good with the Shah-London values, the two-dimensional programs (72 and 128 elements) compare reasonable to good to the Shah-London values, whilst the Nu_i (T) value computed with the two-dimensional program (16 elements) compares poorly.

In contrast, the ¼ fRe value computed with the two-dimensional program (128 and 200 elements) compares excellently with the corresponding Shah-London value, whereas two-dimensional program (16 elements) produced a value that compares reasonable.

Table 7.4. Comparing the computed Nusselt numbers (Nu_i and Nu_o) and friction factors with published values. All these values were obtained for annular ducts subjected to a constant surface temperature at the walls, and $r_i/r_o = 0.5$.

Source	Nu_i (T)	Nu_i (T) - 9.441*	Nu_o (T)	Nu_o (T) - 6.401*	¼ fRe	¼ fRe - 23.813*
Shah and London (1978:259)	9.441	0	6.401	0	23.813	0
Two-dimensional C++ program (16 elements)	9.9020	+0.461	6.5587	+0.1577	23.8238	+0.0108
Two-dimensional C++ program (72 elements)	9.4829	+0.0419	6.4126	+0.0116	23.8156	+0.0026
Two-dimensional C++ program (128 elements)	9.4543	+0.0133	6.4043	+0.0033	23.8133	+0.0003
Two-dimensional C++ program (200 elements)	9.4462	+0.0052	6.4021	+0.0011	23.8127	-0.0003

*Shah-London values: Nu_i (T) = 9.441; Nu_o (T) = 6.401; ¼ fRe = 23.813.

It follows from Tables 7.2, 7.3 and 7.4 that excellent values for Nu_i, Nu_o and ¼ fRe were obtained with the one-dimensional program, whilst the two-dimensional program (200 elements) produced good to excellent values for Nu_i and Nu_o, and excellent values for ¼ fRe. Values computed with the two-dimensional program (16 elements) were by far the least accurate. It is noticeable that the two-dimensional program results are converging as the number of elements are increased, and also that the results are usually converging to the Shah-London values.

In section 7.7 extended lists of computed Nusselt numbers and friction factors are given and discussed for various radius ratios ($0 \leq r_i/r_o \leq 1$).

7.3. Comparisons for trapezoidal ducts

The Nusselt numbers (Nu (H1) and Nu (T)) and friction factors, for fully developed laminar flow in trapezoidal ducts, were determined with the two-dimensional C++ program that was discussed in Chapter 6. These results are tabulated in Tables 7.5 and 7.6 and compared with values reported in the literature. Table 7.5 shows the results for a base angle of 45^o, and Table 7.6 shows the results obtained for a base angle of 60^o. Tables 7.5 and 7.6 show the results obtained for trapezoidal ducts when the aspect ratio equals one and Figure 7.4 illustrates the parameters for a trapezoidal duct. Note that the two-dimensional results are obtained for three separate domains which were initially divided into 4, 9 and 9 blocks respectively. These domains were then, respectively, further divided into 16, 144 and 324 elements by the C++ mesh program.

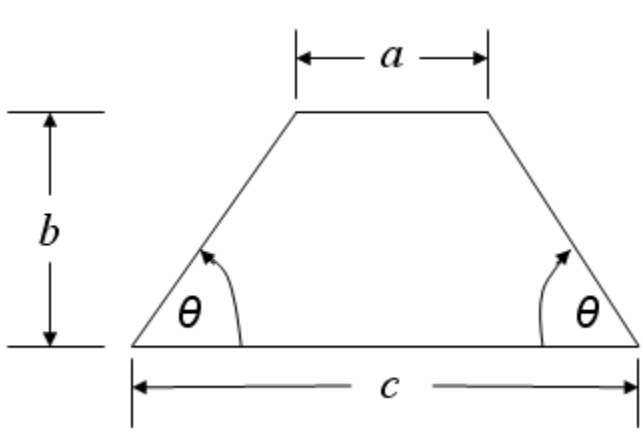

Figure 7.4. A trapezium.

It can be seen in Table 7.5 that the values of *Nu* (H1) computed for trapezoidal ducts (b/a = 1 and θ = 45^o) by employing two-dimensional (16, 144 or 324 elements) programs generally compares good with the Shah-London values. The best values were obtained when 144 or 324 elements were used. No comparisons could be made regarding *Nu* (T) values, because no *Nu* (T) values are available in the literature. However, *Nu* (T) values computed with the two-dimensional (16, 144 or 324 elements) programs compare good to excellently with each other.

Table 7.5. Comparing the computed Nusselt numbers (*Nu* (H1) and *Nu* (T)) and friction factors with published values for trapezoidal ducts (b/a = 1 and θ = 45^o).

Source	***Nu* (H1)**	***Nu* (H1) - 3.268***	***Nu* (T)**	**¼ *f*Re**	**¼ *f*Re - 13.827***
Shah and London (1978:259)	3.268	0	-	13.827	0
Two-dimensional C++ program (16 elements)	3.2762	+0.0082	2.5969	13.8407	+0.0137
Two-dimensional C++ program (144 elements)	3.2722	+0.0042	2.6022	13.8233	-0.0037
Two-dimensional C++ program (324 elements)	3.2722	+0.0042	2.6023	13.8225	-0.0045

***Shah-London values: *Nu* (H1) = 3.268; ¼ *f*Re = 13.827.

The friction factors (¼ *f*Re) follows the same pattern as described for the *Nu* (H1) values. The closest approximation are obtained with the two-dimensional (144 or 324 elements) program, whilst the worst approximation is obtained with the two-dimensional program (16 elements).

It can be seen in Table 7.6 that the values of *Nu* (H1) computed for trapezoidal ducts (b/a = 1 and θ = 60^o) by employing two-dimensional (16, 144 or 324 elements) programs generally compare

excellent with the Shah-London values. The values determined for the domain that are divided into 16 elements differ much more from the Shah-London values than the domains that are divided into 144 or 324 elements.

Table 7.6. Comparing the computed Nusselt numbers (*Nu* (H1) and *Nu* (T)) and friction factors with published values for trapezoidal ducts (b/a = 1 and $\theta = 60^o$).

Source	***Nu* (H1)**	***Nu* (H1) - 3.495***	***Nu* (T)**	**¼ *f*Re**	**¼ *f*Re - 14.151***
Shah and London (1978:259)	3.495	0	-	14.151	0
Yuan *et al*. (2001:4052)	3.461	-0.034	2.822	14.213	0.062
Two-dimensional C++ program (16 elements)	3.4934	-0.0016	2.8348	14.1655	0.0145
Two-dimensional C++ program (144 elements)	3.4945	-0.0005	2.8394	14.1520	0.001
Two-dimensional C++ program (324 elements)	3.4946	-0.0004	2.8395	14.1516	0.0006

***Shah-London values: *Nu* (H1) = 3.495; ¼ *f*Re = 14.151.

Also, note that *Nu* (T) values were not reported by Shah and London (1978:259). *Nu* (T) values computed with the two-dimensional (16, 144 or 324 elements) programs compare good to excellent with each other. These computed values compare reasonable with the *Nu* (T) value reported by Yuan *et al*. (2001:4052).

The friction factors (¼ *f*Re) follow the same pattern as described for *Nu* (H1) values. The closest approximations are obtained with the two-dimensional program (324 elements), whilst the worst approximations are obtained with the two-dimensional program (16 elements).

In general the Nusselt numbers and friction factors shown in Tables 7.5 and 7.6 compare more favourably with the Shah-London values as the number of elements in the two-dimensional domain is increased (i.e. from 16 elements to 144 to 324 elements).

In section 7.8 extended lists of computed Nusselt numbers and friction factors are given and discussed for various base angles and aspect ratios.

7.4. Comparisons for a square duct

The Nusselt numbers (*Nu* (H1) and *Nu* (T)) and friction factors, for fully developed laminar flow in a square duct, were determined with the two-dimensional C++ program that was discussed in Chapter 6. The results obtained for such a square duct (see Figure 7.5) are tabulated in Table 7.7 and compared

with values reported in the literature. Note that the two-dimensional results are obtained for three separate domains which were initially divided into 4, 9 and 9 blocks respectively. These domains were then, respectively, further divided into 16, 36 and 324 elements by the C++ mesh program.

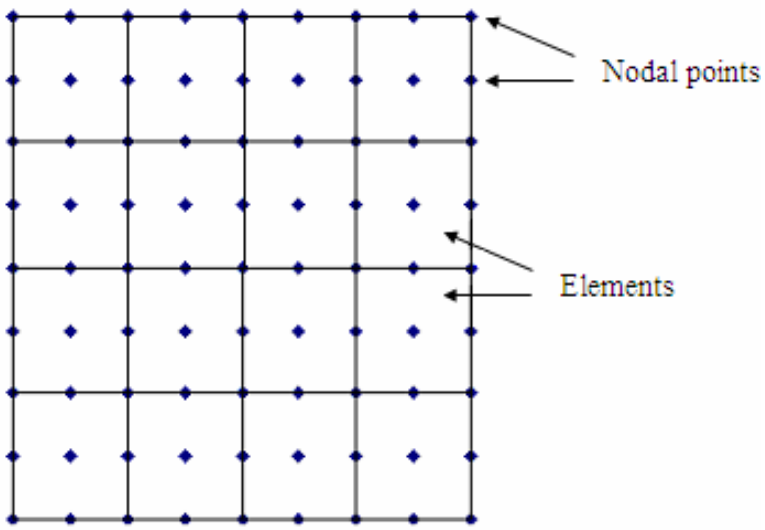

Figure 7.5. A square divided into 16 elements. Note that each element is defined by nine nodal points.

Table 7.7 depicts Nusselt numbers (*Nu* (H1) and *Nu* (T)) and friction factors for square ducts. Values computed with the two-dimensional programs are generally in good agreement with the Shah-London values.

The *Nu* (H1) values determined for the domain that is divided into 16 elements differ much more from the Shah-London values than the domains that are divided into 36 elements, whilst the latter differs more than values obtained with the 324 elements domain. Also, note that the *Nu* (T) values, computed via the different two-dimensional programs, are basically the same for the 16, 36 and 324 elements.

The friction factors followed the same pattern as the *Nu* (H1) values. The closest approximations are obtained with the two-dimensional program (324 elements). A less satisfactory approximation was observed for 36 elements, whilst the worst approximation is obtained with the two-dimensional programs (16 elements).

It follows from Table 7.7 that the *Nu* (H1) values and friction factors compare more favourably with the Shah-London values as the number of elements is increased (i.e. from 16 elements to 36 elements to 324 elements), whilst the *Nu* (T) values at first compare more favourably and then less favourably as the number of elements is increased.

Table 7.7. Comparing the computed Nusselt numbers (*Nu* (H1) and *Nu* (T)) and friction factors with published values for square ducts.

Source	*Nu* (H1)	*Nu* (H1) - 3.6080*	*Nu* (T)	*Nu* (T) - 2.9760*	¼ *f*Re	¼ *f*Re - 14.2271*
Du Toit *et al*. (2000:158)	3.622	+0.014	-	-	14.24	+0.0129
Incropera and De Witt (2005:519)	3.61	+0.002	2.98	+0.004	14.25	+0.0229
Kays (966:117)	3.63	+0.022	2.98	+0.004	-	-
Kays and Crawford (1993:125)	3.61	+0.002	2.98	+0.004	-	-
Kays and London (1984:120)	3.61	+0.002	2.98	+0.004	14.2	-0.0271
Shah and London (1978:259)	3.6080	0	2.9760	0	14.2271	0
Two-dimensional C++ program (16 elements)	3.6008	-0.0072	2.9748	-0.0012	14.2376	+0.0105
Two-dimensional C++ program (36 elements)	3.6063	-0.0017	2.9770	+0.0010	14.2296	+0.0025
Two-dimensional C++ program (324 elements)	3.6079	-0.0001	2.9775	+0.0015	14.2271	0.0000

*Shah-London values: *Nu* (H1) = 3.6080; *Nu* (T) = 2.9760; ¼ *f*Re = 14.2271.

7.5. Comparisons for a rectangular duct

The Nusselt numbers (*Nu* (H1) and *Nu* (T)) and friction factors, for fully developed laminar flow in a rectangular duct (with b/a =1/4), were determined with the two-dimensional C++ program that was discussed in Chapter 6. The results obtained for such a rectangular duct (see Figure 7.6) are tabulated in Table 7.8 and compared with values reported in the literature. Note that the two-dimensional results are obtained for three separate domains which were initially divided into 4, 9 and 9 blocks respectively. These domains were then, respectively, further divided into 16, 36 and 324 elements by the C++ mesh program.

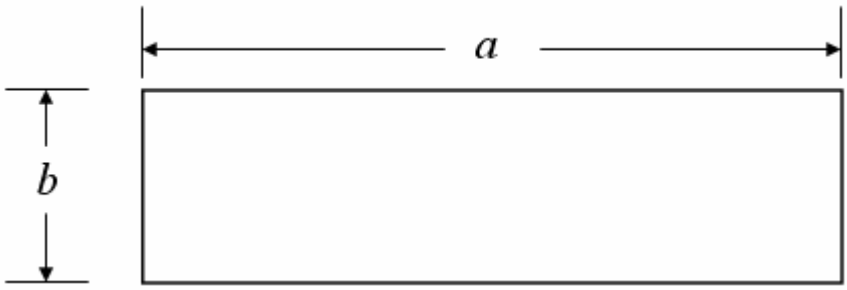

Figure 7.6. A rectangular duct with variables *a* and b.

Table 7.8 shows the values, for *Nu* (H1), *Nu* (T) and ¼ *f*Re, computed for rectangular ducts (*b*/*a* = 1/4). These values, computed by employing two-dimensional programs (16, 144 or 324 elements), are compared with the Shah-London values.

Table 7.8. Comparing the computed Nusselt numbers (*Nu* (H1) and *Nu* (T)) and friction factors with published values for rectangular ducts (*b*/*a* = 1/4).

Source	***Nu* (H1)**	***Nu* (H1) - 5.3311***	***Nu* (T)**	***Nu* (T) - 4.4390***	**¼ *f*Re**	**¼ *f*Re - 18.2328***
Du Toit *et al*. (2000:158)	5.344	+0.0129	-	-	-	-
Incropera and De Witt (2005:519)	5.33	-0.0011	4.44	+0.001	18.25	+0.0172
Kays (1966:117)	5.35	+0.0189	4.44	+0.001	-	-
Kays and Crawford (1993:125)	5.33	-0.0011	4.44	+0.001	-	-
Kays and London (1984:120)	5.33	-0.0011	4.44	+0.001	18.3	+0.0672
Shah and London (1978:259)	5.3311	0	4.4390	0	18.2328	0
Two-dimensional C++ program (16 elements)	5.2567	-0.0744	4.4022	-0.0368	18.3557	+0.1229
Two-dimensional C++ program (36 elements)	5.3088	-0.0223	4.4305	-0.0085	18.2681	+0.0353
Two-dimensional C++ program (324 elements)	5.3306	-0.0005	4.4403	+0.0013	18.2335	+0.0007

*****Shah-London values: *Nu* (H1) = 5.3311; *Nu* (T) =4.4390; ¼ *f*Re = 18.2328.

Good to Excellent correlations exists between the *Nu* (H1), *Nu* (T)) and (¼ *f*Re) values obtained with the two-dimensional program (324 elements) and the Shah-London values. The least acceptable correlation was obtained for values determined with the two-dimensional program (16 elements).

Also, note that these results are generally in a fairly good agreement with all the values reported in the literature.

As in previous cases, it is obvious that the accuracy of the values (as compared to the Shah-London values) obtained for the 324 element-domain is superior to those obtained for the 36 element-domain and even more superior to the values obtained for the 16 element-domain.

7.6. Comparisons for a triangular duct

The Nusselt numbers (*Nu* (H1) and *Nu* (T)) and friction factors, for fully developed laminar flow in a triangular duct, were determined with the two-dimensional C++ program that was discussed in Chapter 6. The results obtained for such a triangular duct (see Figure 7.7) are tabulated in Table 7.9 and compared with values reported in the literature. Note that the two-dimensional results are obtained for three separate domains which were initially divided into 3 blocks each. These domains were then, respectively, further divided into 12, 27 and 48 elements by the C++ mesh program.

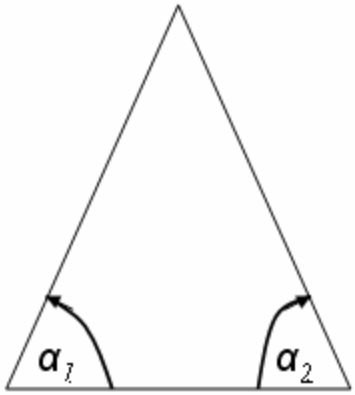

Figure 7.7. A triangle with its left (α_1) and right (α_2) base angles.

All the values for *Nu* (H1), *Nu* (T) and ¼ *f*Re shown in Table 7.9 were obtained for triangular ducts ($\alpha_1 = \alpha_2 = 60^o$). These results were computed with the two-dimensional program for domains divided into 12, 27 or 48 elements. The results obtained for *Nu* (H1) and ¼ *f*Re with the two-dimensional program (27 or 48 elements) compare excellently with the Shah-London values. The least acceptable correlation was obtained for values determined with the two-dimensional program (12 elements).

The correlations of the Nu (T) values with the Shah-London values are less satisfactory than that of *Nu* (H1) and (¼ *f*Re). Contrary to previous findings, the best comparison was observed for 12 elements and the least acceptable correlation was observed for the 48 elements.

Table 7.9. Comparing the computed Nusselt numbers (*Nu* (H1) and *Nu* (T)) and friction factors with published values for triangular ducts ($\alpha_1 = \alpha_2 = 60^o$).

Source	***Nu* (H1)**	***Nu* (H1) - 3.111***	***Nu* (T)**	***Nu* (T) - 2.47***	**¼ *f*Re**	**¼ *f*Re - 13.333***
Chen *et al*. (2000:220)	3.124	+0.013	-	-	13.2695	-0.0635
Du Toit *et al*. (2000:158)	3.158	+0.047	-	-	-	-
Incropera and De Witt (2005:519)	3.11	-0.001	2.49	+0.02	13.25	-0.083
Kays (1966:117)	3.00	-0.111	2.35	-0.12	-	-
Kays and Crawford (1993:125)	3.11	-0.001	2.49	+0.02	-	-
Kays and London (1984:120)	3.11	-0.001	2.47	0	13.33	-0.003
Shah and London (1978:259)	3.111	0	2.47	0	13.333	0
Two-dimensional C++ program (12 elements)	3.1133	+0.0023	2.4868	+0.0168	13.3361	+0.0031
Two-dimensional C++ program (27 elements)	3.1117	+0.0007	2.4939	+0.0239	13.3339	+0.0009
Two-dimensional C++ program (48 elements)	3.1111	+0.0001	2.4949	+0.0249	13.3333	+0.0003

*****Shah-London values: *Nu* (H1) = 3.111; *Nu* (T) = 2.47; ¼ *f*Re = 13.333.

The results obtained with the two-dimensional programs generally compare good with the results reported in the literature. Also, note that there is only a small difference (less than 0.01) between values determined for the domain that is divided into 12 elements and the domain that is divided into 48 elements.

The Nusselt numbers (*Nu* (H1) and *Nu* (T)) and friction factors that were determined for a rectangular duct (b/a = 1/4), a trapezoidal duct (b/a = 1/4 and $\theta = 60^o$) and a triangular duct ($\alpha_1 = \alpha_2 = 60^o$) with the two-dimensional C++ program, were tabulated in Table 7.10.

Comparing a trapezium, a triangle and a rectangle

A trapezium is a shape that is actually a mix between a triangle and a rectangle (or square). It is now interesting to note that the values of *Nu* (H1), *Nu* (T) and ¼ *f*Re obtained for a trapezium are located somewhere between the values obtained for a triangle and rectangle (see Table 7.10).

Table 7.10. Computed Nusselt numbers (*Nu* (H1) and *Nu* (T)) and friction factors for rectangular- (b/a = 1/4), trapezoidal- (b/a = 1/4 and $\theta = 60^o$) and triangular ducts ($\alpha_1 = \alpha_2 = 60^o$).

Duct	***Nu* (H1)**	***Nu* (T)**	**¼ *f*Re**
a. Rectangular (with b/a = 1/4)	5.3306	4.4403	18.2335
b. Trapezoidal (with b/a = 1/4 and $\theta = 60^o$)	5.2449	4.3653	18.0589
c. Triangular (with $\alpha_1 = \alpha_2 = 60^o$)	3.1111	2.4949	13.3333

a. Values from Table 7.8. **b.** Values from Table 7.13. **c.** Values from Table 7.9.

7.7 Friction factor and Nusselt numbers for annular ducts

Friction factors and Nusselt numbers (*Nu* (H1) and *Nu* (T)) for annular ducts with different radius ratios (r_i/r_o), whilst the one wall is at constant surface temperature and the other wall was not subjected to any heat flux, were determined with the one-dimensional C++ program and tabulated (Table 7.11).

The values shown in Table 7.11 are accurate to the second decimal when it is compared with corresponding values (not shown in this study) published by Incropera and De Witt (2005:520).

Influence coefficients, friction factors, the inner Nusselt numbers and outer Nusselt numbers for annular ducts, subjected to the H1 boundary condition, were determined with various radius ratios and tabulated (Table 7.12). Note that: Nu_i and Nu_o are the Nusselt numbers, of the annular ducts, when $q_i'' = q_o''$ (see Eqs (5.37) and (5.38)).

The values shown in Table 7.12 are accurate to the first decimal when it is compared with corresponding values published by Dwyer (1963b:337) (see Table 4.1), and accurate to the second decimal when it is compared with corresponding values (not shown in this study) published by Incropera and De Witt (2005:521).

Table 7.11. Computed Nusselt numbers and friction factors for annular ducts with various radius ratios. All these values were obtained for annular ducts with one wall at constant surface temperature whilst the other wall was not subjected to heat flux.

r_i/r_o	Nu_i (T)	Nu_o (T)	¼ fRe
0.00	-	3.657	16.000
0.05	17.459	4.056	21.567
0.10	11.559	4.114	22.343
0.15	9.331	4.156	22.790
0.20	8.130	4.194	23.088
0.25	7.371	4.232	23.302
0.30	6.845	4.270	23.461
0.35	6.459	4.309	23.583
0.40	6.163	4.348	23.678
0.45	5.928	4.388	23.753
0.50	5.738	4.429	23.813
0.55	5.581	4.471	23.860
0.60	5.449	4.513	23.897
0.65	5.337	4.555	23.926
0.70	5.240	4.598	23.949
0.75	5.156	4.641	23.967
0.80	5.082	4.685	23.980
0.85	5.017	4.729	23.989
0.90	4.959	4.773	23.996
0.95	4.908	4.817	23.999
1.00	4.898	4.898	24.000

Nu_i was obtained for a constant surface temperature at the inner wall, whilst outer wall was not subjected to heat flux. Nu_o was obtained for a constant surface temperature at the outer wall, whilst inner wall was not subjected to heat flux.
Also note that Nu_i (T) has no result for $r_i/r_o=0$, this is because $r_i=0$, which means that the specific annular duct is effectively a circular duct.

Table 7.12. Computed influence coefficients, Nusselt numbers and friction factors for annular ducts with various radius ratios, subjected to the H1 boundary condition.

r_i/r_o	Nu_{ii} (H1)	Nu_{oo} (H1)	θ_i^*	θ_o^*	Nu_i (H1)	Nu_o (H1)	¼ fRe
0.00	-	4.364	∞	0.000	-	4.364	16.000
0.05	17.811	4.792	2.183	0.029	15.056	4.935	21.567
0.10	11.906	4.834	1.384	0.056	31.005	5.121	22.343
0.15	9.687	4.860	1.075	0.081	129.160	5.288	22.790
0.20	8.499	4.883	0.904	0.104	88.531	5.450	23.088
0.25	7.753	4.905	0.793	0.125	37.454	5.606	23.302
0.30	7.241	4.928	0.712	0.145	25.142	5.764	23.461
0.35	6.867	4.953	0.651	0.164	19.676	5.925	23.583
0.40	6.583	4.979	0.602	0.182	16.540	6.087	23.678
0.45	6.360	5.007	0.562	0.199	14.521	6.251	23.753
0.50	6.181	5.037	0.529	0.215	13.123	6.417	23.813
0.55	6.034	5.067	0.500	0.231	12.068	6.589	23.860
0.60	5.912	5.099	0.474	0.246	11.240	6.763	23.897
0.65	5.808	5.132	0.452	0.260	10.599	6.935	23.926
0.70	5.720	5.166	0.432	0.273	10.070	7.106	23.949
0.75	5.644	5.201	0.415	0.287	9.648	7.295	23.967
0.80	5.578	5.237	0.398	0.299	9.266	7.471	23.980
0.85	5.521	5.273	0.384	0.311	8.963	7.653	23.989
0.90	5.470	5.310	0.370	0.323	8.683	7.843	23.996
0.95	5.425	5.347	0.358	0.335	8.450	8.041	23.999
1.00	5.390	5.390	0.346	0.346	8.242	8.242	24.000

Note that Nu_{ii} (H1) and Nu_i (H1) have no results for $r_i/r_o=0$, this is because $r_i=0$, which means that the specific annular duct is effectively a circular duct.

Figures 7.8 and 7.9 follows from the computed results tabulated in Table 7.12. In Figure 7.8 Nu_{ii} (H1), Nu_{oo} (H1) and ¼ fRe are plotted against the radius ratio, for an annular duct subjected to a constant heat flux.

Friction factor and influence coefficients – Annular duct

a

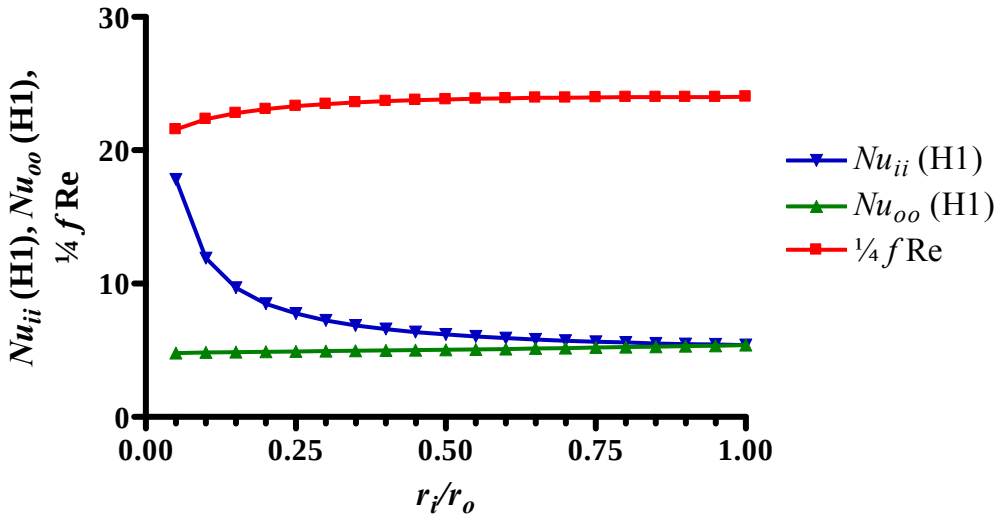

b

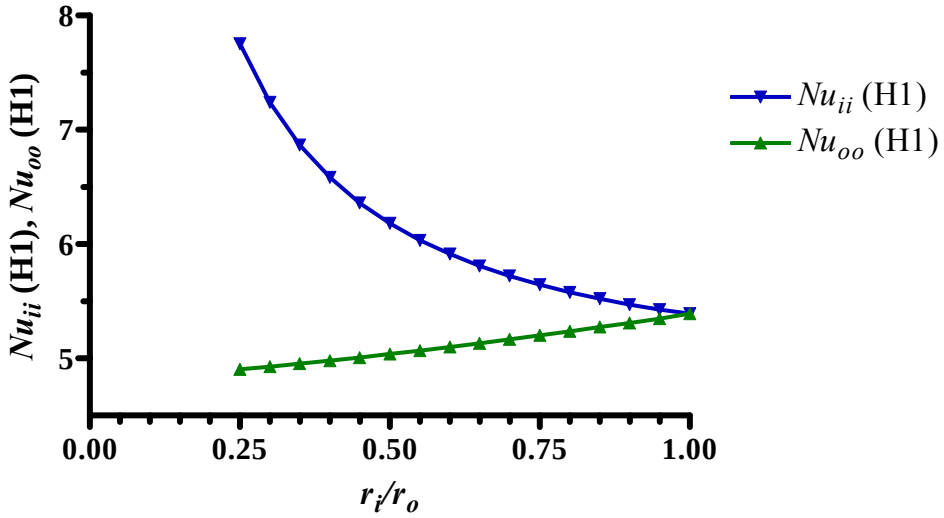

Figure 7.8a. Friction factor and influence coefficients for an annular duct, subjected to constant heat flux, versus radius ratio (from Table 7.12).
Figure 7.8b. Influence coefficients for an annular duct, subjected to constant heat flux, versus radius ratio (from Table 7.12). Results shown for $r_i/r_o \geq 0.25$.

It can be seen from Figure 7.8 that Nu_{oo} (H1) and ¼ fRe increase as r_i/r_o increases, whilst Nu_{ii} (H1) decreases as r_i/r_o increases. The value of Nu_{ii} (H1) decreases sharply for lower values of r_i/r_o (0.05 - 0.35), where after Nu_{ii} (H1) gradually decreases to its minimum value (Nu_{ii} = 5.390 at r_i/r_o = 1.0). On the other hand, the value of Nu_{oo} (H1) gradually increases from 4.792 (at r_i/r_o = 0.05) to its maximum value of 5.390 at r_i/r_o = 1.0. The difference (Nu_{ii} - Nu_{oo}) between the values decreases steadily as r_i/r_o increases and eventually at r_i/r_o = 1.0 ($r_i = r_o$), the difference is zero ($Nu_{ii} = Nu_{oo}$ = 5.390). This was to be expected, because at r_i/r_o = 1.0 the inner and outer boundary have equivalent sizes.

The value of ¼ fRe increases sharply for lower values (to about 0.15) of r_i/r_o, where after ¼ fRe gradually increases to the maximum value (¼ fRe = 24.000).

In Figure 7.9 Nu_i (H1) and Nu_o (H1) are plotted against the radius ratio, for an annular duct subjected to a constant heat flux and when $q_i'' = q_o''$.

It can be seen from Figure 7.9 that Nu_i (H1) increases sharply to a maximum value (Nu_i (H1) = 129.16 at r_i/r_o = 0.15) and then declines sharply to Nu_i (H1) = 19.676 (at r_i/r_o = 0.35), where after Nu_i (H1) declines gradually to a minimum value of 8.242 (at r_i/r_o = 1.0). This anomaly in the values of Nu_i (H1) is due to the heat transfer coefficient, which is used in the definition of the Nusselt number. The value of the heat transfer coefficient is large in the peak area where $0.1 < r_i/r_o < 1/4$. The latter result is because of the fact that the definition of the heat transfer is based on the difference between the wall and the bulk temperature which may be the same under certain circumstances. In contrast to Nu_i (H1), the value of Nu_o (H1) steadily increases as r_i/r_o increases. The difference (Nu_i - Nu_o) between the values decreases steadily as r_i/r_o increases from 0.3 to 1.0, where until $Nu_i = Nu_o$ (=8.242).

Annular duct – Nusselt numbers (with equal heat transfer at the inner and outer boundaries)

a

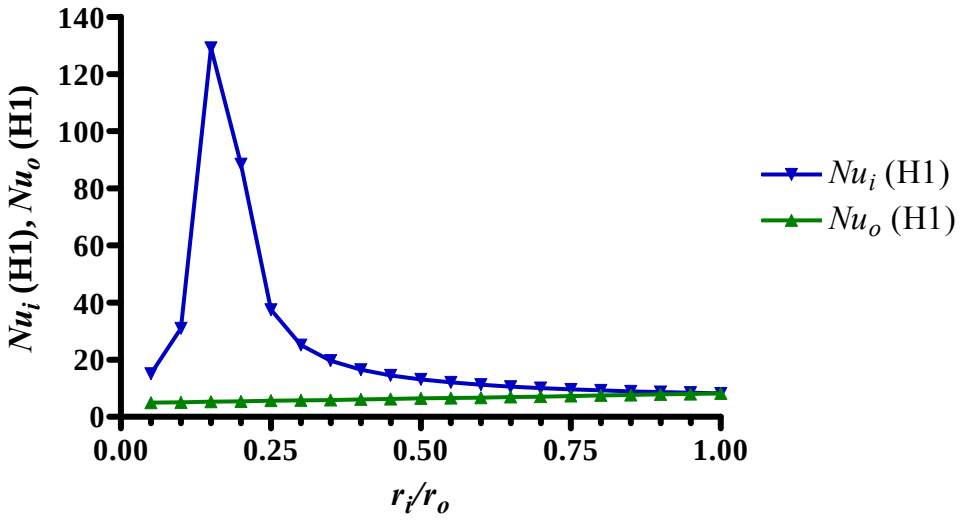

b

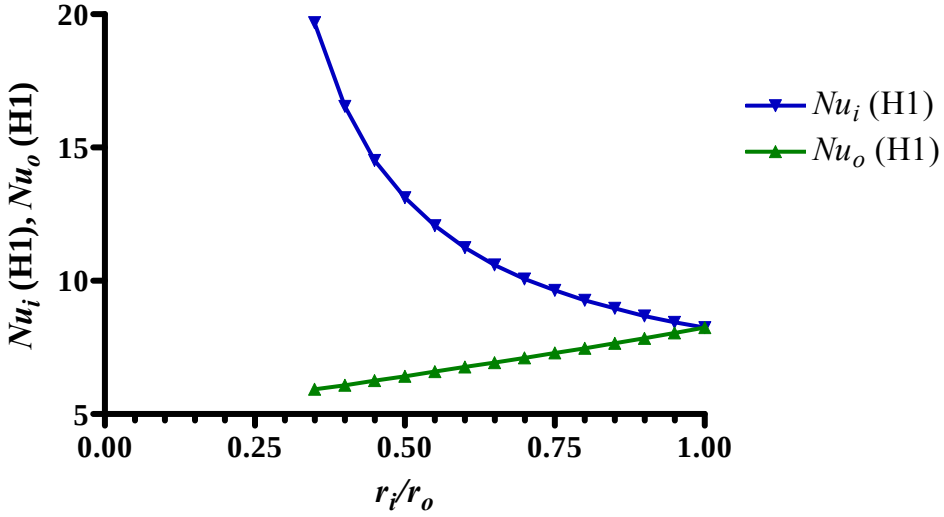

Figure 7.9a. Nu_{ii} (H1) and Nu_{oo} (H1) versus radius ratio, for an annular duct subjected to equal heat transfer at the inner and outer boundaries (from Table 7.12).
Figure 7.9b. Nu_{oo} (H1) versus radius ratio, for an annular duct subjected to equal heat transfer at the inner and outer boundaries (from Table 7.12). Results shown for $r_i/r_o \geq 0.35$.

7.8. Friction factors and Nusselt numbers for trapezoidal ducts

The list of friction factors and Nusselt numbers for trapezoidal ducts, shown in Table 2.1, was the only list of trapezoidal friction factors and Nusselt numbers that could be found in the literature. Note that the values in Table 2.1 are only given for the H1 boundary condition at 30^o, 45^o, 60^o, 75^o and 85^o base angles. Tables 7.13 – 7.17 show friction factors and Nusselt numbers (determined with the two-dimensional C++ program) for trapezoidal ducts that are subjected to the H1 or T boundary conditions.

Table 7.13. Computed Nusselt numbers and friction factors for trapezoidal ducts with different base angles and $b/a = 1/4$.

Base angle	*Nu* (H1)	*Nu* (T)	¼ *f*Re
20^o	3.7704	2.9782	15.1013
25^o	4.0922	3.2876	15.7364
30^o	4.3621	3.5440	16.2737
35^o	4.5881	3.7567	16.7263
40^o	4.7765	3.9328	17.1059
45^o	4.9327	4.0779	17.4221
50^o	5.0608	4.1962	17.6825
55^o	5.1640	4.2912	17.8932
60^o	5.2449	4.3653	18.0589
65^o	5.3053	4.4203	18.1830
70^o	5.3466	4.4576	18.2679
75^o	5.3696	4.4780	18.3153
80^o	5.3746	4.4819	18.3255
85^o	5.3618	4.4695	18.2986
90^o	5.3306	4.4403	18.2335

The tabulated values (Tables 7.13 – 7.17) compare well with corresponding values published by Shah and London (1978:256-260) (Table 2.1).

Table 7.14. Computed Nusselt numbers and friction factors for trapezoidal ducts with different base angles and $b/a = 1/2$.

Base angle	*Nu* (H1)	*Nu* (T)	¼ *f*Re
20°	3.0021	2.2482	13.5508
25°	3.2292	2.4776	13.9698
30°	3.4304	2.6773	14.3473
35°	3.6063	2.8499	14.6804
40°	3.7576	2.9977	14.9687
45°	3.8857	3.1227	15.2130
50°	3.9917	3.2264	15.4142
55°	4.0767	3.3102	15.5736
60°	4.1414	3.3751	15.6920
65°	4.1865	3.4219	15.7698
70°	4.2123	3.4509	15.8074
75°	4.2190	3.4625	15.8046
80°	4.2065	3.4568	15.7610
85°	4.1747	3.4334	15.6758
90°	4.1232	3.3923	15.5482

Table 7.15. Computed Nusselt numbers and friction factors for trapezoidal ducts with different base angles and $b/a = 1$.

Base angle	*Nu* (H1)	*Nu* (T)	¼ *f*Re
20°	2.6163	1.8965	12.7758
25°	2.7735	2.0715	13.0231
30°	2.9190	2.2288	13.2563
35°	3.0511	2.3693	13.4694
40°	3.1690	2.4936	13.6588
45°	3.2722	2.6023	13.8225
50°	3.3608	2.6958	13.9594
55°	3.4348	2.7747	14.0690
60°	3.4946	2.8395	14.1516
65°	3.5405	2.8905	14.2082
70°	3.5734	2.9286	14.2405
75°	3.5943	2.9545	14.2518
80°	3.6049	2.9697	14.2473
85°	3.6081	2.9763	14.2349
90°	3.6079	2.9775	14.2271

Table 7.16. Computed Nusselt numbers and friction factors for trapezoidal ducts with different base angles and $b/a = 2$.

Base angle	*Nu* (H1)	*Nu* (T)	¼ *f*Re
20°	2.4833	1.7775	12.5092
25°	2.6154	1.9364	12.6909
30°	2.7425	2.0777	12.8712
35°	2.8629	2.2102	13.0457
40°	2.9754	2.3316	13.2119
45°	3.0798	2.4424	13.3692
50°	3.1763	2.5432	13.5184
55°	3.2657	2.6350	13.6622
60°	3.3498	2.7191	13.8055
65°	3.4314	2.7979	13.9566
70°	3.5154	2.8754	14.1283
75°	3.6103	2.9584	14.3404
80°	3.7302	3.0595	14.6226
85°	3.8963	3.1995	15.0147
90°	4.1232	3.3923	15.5482

Table 7.17. Computed Nusselt numbers and friction factors for trapezoidal ducts with different base angles and $b/a = 4$.

Base angle	*Nu* (H1)	*Nu* (T)	¼ *f*Re
20°	2.4501	1.7480	12.4440
25°	2.5778	1.9010	12.6145
30°	2.7032	2.0438	12.7902
35°	2.8241	2.1767	12.9677
40°	2.9395	2.2999	13.1458
45°	3.0488	2.4135	13.3250
50°	3.1523	2.5177	13.5084
55°	3.2511	2.6131	13.7021
60°	3.3479	2.7010	13.9172
65°	3.4481	2.7845	14.1726
70°	3.5637	2.8706	14.5009
75°	3.7203	2.9765	14.9596
80°	3.9785	3.1476	15.6513
85°	4.4823	3.5262	16.7403
90°	5.3306	4.4403	18.2335

The values from Tables 7.13 – 7.17 are used to plot *Nu* (H1), *Nu* (T) and ¼ *f*Re against different base angles of trapezoidal ducts and for various aspect ratios (Figures 7.10 – 7.12). In Figures 7.10 - 7.12 the curves ($b/a < 1$) of *Nu* (H1), *Nu* (T) and ¼ *f*Re reach maximum values at base angles of between 70º - 80º, and then decreases as the base angles increase to 90º. The values of *Nu* (H1) and ¼ *f*Re follows the same pattern for when $b/a = 1$, whilst *Nu* (T) only reaches its maximum value at a base angle of 90º. The curves for *Nu* (H1), *Nu* (T) and ¼ *f*Re, for b/a values greater than 1 ($b/a = 2$ or 4), are increasing at a slow steady rate as the base angle is increased (from 20^o - 60^o). At greater base angles (greater than about 60º) the values of *Nu* (H1), *Nu* (T) and ¼ *f*Re increase sharply to reach maximum values, at a base angle of 90º, that are equal to the values with inverse aspect ratios. At a base angle of 90º *Nu* (H1) is equal to 5.3306 for a trapezoidal duct ($b/a = 4$ or 1/4 - see Tables 7.13 and 7.17) and a rectangular duct ($b/a = 1/4$ - see Table 7.8). Of course, the latter result is to be expected, since a trapezium with a base angle of 90º is actually a rectangular. For the same reason, it follows that the *Nu* (H1) values for trapezoidal ducts ($b/a = 2$ or 1/2- see Tables 7.14 and 7.16) are also equivalent at base angles of 90º, namely *Nu* (H1) = 4.1232. Analogous to these results it can be seen in Figure 7.11 that, for trapezoidal ducts with base angles of 90º, *Nu* (T) = 4.4403 ($b/a = 4$ or 1/4 - see Tables 7.13 and 7.17) and *Nu* (T) = 3.3923 ($b/a = 2$ or 1/2 - see Tables 7.14 and 7.16).

It can also be seen in Figures 7.10 - 7.12 that the curves for *Nu* (H1), *Nu* (T) and ¼ *f*Re shift downward as the value of b/a increases from 1/4 to 1. Eventually, for higher values of b/a ($b/a = 2$ or 4) and for base angles smaller than about 70º, it seems that the curves become stationary without any further downward shift. This tendency of *Nu* (H1), *Nu* (T) and ¼ *f*Re to become constant, as the ratio b/a increases, is illustrated in Figure 7.13.

The curves for friction factors (Figure 7.12) follow the same pattern as was described for the curves of *Nu* (H1) and *Nu* (T). For trapezoidal ducts with 90º base angles, ¼ *f*Re = 18.2335 ($b/a = 4$ or 1/4 - see Tables 7.13 and 7.17) and ¼ *f*Re = 15.5482 ($b/a = 2$ or 1/2 - see Tables 7.14 and 7.16).

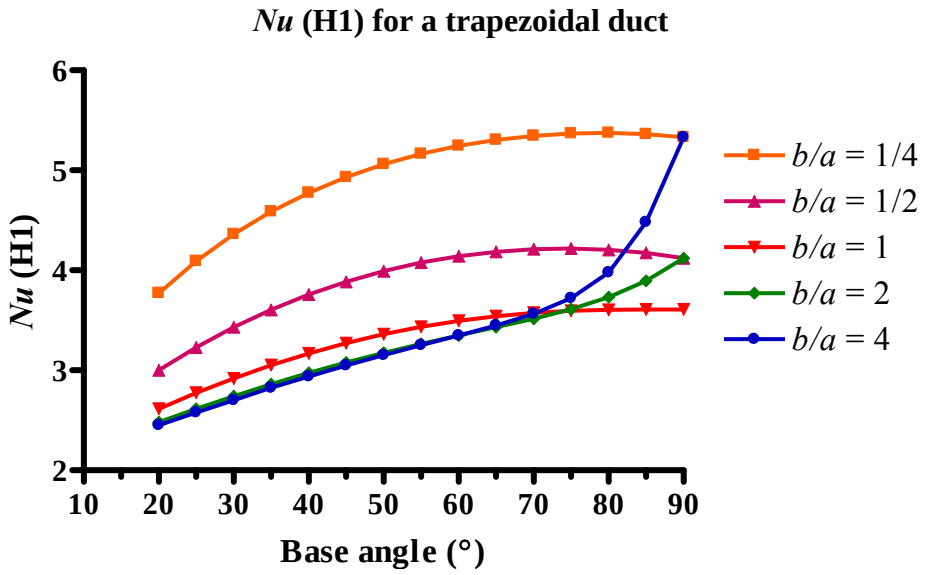

Figure 7.10. Nu_i (H1) versus Base angle, for a trapezoidal duct, subjected to different aspect ratios (from Tables 7.13 – 7.17).

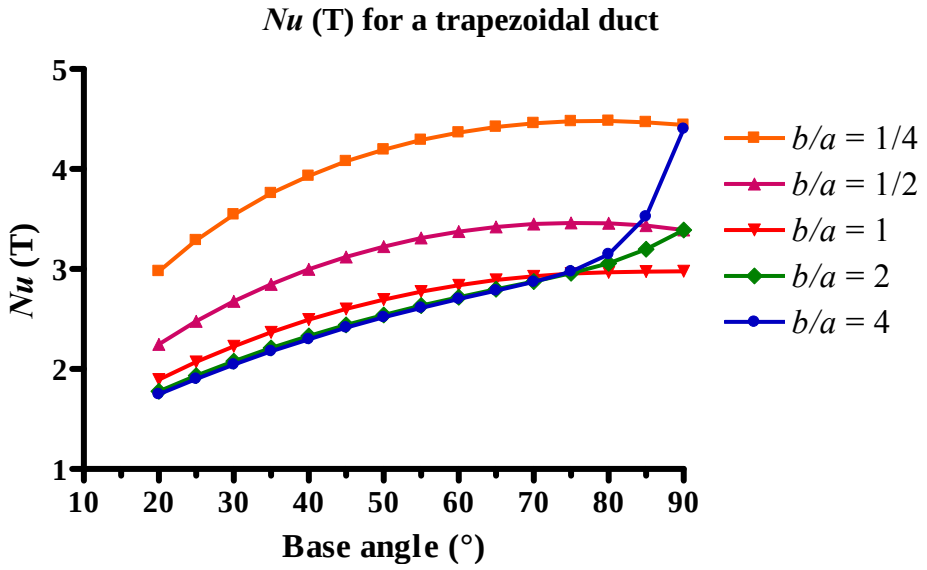

Figure 7.11. Nu_i (T) versus Base angle, for a trapezoidal duct, subjected to different aspect ratios (from Tables 7.13 – 7.17).

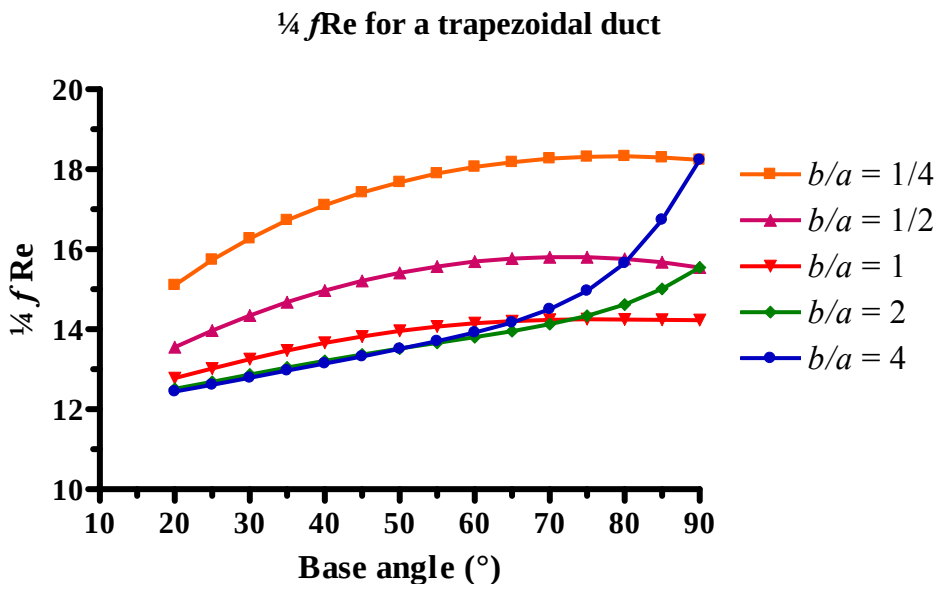

Figure 7.12. ¼ *f*Re versus base angle, for a trapezoidal duct, subjected to different aspect ratios (from Tables 7.13 – 7.17).

The values from Tables 7.13 – 7.17 are used to plot *Nu* (H1), *Nu* (T) and ¼ *f*Re against different aspect ratios for a trapezoidal duct at a 20° base angle (Figures 7.13). In Figure 7.13 the hyperbolic curves of *Nu* (H1), *Nu* (T) and ¼ *f*Re decrease as the aspect ratio increases from *b*/*a* = 1/4 to *b*/*a* = 1. It can be seen that the values of *Nu* (H1), *Nu* (T) and ¼ *f*Re decrease relative insignificantly and eventually tend to become almost constant, as the aspect ratio values increase beyond a value of one.

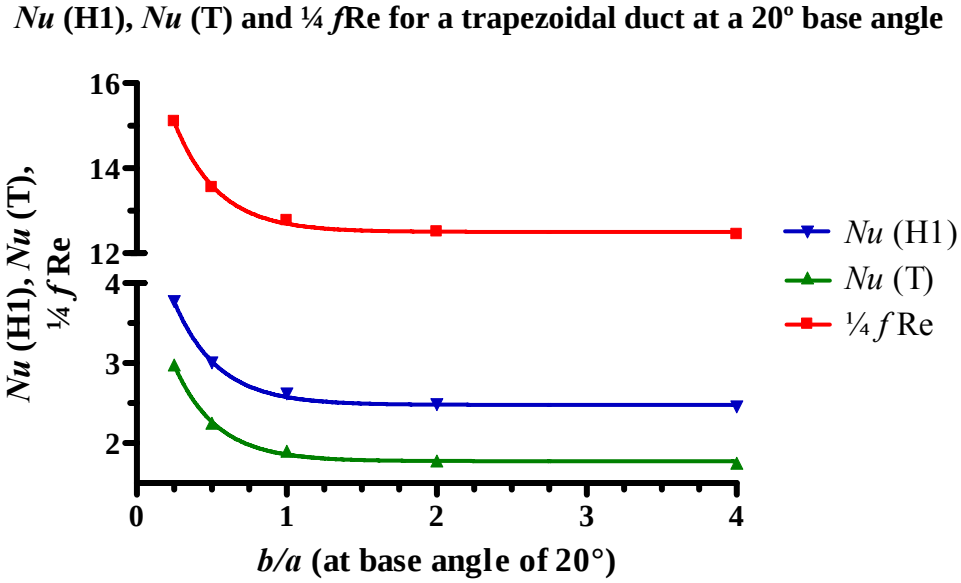

Figure 7.13. This figure illustrates the hyperbolic relationships between *Nu* (H1), *Nu* (T), ¼ *f*Re and different *b*/*a* ratios (at 20° base angle) of trapezoidal ducts.

7.9. Summary

The following C++ results were compared with known values and discussed.

- Nusselt numbers (*Nu* (H1) and *Nu* (T)) and friction factors for one- and two-dimensional fully developed laminar flow in circular ducts.
- Nusselt numbers and friction factors for one- and two-dimensional fully developed laminar flow in annular ducts with both walls subjected to a constant heat flux.
- Nusselt numbers and friction factors for one- and two-dimensional fully developed laminar flow in annular ducts with both walls subjected to a constant surface temperature.
- Nusselt numbers and friction factors for one- and two-dimensional fully developed laminar flow in annular ducts with one wall at constant surface temperature whilst the other wall was not subjected to heat flux.
- Nusselt numbers (*Nu* (H1) and *Nu* (T)) and friction factors for two-dimensional fully developed laminar flow in trapezoidal ducts (with $b/a = 1$, and $\theta = 45^o$).
- Nusselt numbers (*Nu* (H1) and *Nu* (T)) and friction factors for two-dimensional fully developed laminar flow in trapezoidal ducts (with $b/a = 1$, and $\theta = 60^o$).
- Nusselt numbers (*Nu* (H1) and *Nu* (T)) and friction factors for two-dimensional fully developed laminar flow in square ducts.
- Nusselt numbers (*Nu* (H1) and *Nu* (T)) and friction factors for two-dimensional fully developed laminar flow in rectangular ducts (with $b/a = 1/4$).
- Nusselt numbers (*Nu* (H1) and *Nu* (T)) and friction factors for two-dimensional fully developed laminar flow in triangular ducts (with $\alpha_1 = \alpha_2 = 60^o$).

All the above mentioned results have been compared with results reported in the literature, and it was pointed out that the observed correlations were very satisfactory. In general, the C++ results compared exceptionally well with the results published by Shah and London (1978:200-394). Most of the determined values were accurate to the second or third decimal as compared with the published values. It can, therefore, be concluded that the Finite element code generate accurate and usable values.

Friction factors, Nusselt numbers and influence coefficients obtained under various conditions were tabulated in a number of tables.

- Friction factors and Nusselt numbers for annular ducts at various radius ratios. These values were obtained with one wall at constant surface temperature whilst the other wall was not subjected to heat flux.
- Influence coefficients, friction factors and the Nusselt numbers (H1) for annular ducts with various radius ratios.
- Friction factors and Nusselt numbers for trapezoidal ducts with different base angles.

The compiled lists referred to above are more comprehensive than similar lists found in the literature.

The following curves were shown

- In Figure 7.8 Nu_{ii} (H1), Nu_{oo} (H1) and ¼ fRe are plotted against the radius ratio, for an annular duct subjected to a constant heat flux.
    - It can be seen that the difference (Nu_{ii} - Nu_{oo}) between the values decreases steadily as r_i/r_o increases and eventually at r_i/r_o = 1.0 (r_i = r_o), the difference is zero, i.e. (Nu_{ii} = Nu_{oo}).
- In Figure 7.9 Nu_i (H1) and Nu_o (H1) are plotted against the radius ratio for an annular duct subjected to a constant heat flux and when $q_i'' = q_o''$.
    - It can be seen that Nu_i (H1) increases sharply to a maximum value (Nu_i (H1) = 129.16 at r_i/r_o = 0.15) and then declines sharply to Nu_i (H1) = 19.676 (at r_i/r_o = 0.35), where after Nu_i (H1) declines gradually to a minimum value of 8.242 (at r_i/r_o = 1.0). This anomaly in the values of the Nu_i (H1) is due to definition of the heat transfer coefficient, which is used in the Nusselt number definition. The value of the heat transfer coefficient is large in the peak area. That is where 0.1 < r_i/r_o < 0.25.
- In Figures 7.10 – 7.12 Nu (H1), Nu (T) and ¼ fRe are plotted against the base angles for trapezoidal ducts at various aspect ratios.
    - It has been shown that curves with inverse aspect ratios have the same values at a 90^o base angle; this is because a trapezium with a base angle of 90^o is actually a rectangular duct.

- In Figure 7.13 *Nu* (H1), *Nu* (T) and ¼ *f*Re are plotted against the aspect ratio for trapezoidal ducts at a 20^o base angle.
    - It has been shown that the values of *Nu* (H1), *Nu* (T) and ¼ *f*Re firstly decrease rapidly as the aspect ratio ($b/a < 1$) increases, where after (for $b/a > 1$) the increase in the values are less marked and eventually these values become almost stationary.

In the next chapter the obtained results are discussed and the final conclusions are drawn.

8. Discussion and Conclusions

The main objective of this study was to determine Nusselt numbers and friction factors for one- and two-dimensional fully developed laminar flow in ducts. This has been achieved by performing various computations with C++ programs under preset conditions.

Analytic solutions have been given for the computation of:

- the Nusselt number for a circular duct subjected to a constant wall heat flux in the axial direction,
- the friction factors for circular and annular ducts subjected to a constant wall heat flux or a constant wall temperature in the axial direction, and
- the Nusselt numbers for an annular duct with one wall subjected to constant wall temperature in the axial direction whilst the other wall was adiabatic.

It was pointed out that the Nusselt number for a circular duct, subjected to a constant surface temperature at the wall, must be determined iteratively.

The Finite element formulation for fully developed laminar flow in one- and two-dimensional ducts has been used in C++ programs in order to determine the friction factors and Nusselt numbers for different duct shapes.

Friction factor and Nusselt number results were determined for the for the H1 and/or T boundary conditions for the following duct shapes.

- Circular ducts for one- and two-dimensional flow.
- Annular ducts for one- and two-dimensional flow.
- Trapezoidal ducts for two-dimensional flow.
- Square ducts for two-dimensional flow.
- Rectangular ducts for two-dimensional flow.
- Triangular ducts for two-dimensional flow.

The Nusselt numbers and friction factors for circular and annular ducts were determined with the one-dimensional C++ program for different sets of input data

Friction factors, Nusselt numbers and influence coefficients obtained under various conditions were tabulated in a number of tables.

- Friction factors and Nusselt numbers for annular ducts at various radius ratios. These values were obtained with one wall at constant surface temperature whilst the other wall was not subjected to heat flux.
- Influence coefficients, friction factors and the Nusselt numbers (H1) for annular ducts with various radius ratios.
- Friction factors and Nusselt numbers for trapezoidal ducts with different base angles.

The compiled lists referred to above are more comprehensive than similar lists found in the literature.

Final conclusion

The values obtained with the one- and two-dimensional C++ programs have proven to be very accurate when compared to previously published results. The accuracy of the two-dimensional programs generally increased markedly as the number of elements increased, until eventually highly accurate numbers were obtained. Hereafter, the accuracy of the computed values increased minimally if the number of elements was increased beyond a certain point. Excellent agreements were generally found by comparing the determined values with values reported in the literature. It was, therefore, concluded that the finite element method used in this study is a viable method that may be employed to determine accurate and reliable Nusselt numbers and friction factors for a variety of duct shapes.

Suggestions

In a following study a commercial CFD code should be used to determine the friction factor and Nusselt number for three-dimensional fully developed laminar flow.

The commercial code should also be used to study the development of the friction factors and Nusselt numbers as a function of distance from the inlet. One should also investigate the distance that is necessary for the flow to become fully developed, and see whether a pattern can be observed. Viscous dissipation that is not negligible could also be investigated by adapting the codes used in this study.

Bibliography

AQUARO, A.D. & PIEVE, M. 2007. High temperature heat exchangers for power plants: Performance of advanced metallic recuperators. *Applied Thermal Engineering*, 27:389–400.

BARLETTA, A. 2002. Fully developed mixed convection and flow reversal in a vertical rectangular duct with uniform wall heat flux. *International Journal of heat and Mass Transfer,* 45(2):641-654.

BECKER, E.B, CAREY, G.F. & ODEN, J.T. 1981. Finite elements An introduction. London: Prentice-Hall. 485 p.

BEJAN, A. 1993. Heat transfer. New York: John Wiley & Sons. 675 p.

BEVERLY, C.R. & TANNER, R.I. 1992. Numerical analysis of three-dimensional Bingham plastic flow. *Non-Newtonian Fluid Mech.*, 42:85-115.

BUSEDRA, A.A. & SOLIMAN, H.M. 1999. Analysis of laminar mixed convection in inclined semicircular ducts under buoyancy-assisted and -opposed conditions. Part A. *Numerical heat transfer*, 36:527-544.

CHEN, S., CHAN, T.L. & LEUNG, C.W. 2000. Numerical prediction of laminar forced convection in triangular ducts with unstructured triangular grid method. *Numerical Heat Transfer*, 38:209-224.

COELHO, M. & PINHO, F.T. 2006. Fully-developed heat transfer in annuli with viscous dissipation. *International journal of heat and mass transfer,* 49:3349-3359.

COETZEE, R.V. 2005. Volume weighted interpolation for unstructured meshes in the finite volume method. Potchefstroom:North-West University. (Dissertation – PhD) 99 p.

DU TOIT, A. 1997. Finite element method for thermodynamic flow. Potchefstroom:Potchefstroom University for Christian Higher Education. (Dissertation – M.Eng.) 102 p.

DU TOIT, C.G., LE GRANGE, C.G., COETZEE, R.V. & VAN DER MERWE, J. 2000. The determination of the Nusselt Numbers and Friction Factor for laminar flow in closed conduits. (*In* Centre for composite materials and structures. Proceedings international conference on applied mechanics held in Durban on 11 to 13 January 2000. Durban. p. 154-159.)

DU TOIT, C.G. 2002a. Calculation of friction factors and Nusselt numbers for laminar flow in rectangular ducts using finite elements. *Numerical Heat transfer,* 41:397-407.

DU TOIT, C.G. 2002b. Friction factor and Nusselt number for fully developed laminar flow in annuli. (*In* Heat transfer 2002. The twelfth international heat transfer conference in Grenoble, France on 18–23 August 2002. Grenoble. p. 201-206.)

DU TOIT, C.G. 2003. Friction factor and Nusselt number for fully developed laminar flow in a semi-circular duct. (*In* HEFAT 2003. 2nd international conference on heat transfer, fluid mechanics and thermodynamics held in Zambia, Victoria Falls on 24-26June 2003. Victoria Falls. p. 50-55.

DU TOIT, C.G. 2004a. Leereenheid 3: eindige element-metode oorsig en voorbeeld. Potchefstroom: NWU. 31 p. (MEGI322)

DU TOIT, C.G. 2004b. Finite element calculation of the Reynolds friction factors and Nusselt numbers for fully developed laminar flow in annuli. Unpublished paper. 25 p.

DU TOIT, C.G. 2007. Introduction to the Galerkin finite element method. Potchefstroom: NWU. 35 p. (Finite element notes)

DWYER, O.E. 1962. Unilateral heat transfer to liquid metals flowing in Annuli. *Nuclear science and engineering,* 15:58-68.

DWYER, O.E. 1963a. Equations for bilateral heat transfer to a fluid flowing in a concentric annulus. *Nuclear science and engineering*, 15:52-57.

DWYER, O.E. 1963b. On the transfer of heat fluids flowing through pipes, annuli, and parallel plates. *Nuclear science and engineering,* 17:336-344.

ERDOGAN, M.E. & IMRAK, C.E. 2005. The effects of duct shape on the Nusselt number. *Mathematical and computational applications,* 10(1):79-88.

ESCUDIER, M.P., OLIVEIRA, P.J. & PINHO, F.T. 2002. Fully developed laminar flow of purely viscous non-Newtonian liquida through annuli, including the effects of eccentricity and inner-cylinder rotation. *International Journal of Heat and Fluid Flow,* 23:52-73.

FERZIGER, J.H. & Peric, M. 1997. Computational methods for fluid dynamics. Berlin: Springer. 364 p.

GAMRAT, G., FAVRE-MARINET, M. & ASENDRYCH, D. 2005. Conduction and entrance effects on laminar liquid flow and heat transfer in rectangular micro channels. *International Journal of heat and Mass Transfer,* 48:2943-2954.

HAHN, B. 1994. C++ a practical introduction. Manchester: Blackwel*l*. 459 p.

HOLMAN, J.P. 1997. Heat Transfer. New York: McGraw-Hill. 392 p.

INCROPERA, F.P. & DE WITT, D.P. 2005. Fundamentals of Heat and Mass Transfer. New York: John Wiley & Sons. 997p.

JOHNSON, L.W. & RIESS, R.D. 1982. Numerical analysis. 2nd ed. Massachusetts: Addison-Wesley. 563 p.

KAKAC, S., SHAH, R.K. & BERGLES, A.E. 1983. Low Reynolds number flow heat exchangers. Washington: Hemisphere publishing corporation. 1016 p.

KAPALE, U.C. & CHAND, S. 2006. Modeling for shell-side pressure drop for liquid flow in shell-and-tube heat exchanger. *International Journal of heat and Mass Transfer*, 49:601-610.

KAYS, W.M. 1966. Convective heat and mass transfer. New York: McGraw-Hill. 289 p.

KAYS, W.M. & CRAWFORD, M.E. 1993. Convective heat and mass transfer. 3rd ed. New York: McGraw-Hill 601 p.

KAYS, W.M. & LONDON, A.L. 1984. Compact heat exchangers. 3rd ed. New York: McGraw Hill. 335 p.

KOO, J. & KLEINSTREUER, C. 2004. Viscous dissipation effects in micro tubes and micro channels. *International Journal of heat and Mass Transfer,* 47:3159-3169.

LEE, K. 1999. Laminar natural convection heat and mass transfer in vertical rectangular ducts. *International Journal of heat and Mass Transfer*, 42:4523-4534.

LEE, P., GARIMELLA, S.V. & LIU, D. 2005. Investigation of heat transfer in rectangular micro channels. *International Journal of heat and Mass Transfer,* 48:1688-1704.

LEVEQUE, R.J. 2002. Finite volume methods for hyperbolic problems. Cambridge: Cambridge University Press. 558 p.

LUO, D.D., LEUNG, C.W. & CHAN, T.L. 2004. Forced convection and flow friction characteristics of air-cooled horizontal equilateral triangular ducts with ribbed internal surfaces. *International Journal of heat and Mass Transfer,* 47:5439–5450.

MEURIC, O.F.J., CHIU, T.W., WAKEMAN, R.J. & FISHER, K.A. 1997. A numerical study of helical flow of generalised Newtonian fluids in eccentric annuli. *Strojnicky Casopis*, 45:363-373.

MANGLIK, R.M. & FANG, P.P. 1995. Effect of eccentricity and thermal boundary conditions on laminar fully developed flow in annular ducts. *International Journal of heat and fluid flow*, 16:298-306.

MORINI, G.L. 2005. Viscous heating in liquid flows in micro-channels. *International Journal of heat and Mass Transfer,* 48:3637-3647.

PIVA, S. 1995. An analytical approach to fully developed heating of laminar flow in circular pipes. *International communications in heat and mass transfer*, 22(6):815-824.

RAY, S. & DATE, A.W. 2003. Friction and heat transfer characteristics of flow through square duct with twisted tape insert. *International communications in heat and mass transfer*, 46:889-902.

ROSAGUTI, N.R., FLETCHER, D.F. & HAYNES, B.S. 2006. Laminar flow and heat transfer in a periodic serpentine channel with semi-circular cross-section. *International Journal of heat and Mass Transfer*, 49:2912-2923.

ROUSSEAU, P.G. 2007. Thermo system design (MEGI 427). Potchefstroom: NWU. 121 p.

SADASIVAM, R., RAJ, M., MILIND, M. & Jog, A. 1999. Fully developed forced convection through trapezoidal and hexagonal ducts. *International Journal of heat and Mass Transfer*, 42:4321-4331.

SAINI, R.P. & SAINI, J.S. 1997. Heat transfer and friction factor correlations for artificially roughened ducts with expanded metal mesh as roughness element. *International Journal of heat and Mass Transfer,* 40(4):973-986.

SAKALIS, V.D., HATZIKONSTANTINOU, P.M. & KAFOUSIAS, N. 2002. Thermally developing flow in elliptic ducts with axially variable wall temperature distribution. *International Journal of heat and Mass Transfer*, 45:25-35.

SHAH, R.K. 1966. Convective heat and mass transfer. New York: Academic Press. 439 p.

SHAH, R.K. & LONDON, A.L. 1978. Laminar flow forced convection in ducts. New York: Academic Press. 437 p.

SHAMES, I.H. 2003. Mechanics of fluid. New York: McGraw-Hill. 820 p.

SYRJALA, S. 1998. Laminar flow of viscoelastic fluids in rectangular ducts with heat transfer: a finite element analysis. *International communications in heat and mass transfer,* 25(2):191-204.

SYRJALA, S. 2002. Accurate prediction of friction factor and Nusselt number for some duct flows of power-law non-Newtonian fluids. Part A. *Numerical Heat Transfer*, 41:89-100.

TAYLOR, C. & HUGHES, T.G. 1981. Finite element programming of the Navier-Stokes equations. Swansea: Pineridge press. 244 p.

TEAMAH, M.A. 2008. Numerical simulation of double diffusive natural convection in rectangular enclosure in the presences of magnetic field and heat source. *International journal of thermal science*, 47:237-248.

TISELJ, I., HETSRONI, G., MAVKO, B. & MOSYAK, A. 2004. Effect of axial conduction on the heat transfer in micro-channels. *International Journal of heat and Mass Transfer,* 47:2551-2565.

UZUN, I. & UNSAL, M. 1997. A numerical study of Laminar heat convection in ducts of irregular cross-sections. *International communications in heat and mass transfer*, 24(6):835-848.

VALENCIA, A. 1995. Heat transfer enhancement in a channel with a built-in square cylinder. *International communications in heat and mass transfer*, 22(1):47-58.

VAN ZIJL, G.P.A.G. 1990. Segregated finite element solution of the incompressible navier-stokes equations, with equal-order velocity-pressure formulation. Potchefstroom:North-West University. (Dissertation – M. Eng.) 67 p.

VELUSAMY, K., GARG, V.K. & VAIDYANATHAN, G. 1995. Fully developed flow and heat transfer in semi-elliptical ducts. *International journal of heat and fluid flow*, 16:145-152.

VELUSAMY, K. & GARG, V.K. 1996. Laminar mixed convection in vertical elliptic ducts. *International Journal of heat and Mass Transfer,* 39(4):745-752.

WEI, T., FIFE, P., KLEWICKI, J. & MCMURTRY, P. 2005. Scaling heat transfer in fully developed turbulent channel flow. *International Journal of heat and Mass Transfer*, 48:5284-5296.

WHITE, F.M. 1988. Fluid mechanics. 2nd ed. New York: McGraw-Hill. 732 p.

WU, H.Y & CHENG, P. 2003. Friction factors in smooth trapezoidal silicon micro channels with different aspect ratios. *International Journal of heat and Mass Transfer*, 46:2519-2525.

YEH, C. 2002. Numerical investigation of the three-dimensional natural convection inside horizontal concentric annulus with specified wall temp or heat flux. *International Journal of heat and Mass Transfer,* 45:775-784.

YU, B., KAWAGUCHI, Y., KANEDA, M., OZOE, H. & CHURCHILL, S.W. 2005**a**. The computed characteristics of turbulent flow and convection in concentric circular annuli. Part II. Uniform heating on the inner surface. *International Journal of heat and Mass Transfer*, 48:621-634.

YU, B., KAWAGUCHI, Y., OZOE, H. & CHURCHILL, S.W. 2005**b**. The computed characteristics of turbulent flow and convection in concentric circular annuli. Part III. Alternative thermal boundary conditions. *International Journal of heat and Mass Transfer,* 48:635-646.

YUAN, J., ROKNI, M. & SUNDEN, B. 2001. Simulation of fully developed laminar heat and mass transfer in fuel cell ducts with different cross-sections. *International Journal of heat and Mass Transfer,* 44:4047-4058.

YUCEL, N. & DINLER, N. 2006. Numerical study of laminar and turbulent flow through a pipe with fins attached. Part A. *Numerical heat transfer,* 49:195–214.

Appendix A: Literature study

Reference	Boundary conditions	Duct shape	Are the Nusselt numbers calcula-ted?	Are the friction factors calcula-ted?	Is the flow laminar or turbu-lent?	Are there analytic-cal calcula-tions?	Are there numeri-cal calcula-tions?	Numerical method	How does results compare with other results in the literature?	Conclusions
Barletta (2002:641-654)	H1	Rectangular	Yes	Yes	Laminar	Yes	No			An interesting comparison with the analytical solutions for the same heat transfer problem has revealed that important discrepancies exist in the values of ¼ *f*Re and Nu. These discrepancies are due to the different choice of reference temperature for the linearization.

Busedra and Soliman (1999:527-544)	H1, H2	Semicircular	Yes	Yes	Laminar	No	Yes	control volume based finite difference method, SIMPER algorithm, TDMA	Very good	The value of *f*Re increases as the aspect ratio or axial velocity increase for both boundary conditions in upward inclinations. At the horizontal orientation, ¼ *f*Re (H1) exceeds ¼ *f*Re (H2) because of the thermal stratification associated with H2. This trend reverses with upward inclinations.
Coelho and Pinho (2006:3349-3359)	H1, T	Concentric annuli	Yes	No	Laminar	Yes	No			Simpler exact expressions were presented for the Nusselt numbers at the inner and outer walls, normalised temperature distribution and bulk temperature as functions of relevant non-dimensional numbers, the

										expressions' coefficients is given in tables as functions of the radius ratio
Chen *et al*. (2000:209-224)	H1, T	Triangular	Yes	Yes	Laminar	No	Yes	Finite volume method, SIMPLE, Unstructured triangular grid system	Very good	The friction factor and *Nu* showed a strong dependence on the apex angle of the triangular duct. The results indicated that the horizontal duct with the apex angle of 60^{o} produced the best thermal performance.
Du Toit *et al.* (2000:154-159)	T	Closed conduits	Yes	Yes	Laminar	No	Yes	Finite element, finite volume	Very good. Max delta: *Nu* = 1.5% en f < 0.4%	The finite volume and finite element methods are valid and that they can be used to obtain the friction factors and Nusselt numbers for various cross sections for fully developed laminar flow in closed ducts.
Du Toit (2002a:397-407)	H1	Rectangular	Yes	Yes	Laminar	No	Yes	Finite element	Very good	It was shown that there are some discrepancies in the published values for ¼

										*f*Re and *Nu* for fully developed laminar flow in ducts.
Du Toit (2002b:201-206)	H1	Annuli	Yes	Yes	Laminar	No	Yes	Finite element technique	Very good	The results showed the elegance, accuracy and the power, yet relative simplicity, of the finite element approach in this specific case.
Du Toit (2003:50-55)	H1	Semi-circular	Yes	Yes	Laminar	No	Yes	Finite element approach: FEDuct-cgs	Very good	The results showed the elegance, accuracy and the power of the finite element approach for hydraulically and thermally fully developed laminar flow in ducts.
Du Toit (2004b:1-16)	H1	Annuli	Yes	Yes	Laminar	Yes	Yes	Finite element technique	Very good	The results demonstrated that the finite element technique can be used to obtain accurate values for the friction factors and Nusselt numbers.

Dwyer (1963a:52-57)	H1	Concentric annuli	No	No	Laminar	Yes	No			None
Dwyer (1963b:336-344)	H1	Circular, annuli and parallel plates.	Yes	No	Laminar	Yes	Yes		Very good	The annuli's Nusselt number approaches a circular pipe's Nusselt number as the annuli's inner radius approaches zero.
Erdogan and Imrak (2005:79-88)	H1	Rectangular, semicircular, circular, parallel plates	Yes	Yes	Laminar	Yes	No			The Nusselt number depends on the duct shape.
Escudier *et al*. (2002:52-73)	H1	Annuli	No	Yes	Laminar	No	Yes	Finite volume		Graphical results were presented for the friction factors and other kinematic characteristics which were obtained for power-law fluids through eccentric annuli with inner-cylinder rotation. It was shown that some of the results found in the literature for this type of flow are

										incorrect
Gamrat *et al*. (2005:2943-2954)	H1	Rectangular	Yes	No	Laminar	No	Yes	Continuum model	Very good	Was shown that the thermal entrance effects are depended on the Reynolds number. The experimental and numerical heat flux and temperature values differ greatly for very small (0.1 mm spacing) rectangular micro channels
Kakac *et al*. (75-105)	T, H1, H2	Circular, hexagonal, parallel plates, square and rectangular	Yes	No	Laminar	No	Yes			None
Kapale and Chand (2006:601-610)	H1	Shell-and-Tube	No	Yes	Laminar	No	Yes			The results are in good agreement with other results found in the literature.

Kays and Crawford (108-152)	T, H2	Circular duct, Annuli	Yes	Yes	Laminar	Yes	No			None
Koo and Kleinstreuer (2004:3159-3169)	H1	Micro tubes	No	No	Laminar	Dimen-sional analysis and Experi-mentally validated computer simulation	No			The viscous dissipation in micro tubes and micro channels depends greatly on the Reynolds number, aspect ratio, Prandtl number, conduit hydraulic diameter and the Eckert number, the accuracy of the simulation can thus be affected if viscous dissipation is ignored
Lee (1999:4523-4534)	T, H1	Rectangular	Yes	No	Laminar	Yes	Yes	Vorticity-velocity formulation for three-dimensional parabolic flow		The Nusselt number was found to increase with buoyancy ratio. The characteristics of natural convection in vertical rectangular ducts would approach those of two-dimensional vertical

										parallel plate ducts as the aspect ratio increases above 31.
Lee *et al*. (2005:1688-1704)	T, H1	Rectangular micro channels	Yes	No	Laminar	Experi-mental	Yes	3D conjugate approach	Very good	The results confirmed that the simplified thin wall analysis can be used as a computationally economical alternative to a full three-dimensional conjugate analysis.
Luo*et al*. (2004:5439-5450)	H1	Triangular	Yes	Yes	Turbulent	Experi-mental	No			Non-dimensional relationships for average Nusselt number and average friction factor in terms of Reynolds number, relative rib height and relative rib-to-rib spacing have been developed from the experimental results. The maximum percentage deviations for the two equations are ±3.5% and ±8.7%,

										respectively.
Manglik and Fang (1995:298-306)	T, H1	Annuli	Yes	Yes	Laminar	Yes	Yes	Finite difference method (Same as Manglik and Prusa)	Very good	Large non-uniformities in the axial velocity and temperature fields were found when the eccentricities increased and the radius ratios decreased. The flow was found to stagnate in the narrow sections of an annulus while higher flow velocities were reached in the wider sections. It was also found that higher heat transfer coefficients are sustained by the H1 condition, relative to the T condition, except for very high eccentricity values

Morini (2005:3637-3647)	H1	Micro channels	No	Yes	Laminar	Experi-mental	No			By taking the viscous heating and the consequent decrease of fluid viscosity into account, it is possible to explain the decrease of the friction factor when the Reynolds number increases.
Piva (1995:815-824)	H1, T, H5	Circular pipe	Yes	No	Laminar	Yes	No			The results are in good agreement with other results found in the literature.
Promvonge and Eiamsaard (2007:72-82)	H1	Circular duct	Yes	Yes	Turbulent	Experi-mental	No			The present experimental results on heat transfer and flow friction characteristics in a uniform heat-flux tube equipped with nozzle tabulators are reported in terms of Nusselt number and friction factor. The comparisons between the present experimental work and correlations from

										the literature are good.
Ray and Date (2003:889-902)	H1	Square	Yes	Yes	Turbulent, Laminar	No	Yes	SIMPLEC		The laminar local Nusselt number varies axially over H/2 length in a repetitive manner, the maximum local Nusselt number is found at the cross-section of the duct's diagonal and twisted tape's alignment. The Nusselt number's axial variation for turbulent flow is insignificant.
Rosaguti *et al*. (2006:2912-2923)	T, H2	Semi-circular	Ratio	Ratio	Laminar	No	Yes	Finite-volume CFD code ANSYS CFX-5.7		For serpentine channels, the ratio of heat transfer coefficient to friction factor is up to 5.5 times greater than the corresponding ratio in straight passage.

Sadasivam *et al*. (1999:4321-4331)	H1, T	Trapezoidal and hexagonal	Yes	Yes	Laminar	No	Yes	Finite difference techniques	Very good	The results are in very good agreement with other results found in the literature. The article shows the influence of the trapezoidal ducts' geometrical features on the fully developed laminar flow fRe, Nu_H and Nu_T.
Saini and Saini (1997:973-986)	H1	Square	Yes	Yes	Turbulent	Experi-mental				A considerable enhancement of heat transfer can be obtained as a result of providing expanded metal mesh artificial roughness on the absorber plate of a solar air heater duct and that this enhancement is a strong function of the system and operating parameters.

Sakalis *et al*. (2002:25-35)	T	Elliptic	Yes	Yes	Laminar	Yes	Yes	Iterative finite difference pseudo transient ADI, TDMA		As the aspect ratio of the elliptic duct decreases from 0.99 to 0.25 the friction factor increases. For the fully developed thermal flow: as the aspect ratio of the elliptic duct decreases from 0.99 to 0.25 the Nusselt number increases with about 7%
Syrjala (1998:191-204)	H1	Rectangular	Yes	Yes	Laminar	No	Yes	Criminale-Ericksen-Fibley (CEF) model, Reiner-Rivlin models. Using computer program PDE2D		The numerical predictions demonstrate that although the secondary flow arising from the elasticity of the fluid is typically very weak as compared to the main flow in the axial direction, it may markedly enhance heat transfer. The heat transfer enhancement is particularly

										outstanding in the cases of a high Prandtl number. In contrast, the friction factor, and hence the pressure drop, is essentially unaffected by the secondary flow. Advantage of this models are that the stresses are given explicitly in terms of the instantaneous velocity field
Syrjala (2002:89-100)	T, H1	Rhombic, Triangular, Elliptical, Semi-elliptic	Yes	Yes	Laminar	No	Yes	High-order finite element method using computer code PDE2D		Accurate predictions of friction factor and Nusselt number for the fully developed laminar flows of power-law non-Newtonian fluids have been calculated
Teamah (2008:237-248)	T	Rectangular	Yes	No	Laminar	No	Yes	Finite difference method		The magnetic field's strength and the generation or absorption effect greatly influence the heat and mass transfer

										mechanism and flow characteristics inside the enclosure. The presence of a heat sink increases the Nusselt number while a heat source decreases the Nusselt number.
Tiselj *et al*. (2004:2551-2565)	H1	Triangular Micro channels	Yes	No	Laminar	Experi-mental	Yes	CFX5		Experimental and numerical analysis were performed, and showed that the bulk water temperature, as well as the temperature of the heated wall, do not change linearly along the channel, and that the Nusselt number has a singular point where the difference between the temperatures on the wall and the bulk temperature becomes negative, while the flux changes sign

Uzun and Unsal (1997:835-848)	H1, T	Rhombic, Triangular, Sinusoidal, Irregular shapes	Yes	Yes	Laminar	No	Yes	Finite difference method		The elliptic grid generation technique is an appropriate method for irregular boundary duct solutions.
Valencia (1995:47-58)	T	Square cylinder	Yes	No	Laminar	No	Yes	SIMPLE, SIMPLEC, TDMA		The numerical results reveal the oscillatory structure of the flow when the system is operated above a critical channel Reynolds number of about 200 for cylinder with h/H=0.5 and 600 for cylinder with h/H=0.25. With h = cylinder height and H = channel height
Velusamy *et al*. (1995:142-152)	H1	Semi-elliptical	Yes	Yes	Laminar	No	Yes			The friction factor increases as the aspect ratio decreases. While Nu_{H1} increases monotonically as the aspect ratio decreases, Nu_T exhibits a maximum at Aspect ratio = 0.2. The

										friction factor and Nu_{H1} values for Aspect ratio = 0.1 are about 25% higher than those for the semicircular duct.
Velusamy and Garg (1996:745-752)	H1, T	Elliptic	Yes	Yes	Laminar	No	Yes	Control volume based discrimination method		During mixed convection in elliptical ducts, fluid with a high axial velocity exists around the fool. For a given Rayleigh number, the lower the aspect ratio, the higher is the maximum velocity and the closer it is to the loci of the duct. The Nusselt number and friction factor is high if the aspect ratio is low.
Wei *et al.* (2005:5284-5296)	H1	Channel flow	No	No	Turbulent	Experi-mental	No			The results provide a description of scaling behaviours of the temperature and turbulent heat transfer profiles.

Wu and Cheng (2003:2519-2525)	H1	Trapezoidal micro channels	No	Yes	Laminar, Turbulent	Experi-mental	No			The experimental data agree with the analytical solution based on the Stokes flow theory. The transition from laminar to turbulent flow occurred at Re = 1500-2000.
Yeh (2002:775-784)	T, H1	Annuli	No	No	Laminar	No	Yes	SIMPEC and QUICK		It was found that higher temperature around the inner cylinder occur in the region near its top. The maximum inner cylinder surface temperature occurs right at the top of the inner cylinder.
Yu *et al*. (2005a:621-634)	H1	Concentric circular annuli	Yes	No	Turbulent	Yes	Yes		Very good	The results was very accurate
Yu *et al*. (2005b:621-634)	H1, H2	Concentric circular annuli	Yes	No	Turbulent	No	Yes		Very good	The numerical results are in good agreement with experimental results.

Yuan *et al*. (2001:4047-4058)	H1, T	Rectangular, Trapezoidal	Yes	Yes	Laminar	No	Yes	Finite volume method, with SIMPLE-HT, SIMPLEC, TDMA		Mass injection through one wall increases the friction factor and decreases the Nusselt number, and vice versa.
Yucel and Dinler (2006:195-214)	H1	Circular	Yes	Yes	Turbulent, Laminar	Yes	Yes	Finite-volume method, SIMPLE		For laminar flow cases (Re <= 1 500) without fins, the mean Nusselt number remains constant at about 3.66 for fully developed momentum and thermal boundary-layer cases. However, with increasing fin heights the mean Nusselt numbers decrease slightly due to the high conductivity ratio of the fins. For turbulent cases, increase in Reynolds number increases the disturbance in the flow and causes an increase in the mean Nusselt number.